Universität für Bodenkultur Wien
Department für Agrarbiotechnologie IFA Tulln
Institut für Umweltbiotechnologie

Antonino BIUNDO M.Sc.

DISSERTATION

Enzyme Optimization for Polymer Modification

Zur Erlangung des Doktorgrades an der Universität für Bodenkultur Wien

Univ. Prof. Dipl.-Ing. Dr. techn. Georg Gübitz

Universität für Bodenkultur Wien

Department für Agrarbiotechnologie IFA Tulln

Institut für Umweltbiotechnologie

2017

Table of Contents

Preamble

This thesis is divided into three main sections.

The first section (Chapter 1 and 2) present to the reader the aim of this work and a general introduction to hydrolysis reactions catalyzed by lipases and esterasesfollowed by a more detailed description of the application of this class of enzymes for hydrolysis and functionalization of polyesters.

The second section (Chapter 3 to 6) consists of three publications that were published during the thesis on polyester hydrolysis. The first one exploits the potential of a wild-type from the anaerobic species *Pelosinus fermentans* to hydrolyze the biodegradable polyester poly(butylene adipate-*co*-terephthalate) (PBAT).

Chapters 4 and 5 describe two approaches for improving the activity of a lipase from *Clostridium botulinum* (Cbotu_EstA) on polyesters based on single amino acid substitutions and domain deletion, respectively.

Chapter 6 describes a novel approach to change the affinity of two cutinases in order to improve their ability to act on bulky polyamides.

The third section (Chapter 7 and 8) closes this thesis with a general conclusion and an appendix, listing all scientific publications, oral and poster presentations, secondments and awards.

Abstract

The work described in this thesis was carried out within the EU- FP 7 REFINE project. The goal of the project was the combination of knowledge in polymer and material sciences, biotechnology, ecological impact and Life Cycle Analysis to lead towards a greener and more sustainable society.

Accordingly, the focus of this thesis was to study enzymes acting on polyesters in order to develop an environmentally friendly method for polymer hydrolysis and functionalization.

In a first step, the enzymatic hydrolysis of the biodegradable polyester poly(butylene adipate-*co*-terephthalate) (PBAT) was studied with the wild-type enzyme *Pelosinus fermentans* Lipase 1 (PfL1). Biochemical characterization of the purified enzyme with small substrates showed thermoalkalophilic properties (T_{opt}=50 °C, pH_{opt}=7.5) and a preference for hydrolysis of medium chain length *para*-nitrophenyl esters (C8). Analysis of the 3D structure of the enzyme revealed the presence of an extra domain surrounding a zinc ion, and a lid structure, which are characteristic of members of the I.5 lipase family. Investigation of the hydrolysis of the biodegradable polyester PBAT showed a higher activity of PfL1 when compared to the commercial lipase *Candida antarctica* Lipase B (CaLB) based on quantification of hydrolysis products by using liquid chromatography-mass spectrometry (LC-MS).

Two mutagenesis approaches for improving the enzyme activity on polyesters were investigated. Investigation of the 3D structure of the PBAT hydrolyzing-polyesterase from *Clostridium botulinum* (Cbotu_EstA) exhibited features which were similar to those of the members of the I.5 lipase family. Analysis of the extra domain that carries the zinc ion in terms of polyester hydrolysis led to the production of nine different variants. The substitution of each of the residues of the zinc-binding site suppressed completely the activity of the enzyme reducing its catalytic efficiency on small substrates and its activity on the bulky substrate. Nonetheless, production of the variants of the zinc cavity and surface of the zinc-binding domain led to improved release of small building blocks from the polymeric substrate, albeit catalytic efficiency on the small substrate *para*-nitrophenyl butyrate did not increase. Two variants, S129A and S199A, which are present on the surface of the zinc-binding domain, at the entrance to the cavity, released the highest amount of hydrolysis products as compared to the other variants.

Further analysis of the 3D structure of Cbotu_EstA revealed an uncommon feature for the I.5 lipase family, which consisted of an extra N-terminal domain covering the lid structure of the enzyme. The enzyme was redesigned to improve the hydrolysis of synthetic polyesters which led to the production of the truncated variant del71Cbotu_EstA. The del71Cbotu_EstA variant showed increased activity on the widespread polyester polyethylene terephthalate (PET), which may not be attacked by the wild-type enzyme Cbotu_EstA. The removal of the 71 amino acids at the N-terminus of the enzyme exposed a hydrophobic patch on the surface, which permitted improved sorption on hydrophobic polyesters.

In summary, members of the I.5 lipase family are very important enzymes, which can be used for hydrolysis and functionalization of polyesters.

Finally, the possibility to convert “polyesterases” into “polyamidases” was investigated. Analysis of the 3D structure of amidases and proteases revealed that a H-bond acceptor needs to be present to permit the hydrolysis of amide bonds. Substitution of specific amino acids in the structure of two other members of the carboxylesterase superfamily, namely the polyester-hydrolyzing cutinase from *Humicola insolens* (HiC) and the cutinase 1 from *Thermobifida cellulosilytica* (TcC), were carried out to provide a H-bond acceptor, either through the side chain of amino acids or through a water molecule which is present in the active site of the enzyme and forms a bridge between the enzyme structure and the substrate. The variant HiC L64H/I167Q, which showed the presence of a water molecule in the structure *via* molecular dynamic simulation, showed a complete loss of the ability to hydrolyze the polyester PET. This variant was able to increase the hydrophilicity of the surface of the polyamide Nylon 6,6, thereby, producing high amounts of carboxylic groups. Moreover, the enzyme was able to release higher amounts of building blocks from the surface.

All three examples of mutagenesis show that enzyme engineering can dramatically change and improve the activity of enzymes on polymeric substrates.

Kurzfassung

Die in dieser Dissertation beschriebenen Arbeiten wurden im Rahmen des EU-FP 7 REFINE-Projektes durchgeführt. Ziel des Projektes war die Kombination von Wissen in Polymer- und Materialwissenschaften, Biotechnologie, Umweltwissenschften und Lebenszyklusanalyse zur Entwicklung einer umweltfreundlicheren und nachhaltigeren Gesellschaft.

Dementsprechend war der Schwerpunkt dieser Arbeit die Untersuchung von Enzymen mit Aktivität auf Polyestern zur Entwicklung von umweltfreundlichen Verfahren zur Polyesterhydrolyse und Funktionalisierung.

In einem ersten Schritt wurde die enzymatische Hydrolyse des biologisch abbaubaren Polyesters Poly(butylenadipat-co-terephthalats) (PBAT) mit dem Wildtyp-Enzym *Pelosinus fermentans* Lipase 1 (PfL1) untersucht. Die biochemische Charakterisierung des gereinigten Enzyms auf kurzkettigen Substraten zeigte thermoalkalophile Eigenschaften (T opt = 50 °C, pH opt = 7,5) und eine Bevorzugung der Hydrolyse von Para-Nitrophenylestern mittlerer Kettenlänge (C8). Die Analyse der 3D-Struktur des Enzyms zeigte die Anwesenheit einer zusätzlichen Domäne, die ein Zinkion umgibt, und eine Lid-struktur die für Mitglieder der I.5-Lipase-Familie charakteristisch ist. Die Untersuchung der Hydrolyse des biologisch abbaubaren Polyester-PBAT ergab eine höhere Aktivität von PfL1 im Vergleich zur kommerziellen *Candida antarctica* Lipase B (CaLB) auf Basis der Quantifizierung von Hydrolyseprodukten mittels Flüssigchromatographie-Massenspektrometrie (LC-MS).

Zwei Mutageneseansätze zur Verbesserung der Enzymaktivität auf Polyestern wurden untersucht. Die Untersuchung der 3D-Struktur der PBAT-hydrolysierenden Polyesterase aus *Clostridium botulinum* (Cbotu_EstA) zeigte Eigenschaften, die denen der Mitglieder der I.5-Lipase-Familie ähnlich waren. Die Analyse der zusätzlichen Domäne, die das Zinkion umgibt führte zur Herstellung von neun verschiedenen Mutanten. Die Substitution der Aminosären der Zinkbindungsstelle führte zu einer deutlichen Verringerung der Aktivität des Enzyms auf kleinen Substraten. Nichtsdestoweniger führten Mutationen im Bereich der Zinkbindungsdomäne zu einer verbesserten Hydrolyse der Polyester.

Eine Analyse der 3D-Struktur von Cbotu_EstA zeigte eine zusätzliche N-terminale Domäne die möglicherweise die Hydrolyse von Polyestern behindert. Daher wurde eine verkürzten Variante del71Cbotu_EstA generiert die tatsächlich im Gegensatz

zum Wildtyp-Enzym Cbotu_EstA eine erhöhte Aktivität auf dem wichtigen Polyester Polyethylenterephthalat (PET) aufwies. Die Entfernung der 71 Aminosäuren am N-Terminus des Enzyms legte einen hydrophoben Bereich auf der Oberfläche frei was vermutlich eine verbesserte Bindung an hydrophobe Polyester ermöglichte.
Zusammenfassend sind Mitglieder der I.5-Lipase-Familie sehr interessante Enzyme im Hinblick auf die Hydrolyse und Funktionalisierung von Polyestern.
Schließlich wurde die Möglichkeit, "Polyesterasen" in "Polyamidasen" umzuwandeln untersucht. Die Analyse der 3D-Struktur von Amidasen und Proteasen zeigte, dass ein H-Bindungsakzeptor vorhanden sein muss, um die Hydrolyse von Amidbindungen zu ermöglichen. Basierend darauf wurden Mutanten der Polyester-hydrolysierenden Cutinase aus *Humicola insolens* (HiC) und der Cutinase 1 aus *Thermobifida cellulosilytica* (TcC) generiert und H-Bindungsakzeptoren eingebaut. Die Mutante HiC L64H/I167Q, die in Simulationen die Anwesenheit eines Wassermoleküls vorloren ihre Fähigkeit PET zu hydrolysieren vollständig. Andererseits, konnte diese Mutante Nylon 6,6 hydrolysieren was durch eine Eröhung der Hydrophilie der Oberfläche und Freisetzung von Hydrolyseprodukten gezeigt wurde. Alle drei Beispiele für Mutagenese zeigen, dass mittels Enzyme-engineering die Aktiviät von Enzymen auf Polymeren massiv verändern und verbessert werden kann.

1

Aim of the thesis

The work described in this thesis was conducted within the REFINE project, founded by the 7th Framework Programme for Research and Technological Development of the European Union. The goal of the project was to develop a green technology, directly validated and integrated by industry with new skills and expertise in sustainable green materials, manufacturing, technologies and applications for a greener and more sustainable society. Different approaches were carried out, separately or synergistically, by the partners, such as enzymatic processing, synthesis in supercritical environments and the use of terpenes and polyols, among others. This project was based on the unique combination of knowledge along the production chain in polymer and materials science, biotechnology and applications, ecological impact and Life Cycle Analysis.

Due to the fact that lipases can be activated at the interface through the so called interfacial activation mechanism, members of the lipase superfamily displaying thermal stability are promising candidate for polyester hydrolysis, in which higher temperatures can increase the mobility of the polymer chain, thus leading to increased hydrolysis, especially at the surface for the production of functional groups. Furthermore, in order to improve the activity of lipases, analysis and substitution of specific amino acids can be carried out.

Therefore to achieve this aim, a number of objectives were planned in this thesis, including:

1. Investigating the activity of the wild-type enzyme PfL1 for the hydrolysis of different polyesters, especially biodegradable, such as PBAT.
2. Analyzing the overall structure of the PBAT-hydrolyzing enzyme Cbotu_EstA in order to improve the activity of the enzyme and produce variants able to better hydrolyze the polyester PBAT.
3. Enlarging the range of substrate acceptance of Cbotu_EstA in order to hydrolyze the widespread polymer PET.
4. Converting cutinases into amidases

2

Introduction

2.1 Enzymes and polymers

Proteins are biopolymers, which consist of twenty amino acids as monomers. The spatial distribution of the twenty amino acids can confer specific catalytic activities specific for different classes of enzymes. Enzymes have been used by human beings since the ancient Egypt to produce goods as drinks or food. The first enzyme, diastase, which catalyzes the hydrolysis of starch to maltose, was discovered by the French chemist Anselme Payen in 1833. Half a century later, the German physiologist Wilhelm Kühne made use of the term “enzyme” for the first time, which comes from the Greek work ένζυμον, to explain the process of leaven in a dough.

Enzymes are ubiquitous present in Nature. They direct their activity against natural compounds to improve the speed of a reaction up to 10^{17} times by decreasing the activation energy [1] (Fig. 1).

Normally, enzymes operate in mild conditions and they possess high efficiency and high selectivity towards the natural target compounds. In particular, in order to act on specific substrates, enzymes have to recognize the reagents as target compounds.

More often than not, industrially relevant reactions do not involve natural compounds, but chemicals which contain non-natural modifications [2]. For this reason, in order to increase the activity of enzymes, a modification of either specific (rational design) or random (directed evolution) amino acids and/or domains can improve the activity of biocatalysts towards industrially relevant compounds [3].

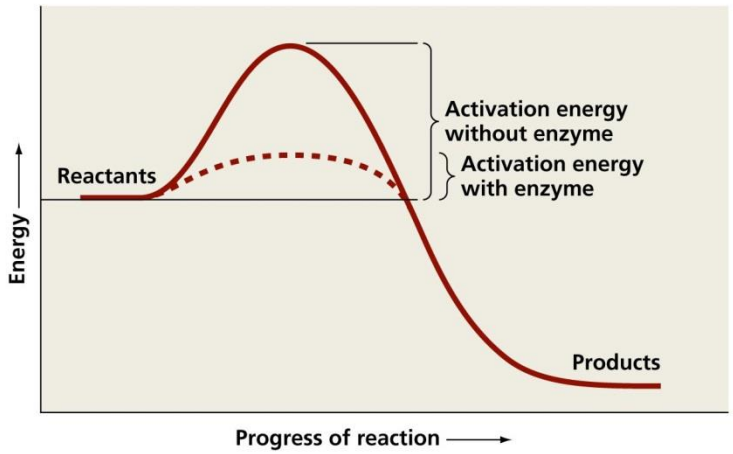

Figure 1. Energy profile diagram for an enzyme catalyzed reaction (dotted line) and the corresponding uncatalyzed reaction (full line) where the reactants are converted into the products.

In polymer chemistry, enzymes have been used both in the synthesis and in the hydrolysis of polymers either to produce specific substitutions or to improve functionalization and the recycling of polymers, respectively [4–6]. Both processes can use enzymes in order to develop environmentally friendly approaches (Fig. 2).
Different features of the two components, the polymer and the enzyme, have to be taken into account in order to improve the specificity of the reaction. Polymeric structures present at the surface of a material can be recognized by enzymes and functional groups can be formed. Degradable and non-degradable polyesters can show differences in biodegradability. Enzymes can act differently on specific polymers. Enzymes can possess specific characteristics and the activity on polymers can produce features that are important for the further use of the material. In order to identify specific characteristics of the enzyme in focus, analysis of solved structures of enzymes, or with the aid of modelling, can aim on specific residues which can be substituted, and variants be produced to display the function and ameliorate the activity of the enzyme.

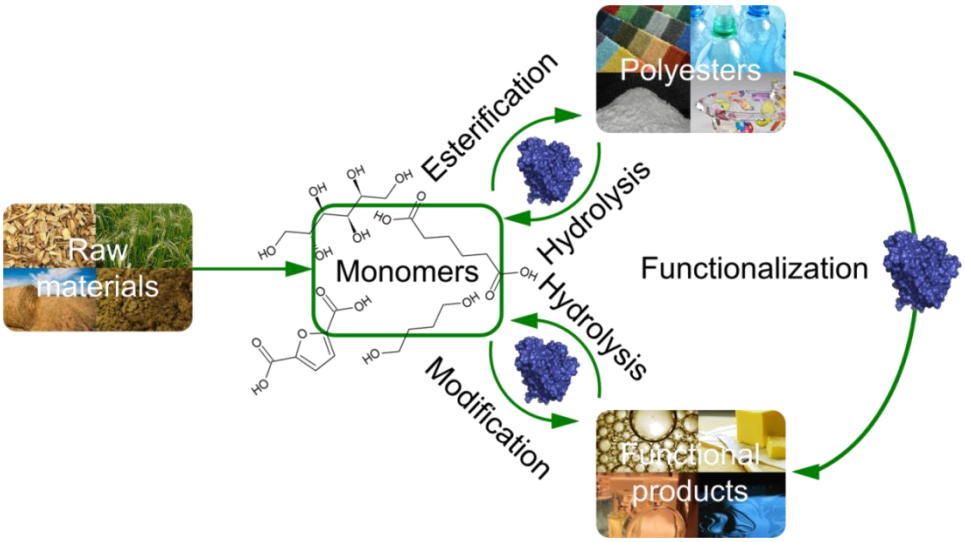

Figure 2. Enzymatic circle for the synthesis, functionalization, modification, and hydrolysis of bio-based polyesters (Permission obtained by Elsevier) [7].

2.2 Enzymatic hydrolysis of polymers

Biodegradability

Polymers are compounds characterized by repetition of single or multiple subunits. Natural polymers are present in the environment and can be used by the producing organism as energy source, such as polyhydroxyalkanoates (PHA) [8] or starch [9], genetic material, such as DNA and RNA, barriers against the attack of microorganisms, such as cutin and suberin [10], and executives to express the genetic information, such as proteins. Since the discovery of the polyamide Nylon 6,6 (Fig. 3A) in 1931 at DuPont, synthetic polymers have been synthesized to satisfy specific human needs [11]. The second class of polymers developed by man-made processes was the class of polyesters, discovered in the early 1940s at Calico Printers, with the production of the worldwide used polyethylene terephthalate (PET) (Fig. 3B).

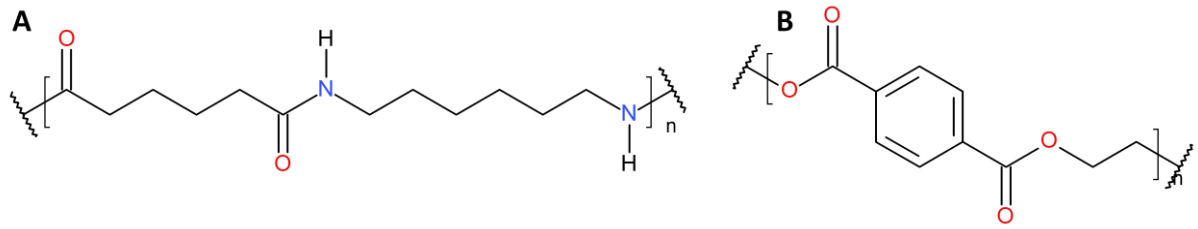

Figure 3. Chemical structure of the synthetic polyamide Nylon 6,6 (**A**) and synthetic polyester polyethylene terephthalate (PET).

Polymers have shown ability to be biodegraded only when the polymer chain is interrupted by hetero-atoms such as O or N or by the presence of C–C double bond. In order to start the biodegradation of the material, extracellular enzymes, constitutively expressed or induced by the presence of the material, have to hydrolyze the polymer in its building blocks. These processes have been reported to be affected by different parameters of the polymer, such as crystallinity [12], viscosity and melting point [13].

Although, polyamides possess both nitrogen and oxygen atoms in their structure, they have been shown to be less degraded than polyesters. This is due to their polymer structure, which presents with different H-bonds, that pack the polymer structure, thus displaying a very strong and resistant structure. Nylon 6,6 and Nylon 6

are the most widely used synthetic polyamides. The H-bonds, which are present in their structure, allow for the use these materials in different applications, such as in textile. However, the H-bonds, which are present in Nylon 6,6 are shorter and, therefore stronger than the ones present in Nylon 6. For this reason Nylon 6,6 may be considered the most important member of the Nylon family.

Polyesters are principally used for commercial applications, such as food packaging [14–16] and textile production [17]. Common characteristics are shared among synthetic polyesters, such as inertness and resistance to various chemicals. These two properties allowed man-made polyesters to find usage in different applications, which decreases their biodegradability in the environment and enlarges plastic waste present especially in water streams.

Biodegradability can be described as an event which takes place through the action of enzymes and/or chemical decomposition associated with living organisms or their secretion products, with the aid of abiotic reactions, such as photodegradation, oxidation and hydrolysis [18]. Enzyme expression can be induced by the presence of polymers in order to hydrolyze specific bonds. Further modification and assimilation of the building blocks can lead to a complete degradation and removal of the polymer by specific microorganisms (Fig. 4)

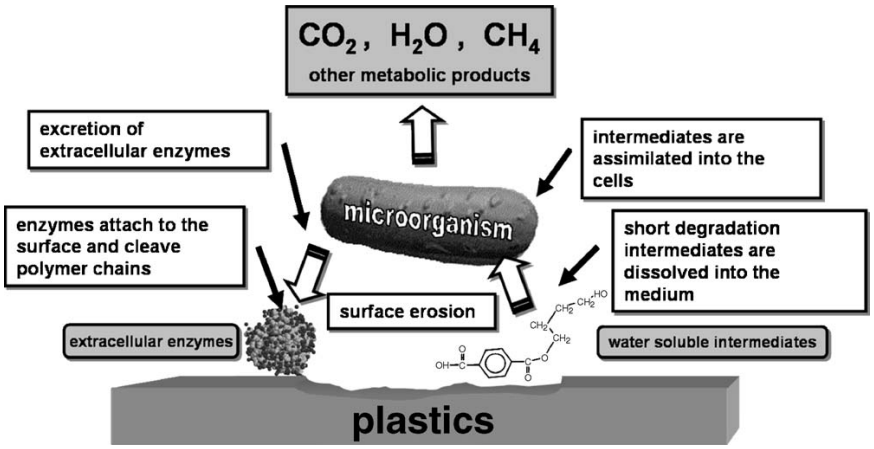

Figure 4. General scheme of biodegradation showing enzymatic hydrolysis of polymer (Permission obtained by Elsevier) [19].

Studies on biodegradability tests of polyesters revealed that aliphatic polyesters are mostly biodegradable [20] but that they lack different properties that are exhibited by polyesters, which contain aromatic moieties, such as PET. Nevertheless, it has been reported that aliphatic polyesters show differences in biodegradability tests as shown

by the different mobility of the polymer chain, and in correlation to the temperature at which the degradation takes place [21]. The latter differences are indicative of differences in the ability of enzymes and microorganisms to degrade these materials.

Polyethylene terephthalate (PET) is the worldwide used thermoplastic polyester, which present with different characteristics, such as gas barrier and resistance to chemicals, which make it an ideal candidate for use in food packaging (such as plastic bottles), textile (fibers), and thermoforming (manufacturing) [22]. PET has an estimated global market of 50 Mton/year [7] against the 299 Mton/year of global plastic production in 2013 [23].

PET is formed by subunits that contain terephthalic acid and ethylene glycol. The aromatic part of the polyester, terephthalic acid, provides excellent material properties and reduces the ability of microorganisms to attack this polymer in order to continue the biodegradability process.

Yoshida et al (2016) have recently reported the ability of the bacterium *Ideonella sakaiensis*, to degrade and assimilate PET [24], showing how evolution of enzymes can improve their activity especially towards non-natural compounds.

Regarding biodegradable polymers, aliphatic polyesters have shown higher degree of biodegradability, in contrast to PET. Generally, polymers which are easily degraded by microorganisms exhibit poor material properties.

In order to find a compromise between biodegradability and industrially relevant properties, copolyesters have been developed by using terephthalic acid as the aromatic component and by maintaining part of the aliphatic constituents [25].

Müller et al. (2001) and Marten et al. (2003 and 2005) have studied the behavior of enzymes on hydrolysis of polyesters that contain or lack aromatic moieties [21,26,27]. As described above, the biodegradability of polyesters begins with the hydrolysis of ester bonds. This process takes place on the surface of the material where enzymes, released in the environment, can find specific bonds and hydrolyze them to release water soluble intermediates, which can then be assimilated by microorganisms or undergo to subsequent transformations.

Aliphatic-aromatic copolyesters have been reported to show industrially relevant properties [18] with reasonable biodegradability. The commercial materials poly(butylene adipate-*co*-terephthalate (PBAT) (Fig. 5A) have been developed by different companies, such as BASF and Eastman-Chemical, with the name Ecoflex® and Eastar Bio®, respectively, and it has been pointed out for its biodegradable and

physical properties [28,29]. Nowadays, polyhydroxybutyrate (PHB), as a member of the class of polyhydroxyalkanoates (PHA), and poly-Lactic acid (PLA) (Fig. 5B and 5C) are commercialized and find applications in different fields. Both polymers, PHB and PLA, are classified as aliphatic polyesters and they are fully biodegradable [30–33]. PHB, which is produced by bacterial fermentation, is usually blended with other polymers especially in packaging, to improve the biodegradability [34]. PLA can also find applications in packaging, but also in biomedical applications [35].

Recently, the bio-based polyethylene furanoate (PEF) (Fig. 5D) has been studied to analyze its advantages and its potential to be hydrolyzed by enzymes [36]. The furane structure present in this polymer would resemble the aromatic moiety of terephthalic acid, but the completely renewable resources, where the furanoic acid comes from, makes this polymer extremely competitive to the fossil derived PET.

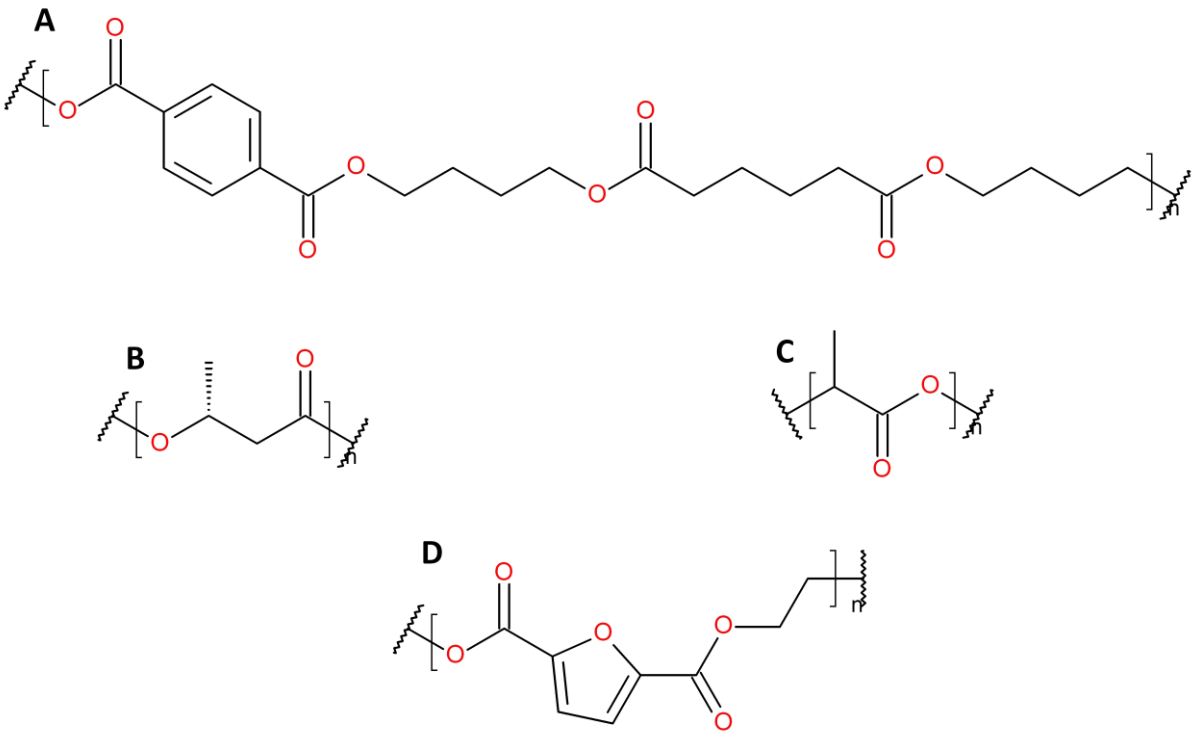

Figure 5. Chemical structure of biodegradable polyesters. (**A**) Poly(butylene adipate-*co*-terepthalate) (PBAT); (**B**) polyhydroxybutyrate (PHB); (**C**) polylactic acid (PLA); (**D**) polyethylene furanoate (PEF).

Functionalization

As described above, extracellular enzymes produced in the presence of polyesters are mostly hydrolases, which act on the surface of the polymeric substrate, that release water soluble building blocks. This process of surface hydrolysis has been

reported to be useful also for modification of polyesters and for their functionalization for different application [4,37–39].

Synthetic polymers, both polyesters and polyamides, such as PET and Nylon 6,6, respectively, are highly hydrophobic and act as a barrier for gasses and odors, and these properties are optimal for food packaging [15]. However, hydrophobicity of polymers negates the possibility of using these materials for textile production as humidity cannot penetrate the material and skin respiration cannot take place. For this reason, the functionalization of polymers is an important step in textile production, as well as in other industrial fields, such as the production of medical devices, where the hydrophilic surface of PET can reduce the attack of microorganisms [40]. Functional groups present onto the surface can also be used as anchors for bioactive molecules or dyes in order to produce drug delivery tools and for polymer processing [41–43].

In order to couple different bioactive compounds on the surface of polymers, three steps are generally followed: (I) production of functional groups on the polymer surface, (II) anchoring of one end of linkers which can be attached to the functional groups, (III) attachment of the bioactive compound of interest on the second end of the linker [42] (Fig. 6).

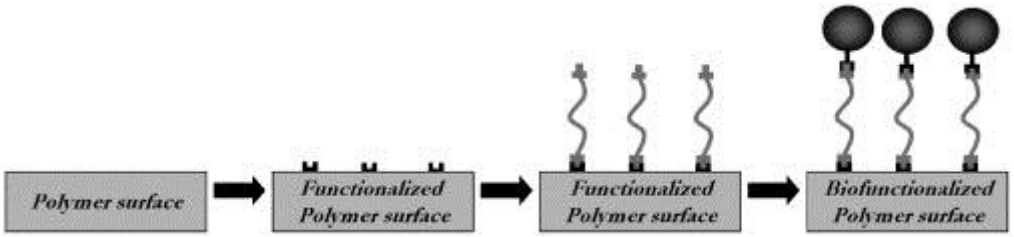

Figure 6. Scheme of biological surface modification showing production of functional groups, binding of linkers and joining of bioactive compounds (Permission obtained by Elsevier) [42].

Nowadays, wet chemical [44] and ionized gaseous [45] methods are used to produce hydrophilic groups [46] (Fig. 7). Nevertheless, one of the most common methods following the wet chemical approach uses alkaline substances, which produces by-products, that can be found in wastewater, and it also involves a weight loss of up to 15% with changes in bulk properties [47]. Instead, plasma treatment, with regard to ionized gasses, is limited because of its complicated use and the difficulty in controlling the modification [48].

Hydrolases have been used to modify the surface of polymeric fibers used in textile production, such as PET, polyamide and polyacrylonitriles [6]. Native and mutated enzymes have been employed to produce functional groups.

Differences in results using either wet chemistry or enzymatic treatment rely on the structure of the polymeric material. In the structure of polymers, molecules are disposed in different ways depending on the polymerization route. For instance, Donelli et al. (2010) have reported that enzymes are more able to hydrolyze amorphous PET, while alkaline treatment can attack mostly crystalline polyesters [49]. Analysis of the polyester surface by means of water contact angle (WCA), Fourier Transform Infrared spectroscopy (FTIR) and Attenuated Total Reflectance mode (ATR) have largely been used to identify the production of functional groups with enzymes and other methods [50].

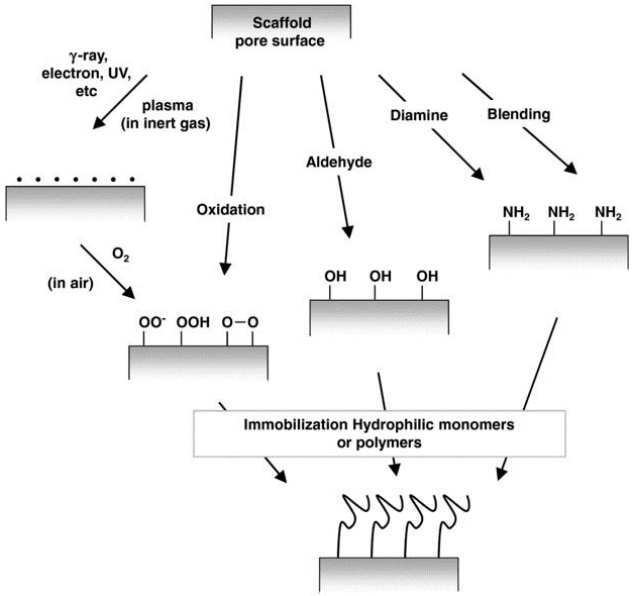

Figure 7. Overview of functionalization methods (Permission obtained by Institute of Physics - Journals) [51].

Amorphous or crystalline polymers can be produced by cooling thermopolymers at room temperatures with sudden changes of temperature or by a slowly decrease of temperature, respectively.

Polymers can also show semi-crystalline morphology, where both amorphous and crystalline lamellae, called crystallites, are present. The regions where both structures are present are named spherulites.

Hydrolytic enzymes that act on the surface of polyesters leave the bulk properties of the material intact without using large amounts of chemicals and energy [22]. As explained in the biodegradability section, enzymes have been reported to attack aliphatic polyesters with ease, while aromatic polyesters, that mostly contain terephthalic acid, such as PET, are resistant to enzymatic attack [25].

Nevertheless, different hydrolytic enzymes have been reported to be able to hydrolyze both aromatic polyesters and aliphatic-aromatic copolyesters. This is possible, especially in the amorphous region of spherulites, where the polymer chains are more motile and can be placed into the active site of the enzyme. As reported by Marten et al. (2003), the temperature difference between the melting temperature of the polymer and the hydrolysis temperature controls the hydrolysis process [21]. One of the most important physical properties of the polymer for the enzymatic hydrolysis is the glass transition temperature (T_g) of amorphous polymers or the melting temperature (T_m) of semi-crystalline materials, which possess amourphous regions conferring a T_g to these polymers. Enzymes, which are stable and active near these two temperatures, can have a better performance on the polyester hydrolysis, depending on the focused material.

In order for enzymes to initiate their attack on polyester surfaces, adsorption processes have to be carried out by the enzyme, and this is mostly enhanced by the presence of hydrophobic domains on the surface of enzymes, which can in turn recognize the hydrophobic surface of polyesters, thereby increasing the yield of hydrolysis [52].

Different studies on enzymes, which are active and stable at higher temperatures, have been widely reported in relation to surface functionalization of polyesters.

2.3 Polyester-hydrolyzing enzymes

Enzymes that belong to the EC 3.1.1, classified as hydrolases acting on ester bonds, have been widely used to perform hydrolysis of polyesters for biodegradation and functionalization.

Esterases (EC 3.1.1.1), lipases (EC 3.1.1.3) and cutinases (3.1.1.74) are well studied biocatalysts thanks to their ability to hydrolyze ester bonds both in soluble and insoluble compounds. These three classes of enzymes share a common structure, namely the α/β-hydrolase fold, which is also present in some serine proteases [53]. This structure consists of a core that is usually formed by eight β-strands surrounded by different α-helices (Fig. 8). The active site of enzymes, which contain this fold, known as catalytic triad, is highly conserved and consists of: one nucleophilic residue (serine, cysteine, or aspartic acid), one acidic residue (aspartic acid or glutamic acid), and one His residue, which is strictly conserved [54].

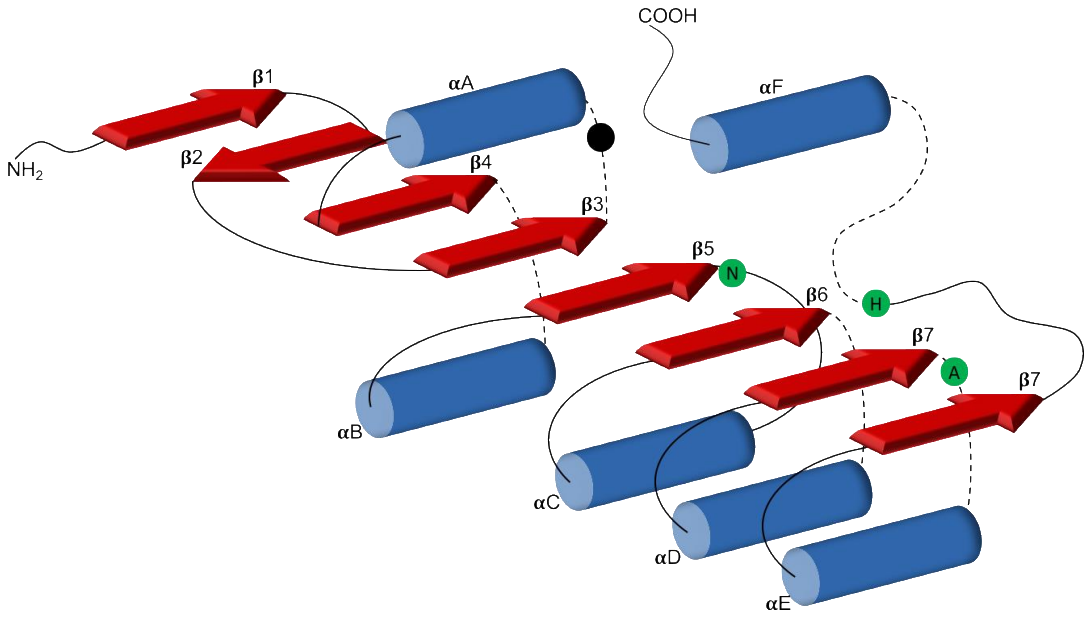

Figure 8. Graphic representation of α/β-hydrolase fold. Eight β-sheets (*red arrows*) are connected through six α-helices (*blue cylinders*). The catalytic triad (*green circles*) contains a nucleophile (N), an acidic residue (A) and a His residue (H). The residues forming the oxyanion hole (*black circle*) are present between the β-sheet β3 and the α-helix αA. Dashed lines represent where domain addition can take place.

The nucleophilic residue is frequently located in a pentapeptide characterized by the sequence Sm-X-Nu-X-Sm [55,56]. The Sm (a small residue) consists of a Gly residue, but also of an Ala residue that can be found in the first position, especially in specific families of the lipase class (e.g. the I.5 lipase family) while X is any amino acid and Nu is the nucleophilic residue. This pentapeptide forms a specific structure in the enzyme, which is called “nucleophilic elbow”, and the differences in the first Sm residue can differentiate the sharpness of this structure for the attack on the substrate [57] (Fig. 9).

Analysis of the behavior of these enzymes has shown promiscuity with regard to conditions, substrates and catalysis. In terms of condition promiscuity, enzymes can act under different conditions that deviate from their natural and optimal ones. For instance, activity in anhydrous environments can lead to a reaction, opposite to that of the hydrolysis of esters, synthesizing esters and polyesters [5], as well as to epoxidation and Baeyer-Villiger oxidation in ionic liquids [58]. Furthermore, concerning substrate promiscuity, enzymes can hydrolyze different esters. Last but not least, with respect to catalytic promiscuity, enzymes catalyze different reactions with different transition states, either by the native enzyme or by variants of the native enzyme where substitutions may redirect the enzyme to perform different reactions, such as aldol and Michael addition [59,60].

In order to perform the native reaction, a common hydrolytic mechanism is present.

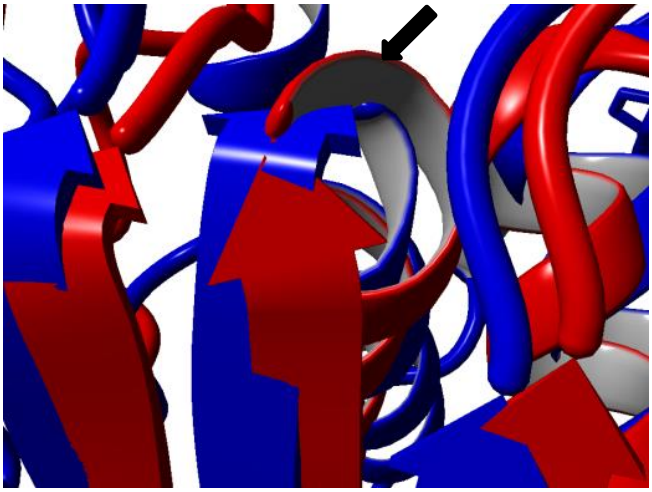

Figure 9. Nucleophilic elbox (*black arrow*) contained in the structure of *Pelosinus fermentans* Lipase 1 (PfL1) (*blue*) and *Thermobifida cellulosilytica* cutinase (TcC) (*red*), containing Ala and Gly as first Sm residue in the pentapeptide surrounding the nucleophilic Ser residue, respectively.

Hydrolysis mechanism

In enzymes, which show the α/β-hydrolase fold, the mechanism starts when the acidic residue of the catalytic triad attacks the histidine, which can furthermore activate the nucleophilic residue to attack an electrophilic species. In the case of carboxyl esterases, the carbonyl carbon of an ester bond is the electrophilic species. In the case of carboxyl esterases, this attack forms a tetrahedral intermediate, which possesses a negative charge, stabilized by the presence of the so called “oxyanion hole” (Fig. 7). The oxyanion hole is a region of the enzyme cavity formed by the backbone of surrounding residues. In the presence of a water molecule, the alcohol molecule is restored and released, leading to the acyl-enzyme form of the protein. After the hydrolysis of the complex acyl-enzyme, the carboxylic acid is released and the enzyme is regenerated [61]. The ionized carboxylic acid is expelled by the electrostatic repulsion, which is present between the carboxylate group and the active site, that is known as “electrostatic catapult” mechanism [56,62] (Fig. 10).

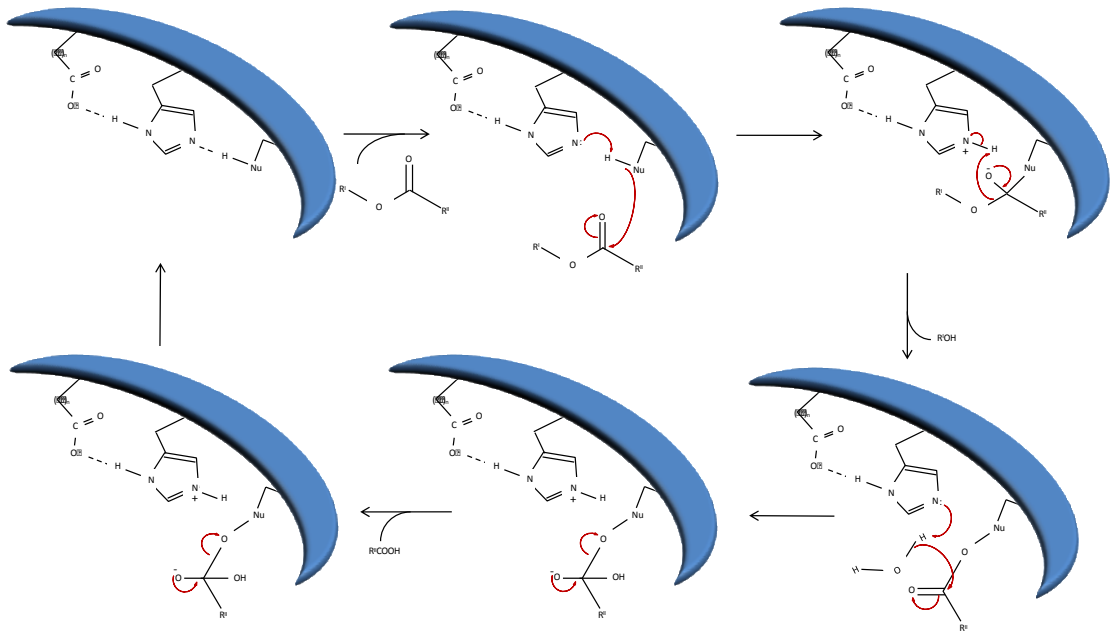

Figure 10. Reaction mechanism for the hydrolysis of ester bonds by enzymes containing the catalytic triad. Nu = O, S or COO for Ser, Cys or Asp, respectively; n = 1 or 2 for Asp or Glu, respectively; R^{I} and R^{II} = H, C_nH_m.

Cutinases, esterases and lipases share this mechanism but with specific differences. Cutinases, in contrast to esterases and lipases, present the catalytic triad on the surface of the enzyme (Fig. 11).

This feature leads to the specific function of the enzyme, which is able to act on insoluble natural polyesters, such as cutin. Another interesting feature of cutinases is the presence of hydrophobic domains on their surface, which can aid the adsorption of the enzyme on the polyester for a better hydrolysis.

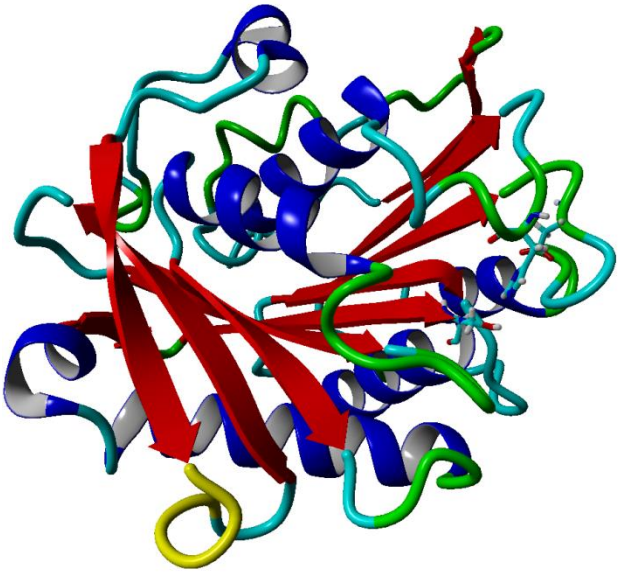

Figure 11. Overall structure of the *Thermobifida cellulosilytica* cutinase (TcC) showing the active site constituted of Ser131/His209/Asp177 at the surface of the enzyme (*sticks*).

Esterases and lipases contain the catalytic triad buried inside the globular structure of the enzyme. In the case of esterases, only small esters can enter the structure and can be hydrolyzed by the enzyme by releasing the alcohol and the ionized carboxylic acid. On the other hand, lipases contain an active site which is buried under a domain formed by α-helices. The number of α-helices varies in different lipases. This domain is called “lid” and permits the presence of a double conformation of lipases (Fig. 12).

Crystallographic studies showed that lipases can be found in two different conformations: closed and open. The closed conformation is the form which is present when the enzyme is in solution, and a basal activity is performed by the enzyme, which in certain cases can be absent. In the presence of an interface, which is formed by insoluble compounds, and in high concentrations of the substrate, the formation of the open conformation can be induced. This mechanism is known as interfacial activation, which increases the activity of lipases [63].

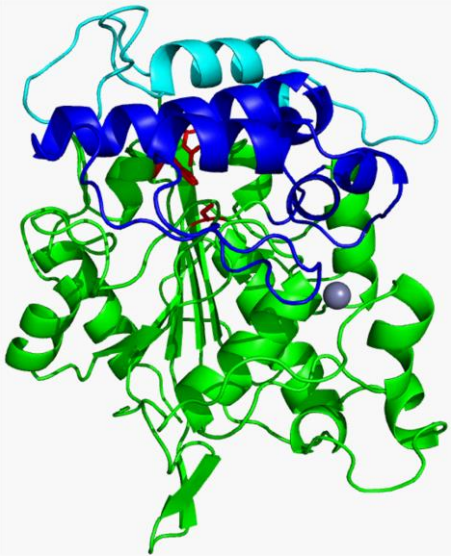

Figure 12. Overall structure of the *Pelosinus fermentans* Lipase 1 (PfL1) showing the α/β-hydrolase core (*green*) and the two insertions forming the lid domain (*cyan* and *blue*). The catalytic triad is shown as *sticks* (*red*). The zinc ion is shown as a *sphere* (*grey*) (From Biundo et al. **2016**, *Appl. Microbiol. Biotechnol.*, DOI: 10.1007/s00253-015-7031-1).

In the interfacial activation, the lid domain moves and permits the entrance to the substrate inside the active site of the enzyme.

In lipases, the lid domain is important to protect the high hydrophobicity of the active site, which usually accepts molecules, such as triglycerides or long chain aliphatic esters. Only when an interface is present, the lid domain changes conformation and permits the entrance to substrate molecules. This movement is also aided by the hydrophobic residues which are present in the inner part of the lid structure. In the open conformation of lipases, these hydrophobic residues can bind to the carbon chain of insoluble compounds by hydrophobic interactions (Fig. 13).

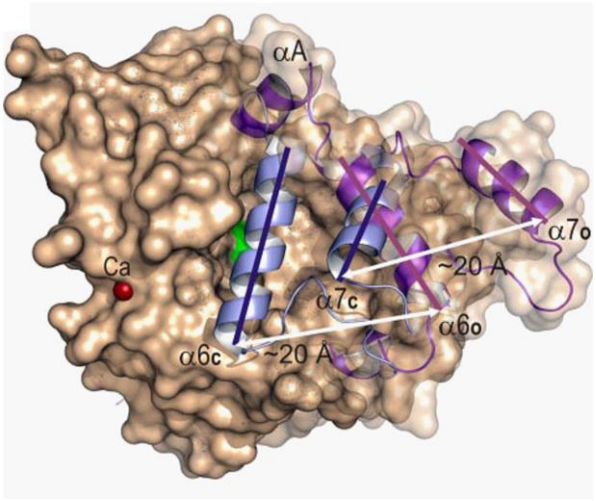

Figure 13. *Geobacillus thermocatenulatus* Lipase 2 (BTL2) structural rearrangement upon activation, showing the molecular surface (*brown*) with the catalytic Ser residue (*green*). Lid changing from the closed (inactive state) to the open (active state) structures are represented. The two helices of the lid are represented in the closed (*blue*) and in the open (*purple*) state. A 20-Å rearrangement of each helix of the lid structure is shown (Permission obtained by The Journal of Biological Chemistry) [64].

Recombinant expression

Carboxyl esterases are widely distributed in the three living kingdoms. In order to be used in biotechnological and environmental applications, industries need large amounts of enzymes which cannot be atained by native organisms. Different hosts have been used for the heterologous expression of carboxyl esterases in order to improve the expression. DNA sequences of tags have been fused to enzyme genes for high purification of the biocatalyst. Bacterial and fungal host systems are the most widely used thanks to their ability of producing high amounts of enzymes and their ease at manipulating them. Table 1 presents different approaches for the expression of carboxyl esterases in order to produce high active enzymes in massive amounts for polyester hydrolysis.

Thermophilic microorganisms were reported to express enzymes that were able to hydrolyze polyesters [65–71]. This particular property of thermophilic enzymes can be explained by the higher temperature optimum as compared to mesophilic enzymes.

Thermophiles are known to produce enzymes with increased interactions, such as electrostatic, disulfide bonds and hydrophobic interactions [72]. The presence of glycosylation patterns, that are present in enzymes of fungal organisms or plants, is

also important to confer stability to the enzyme. In order to maintain the native post-translation modifications (PTM) fungal enzymes are usually expressed in eukaryotic systems, namely *Saccharomyces cerevisiaea* or *Pichia pastoris*, while bacterial enzymes are commonly expressed in *Escherichia coli* (Table 1). It has been reported that also mesophilic microorganisms can express thermophilic enzymes which are resistant to temperatures that are higher to the organism's optimum growth temperature [73].

Carboxyl esterases from mesophilic species, which are able to act on polyesters, have been found in two mesophilic species, *Pelosinus fermentans* and *Clostridium botulinum* [74,75].

Table 1. Heterologous hosts used for recombinant expression of hydrolases and their polymeric substrates.

Expression host	Enzyme	Substrate	Reference
Escherichia coli	*Thermobifida cellulosilytica* cutinase	PET, PBAT	[67], [76]
	Pelosinus fermentans lipase	PBAT	[77]
	Clostridium botulinum esterase	PBAT	[78]
	Fusarium oxysporum cutinase	PET	[79]
	Thermobifida fusca carboxylesterase	PET	[70]
	Marinobacter sp. PHB depolymerase	PHB	[80]
	Thermobifida alba cutinase	PET	[68]
	Thermobifida fusca cutinase	PET, PTT	[66,81], [82]
	Saccharomonospora viridis cutinase	PET	[83]
	Thermomonospora curvata polyester hydrolase	PET, PCL	[84]
Streptomyces rimosus	*Thermobifida* sp. hydrolase	PBAT	[85]
Brevibacillus choshinensis	*Bacillus pumilus* PBAT hydrolase	PBAT, PBSu, PCL, PESu	[86]
Saccharomyces cerevisiae	*Fusarium solani pisi* cutinase	PET, PTT	[87], [82]
Pichia pastoris	*Aspergillus oryzae* cutinase	PCL	[88], [89]
	Fusarium solani cutinase	PET, PVAc, PCL	[90], [91], [89]
	Aspergillus fumigatus cutinase	PCL	[89]
	Humicola insolens cutinase	PCL	[89]
	Alternaria brassicicola cutinase	PCL	[89]
	Thielavia terrestris cutinase	PCL	[92]
Trichoderma reesei	*Melanocarpus albomyces* steryl esterase	PET	[93]
Aspergillus oryzae	*Aspergillus oryzae* cutinase	PBSA	[84]

These two enzymes present features specific of members of the I.5 lipase family, such as a lid that covers the active site and a zinc-binding domain that contains a zinc ion coordinated by four amino acids, two His residues and two Asp residues (Fig. 14).

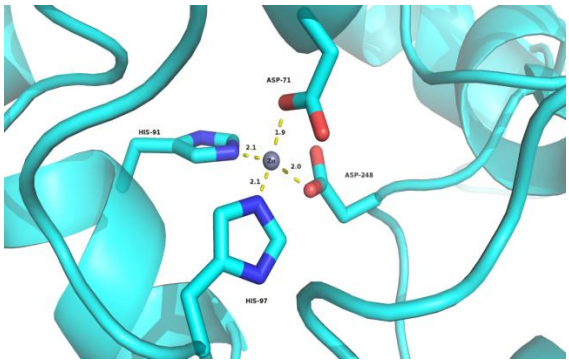

Figure 14. Zinc-coordination site of *P. fermentans* Lipase 1 (PfL1) formed by two Asp and two His residues (*sticks*). The zinc ion is shown as sphere (*grey*) From Biundo et al. **2016**, *Appl. Microbiol. Biotechnol.*, DOI: 10.1007/s00253-015-7031-1).

The zinc-binding domain confers a higher molecular weight to the members of the I.5 lipase family (40-45 kDa) as compared to classical microbial lipases (ca. 30 kDa). The zinc-binding domain was also reported to stabilize the open state for interfacial activation at higher temperatures. This feature permits enzymes from mesophilic organisms to show an increased thermostability as compared to their homologous enzymes, which lack the zinc-binding domain [94]. This characteristic has been reported to be important for the two enzymes to be able to hydrolyze the biodegradable polyester PBAT.

Improvement of enzymatic hydrolysis of polyester

Evolution of organisms is based on mutations in the DNA of ancestors. Mutations are permanent alterations of DNA molecules caused by an introduction of erroneous nucleotides during replication or by environmental factors, which create modification of certain nucleotides. Mutations that occur at the level of protein-encoding genes, change codons of the Open Reading Frame (ORF), which modify the subsequent primary structure of translated proteins. These alterations of the genetic code can also be applied in the laboratory level, thus “evolving” wild-type proteins to generate one or multiple variants carrying random or specific substitutions of amino acids.

Random mutations can be carried out by directed evolution approaches, which can be used to create libraries of variants in order to study the relationship between the structure and the function of proteins, as well as to increase the activity of enzymes [95]. Random and focused mutagenesis are the most commonly used methods to perform directed evolution. In random mutagenesis the entire gene is mutagenized by error-prone PCR [96]. By contrast, in focused mutagenesis degenerated codons are used to introduce multiple mutations in a single codon [97,98]. Rational design is another approach to modify proteins in which the 3D structure is already solved. This approach has been reported to make use of site-directed mutagenesis techniques (Fig. 15).

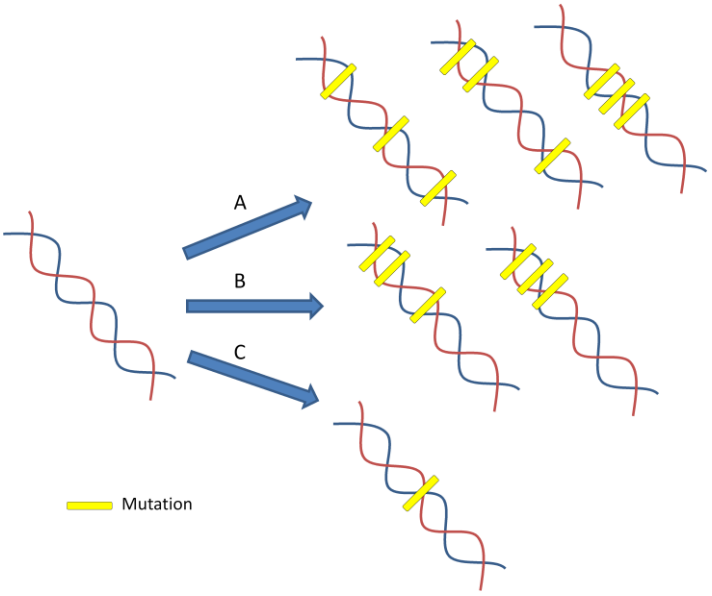

Figure 15. Overview of the different approaches for enzyme engineering. (**A**) Random mutagenesis leads to a library of clones containing mutations randomly on the entire sequence of the gene. (**B**) Focused mutagenesis leads to the formation of mutations only on a certain region of the gene. (**C**) Rational design leads to single mutations which can change specific codon and lead to certain substitutions of amino acids.

In order to improve the activity of the enzyme towards polyester substrates, both directed evolution and rational design approaches have been carried out for improved activity as well as improved thermostability of the enzyme (Fig. 15).

Also, both approaches have been used to improve the activity on aromatic/aliphatic copolyesters of the enzyme Est119 from *Thermobifida alba* [99].

Rational design approaches have been widely used for enzymes with solved 3D structures in order to enlarge the active site, as in the case of cutinases from *F. solani pisi* [100], *T. fusca* [81] (Fig. 16).

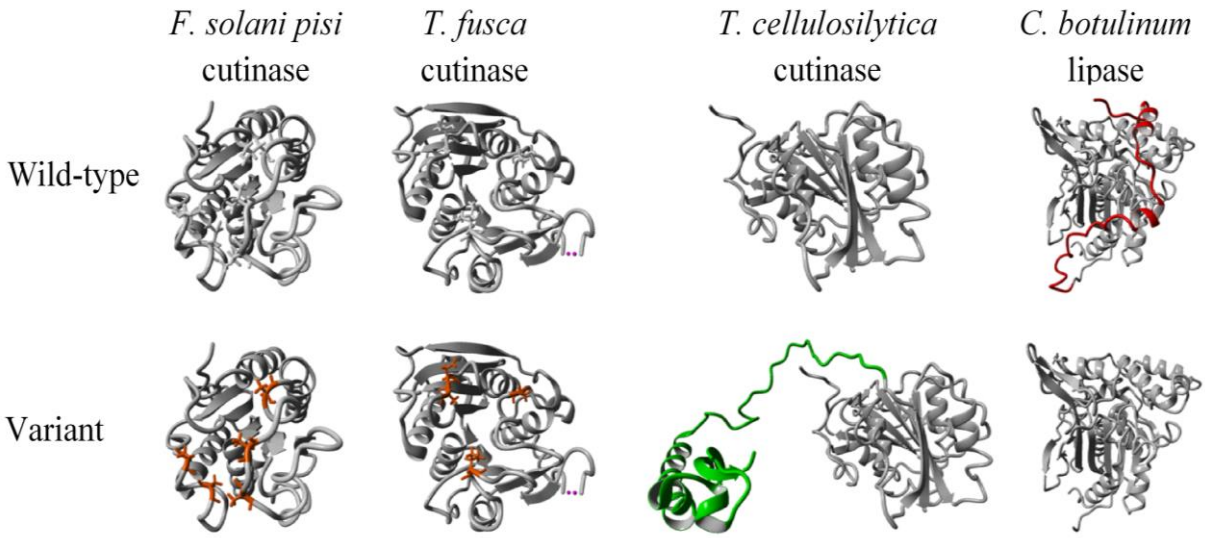

Figure 16. Different approached to modify carboxylesterases in order to enhance their activity on non-natural polyesters. Amino acid exchanges are indicated in orange, domain insertion in green and deletion in red. All the 3D structures were analyzed using the program YASARA view (v. 14.7.17) [101] (From Biundo et al. **2016**, *Biotechnol. J.*, DOI: 10.1002/biot.201600450) [102].

Highly hydrophobic domains of proteins can attach onto the hydrophobic surface of polyesters. Hydrophobins, for instance, are small proteins secreted by fungi, which contain eight Cys residues, which can be adsorbed onto hydrophobic surfaces and to interfaces between hydrophilic and hydrophobic phases [103]. These proteins, as in the case of hydrophobins from *Trichoderma reesei* (Fig. 17) and *Aspergillus oryzae*, were also reported to be important to recruit heterologous and native polyesterases which could hydrolyze natural and synthetic biodegradable polyesters, such as cutin and suberin and poly(butylene succinate-*co*-adipate) (PBSA), respectively [104,105]. Furthermore, fusion of two different members of hydrophobins from *Trichoderma* spp. were reported to stimulate the enzymatic hydrolysis of PET [106].

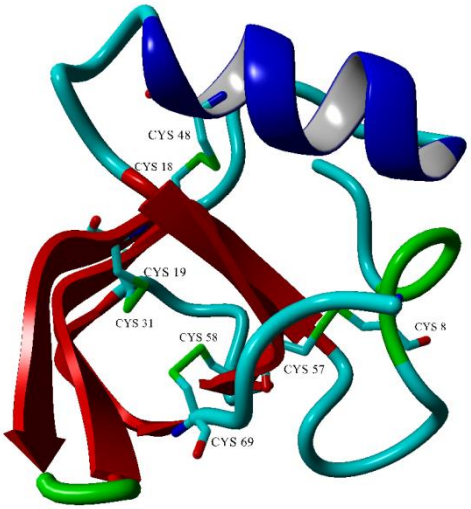

Figure 17. Overall structure of the hydrophobin from *Trichoderma reesei* showing the eight Cys residues forming disulfide bonds (*sticks*).

Improved adsorption of enzymes on hydrophobic surfaces by fusing members of this class of proteins, such as hydrophobins, with polyesterases could enhance the enzymatic activity on synthetic non-biodegradable polyesters, namely PET, as reported in the case of the fusion of the cutinase from *Thermobifida cellulosilytica* (TcC) with hydrophobins from *Trichoderma* [107].

Other approaches have been used to improve the adsorption of polyester-hydrolyzing enzymes to enhance the cleavage of ester bonds on the polymeric surface. In order to mimic natural mechanisms, fusion of the polymer binding module present in the polyhydroxyalkanoate depolymerase from *Alcaligenes faecalis* was used to increase the activity of TcC on poly(1,4-butylene adipate) (PBA) [108] and on PET [109].

Moreover, in order to improve the hydrophobicity of the enzyme for enhanced adsorption, analysis of the 3D structure can help to identify hydrophobic patches, which are hidden underneath superficial domains of enzymes. Deletion of these domains can increase the hydrophobicity of the enzyme, thus reducing the size of the enzyme instead of increasing it, which is important to reduce the production costs in the industry. For instance, an improved polyester hydrolysis activity, with broader range of substrate recognition was achieved by the deletion of an extra domain at the N-terminus of the polyesterase from *Clostridium botulinum* (Cbotu_EstA), which was reported to hydrolyze the biodegradable copolyester PBAT [102] (Fig. 16) thanks to its high thermostability.

Enzymes can be inhibited by released products, which can bind to the structure of enzymes and inhibit the activity. For instance, hydrolysis of the polyester PET can produce terephthalic acid (Ta) and mono-(2-hydrolyethyl) terephthalate (MHET) (Fig. 18), which can act as strong inhibitors of carboxylesterases. In order to overcome this effect in the hydrolysis of PET, site directed mutagenesis was shown to be an approach that reduces the product inhibition in the case of the cutinase from *T. fusca* KW3 [110].

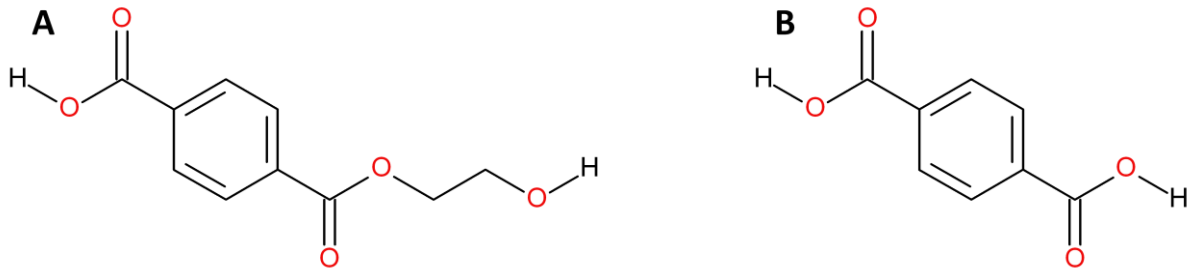

Figure 18. Chemical structure of release products from the hydrolysis of PET. (**A**) Mono-(2-hydrolyethyl) terephthalate (MHET) and (**B**) terephthalic acid (Ta).

The combination of molecular techniques with chemical modifications could lead to designing second generation biocatalysts (e.g. lipases), with enhanced activity or with novel involvement in organic chemistry reactions which are not present in Nature [111].

Improvement of enzymatic hydrolysis of polyamides

The ability of microorganisms to evolve and adapt to specific environments allowed the bacterium *Ideonella sakaiensis* to hydrolyze and assimilate the polyester PET [24]. Although, bacterial species were reported to hydrolyze Nylon oligomers produced by a Nylon factory [112–114], the ability of microorganisms to hydrolyze and assimilate polyamide materials has not been reported.

Amide bonds are formed by the condensation of amine and carboxylic groups. They can be present in proteins and they known as peptide bonds (Fig. 19).

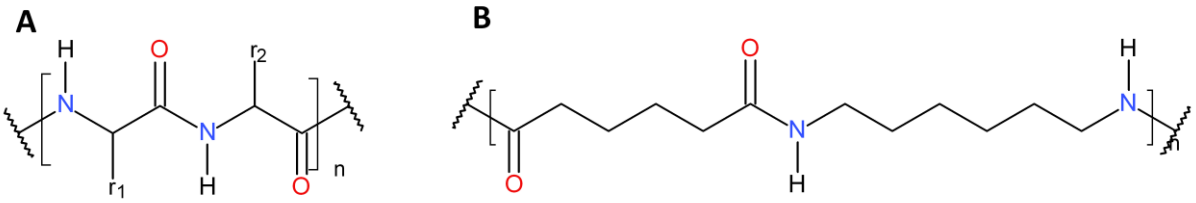

Figure 19. Differences in backbone architectures between (**A**) proteins and (**B**) polyamides (namely Nylon66).

Amidases and proteases possess the ability to hydrolyze these bonds. Structurally, amidases and proteases possess a similar hydrolysis mechanism to carboxylesterases, which leads to the formation of a H-bond between the active site of the enzyme and the carbonyl oxygen of the substrate, which makes the carbonyl carbon of the substrate more electrophilic and vulnerable to attacks by an activated nucleophile [115,116]. However, carboxylesterases are not successfully able to hydrolyze amide bonds, while they are able to hydrolyze different polyesters [43,49,52,67,68,71,89,91,117]. This restriction is due to the electronic conformation of amide bonds, where the lone pair of the scissile nitrogen of the amide bond, which faces antiperiplanar due to stereoelectronic requirements, results in a non-productive conformation in the enzyme active site. In amidases, residues that are present in the active site can form a H-bond for the stabilization of the transition state (TS) complex [118,119]. The stabilization can aid the nitrogen of the amide bond to invert its configuration, during amide bond cleavage, to produce a catalytically competent tetrahedral intermediate (TI) [120,121].

Polyamides, as well as polyesters, possess a hydrophobic surface, on which enzymes, that possess hydrophobic patches on the surface, can adsorb and can start the hydrolysis of the amide bonds. Cutinases, thanks to their hydrophobic patches on the surface [122], can adsorb on the polyamide surface and enhance the hydrolysis of amide bonds, releasing building blocks. For instance, hydrolysis of the polyamide Nylon 6,6 can produce adipic acid (AA) and hexamethylene diamide and their oligomers (Fig. 20).

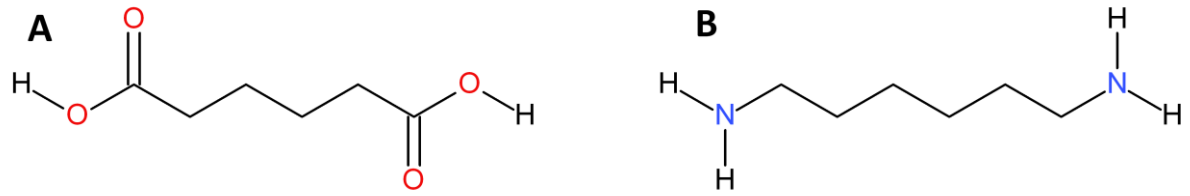

Figure 20. Chemical structure of release products from the hydrolysis of Nylon 6,6. (**A**) Adipic acid and (**B**) Hexamethylene diamine.

The introduction of a H-bond acceptor into the structure of two members of the carboxylesterase family, namely *Candida antarctica* lipase B (CaLB) and *Humicola insolens* cutinase (HiC) has shown the improved ability of these two members to hydrolyze amide-containing substrates [119]. The combination of the presence of the H-bond acceptor and the ability of cutinases to adsorb onto hydrophobic surfaces may improve the activity of these enzymes for polyamide hydrolysis.

Analysis of the 3D structure of the enzyme can lead to improvements in the activity of enzymes in terms of polyester and polyamide hydrolysis. Further study can pave the route for a greener and environmentally friendly approach for both the recycling of building blocks and for the functionalization of polyester and polyamide surfaces to avoid wet chemistry and high energy methods.

2.4 References

[1] A. Radzicka & R. Wolfenden, **1995**, *Science*, 267, 90–3.

[2] R. Patel, **2006**, *B. Curr. Org. Chem.*, 10, 1289–321.

[3] H. Renata et al., **2015**, *Angew*. *Chemie Int. Ed.*, 54, 3351–67.

[4] S. Sen & J. Puskas, **2015**, *Molecules*, 20, 9358–79.

[5] S. Kobayashi & A. Makino, **2009**, *Chem*. *Rev*., 109, 5288–353.

[6] G.M. Guebitz & A. Cavaco-Paulo, **2008**, *Trends Biotechnol.*, 26, 32–8.

[7] A. Pellis et al., **2016**, *Trends Biotechnol.*, 34, 316–28.

[8] L.L. Madison & G.W. Huisman, **1999**, *Microbiol. Mol. Biol. Rev.*, 63, 21–53.

[9] F. Grimaud, **2008**, *J. Exp. Bot.*, 59, 3395–406.

[10] M. Pollard et al., **2008**, *Trends Plant Sci.*, 13, 236–46.

[11] J.K. Smith et al, **1985**, *Science*, (80) 229, 436–42.

[12] M. Mochizuki et al., **1995**, *J. Appl. Polym. Sci.*, 55, 289–96.

[13] Y. Tokiwa et al., **1990**, *ACS Symp. Ser.*, 136–48.

[14] C. Silvestre et al., **2011**, *Prog. Polym. Sci.*, 36, 1766–82.

[15] S.V.N. Vijayendra & T.R. Shamala, **2014**, *Crit. Rev. Biotechnol.*, 34, 338–57.

[16] V. Siracusa et al., **2008**, *Trends Food Sci. Technol.*, 19, 634–43.

[17] J. Pal et al., **2013**, *Mater. Sci. Eng. C.*, 33, 4213–20.

[18] W. Amass et al., **1998**, *Polym. Int.*, 47, 89–44.

[19] R.-J. Mueller, **2006**, *Process Biochem.*, 41, 2124–8.

[20] Y. Tokiwa & T. Suzuki, **1981**, *J. Appl. Polym. Sci.*, 26, 441–8.

[21] E. Marten et al., **2005**, *J. Polymer. Mater.*, 26, 157-66.

[22] W. Zimmermann & S. Billig, **2010**, *Adv. Biochem. Engin./Biotechnol.*, 97–120.

[23] PlasticsEurope, Plastics - the Facts 2014/2015, **2014**.

[24] S. Yoshida et al., **2016**, *Science*, 351, 1196–9.

[25] D. Kint & S. Muñoz-Guerra, **1999**, *Polym. Int.*, 48, 346–52.

[26] R.-J. Müller et al., **2001**, *J. Biotechnol.*, 86, 87–95.

[27] E. Marten et al., **2005**, *Polym. Degrad. Stab.*, 88, 371–81.

[28] U. Witt et al., **1995**, *J. Environ. Polym. Degrad.*, 3, 215–23.

[29] U. Witt et al., **2001**, *Chemosphere*, 44, 289–99.

[30] C. Haas et al., **2015**, *Chem*. *Biochem*. *Eng*. *Q.*, 29, 99–112.

[31] F. Wang & S.Y. Lee, **1997**, *Appl*. *Environ*. *Microbiol*., 63, 3703–6.

[32] M. Smerilli et al., **2015**, *J. Chem. Technol. Biotechnol.*, 90, 648–57.

[33] M. Dusselier et al., **2013**, *Energy Environ*. *Sci.*, 6, 1415.

[34] E. Bugnicourt et al., **2014** *Express Polym*. *Lett*..

[35] M. Jamshidian et al., **2010**, *Compr. Rev. Food Sci. Food Saf.*, 9, 552–71.

[36] A. Pellis et al., **2016**, *J. Biotechnol.*, 235, 47–53.

[37] A. Ortner et al., **2017**, *Green Chem*.

[38] A. Pellis et al., **2015**, *Biotechnol*. *J.*, 10, 1739–49.

[39] Y.-L. Hsieh & L.A. Cram, **1998**, *Text*. *Res*. *J.*, 68, 311–19.
[40] J.X. Li et al., **2007**, *Surf. Coatings Technol.*, 201, 8155–9.
[41] A. Laskarakis et al., **2008**, *Thin Solid Films*, 516, 1443–8.
[42] J.M. Goddard & J.H. Hotchkiss, **2007**, *Prog*. *Polym*. *Sci*., 32, 698–725.
[43] A. Pellis et al., **2016**, *Process Biochem*.
[44] M. Tanahashi et al., **1994**, *J. Appl. Biomater.*, 5, 339–47.
[45] L. Brown et al, **2006**, *Lab Chip*., 6, 66–73.
[46] T. Brueckner et al., **2008**, *J. Polym. Sci. Part A Polym. Chem.*, 46, 6435–43.
[47] S.H. Zeronian & M.J. Collins, **1989**, *Text*. *Prog*., 20, 1–26.
[48] C.-M. Chan et al., **1996**, *Surf*. *Sci*. *Rep*., 24, 1–54.
[49] I. Donelli et al., **2010**, *Polym*. *Degrad*. *Stab*., 95, 1542–50.
[50] I. Donelli et al., **2009**, *Biotechnol. Bioeng.*, 103, 845–56.
[51] S.H. Oh & J.H. Lee **2013** *Biomed*. *Mater*., 8, 14101.
[52] M.A.M.E. Vertommen et al., **2005**, *J. Biotechnol.*, 120, 376–86.
[53] M. Nardini & B.W. Dijkstra, **1999**, *Curr. Opin. Struct. Biol.*, 9, 732–7.
[54] H. Jochens et al., **2011**, *ChemBioChem*., 12, 1508–17.
[55] U.T. Bornscheuer, **2002**, *FEMS Microbiol*. *Rev*., 26, 73–81.
[56] C.D. Anobom et al., **2014**, *Biomed. Res*. *Int*., 684506.
[57] J.D. Schrag & M. Cygler, **1997**, *Methods Enzymol*., 284, 85–107.
[58] A.J. Kotlewska et al., **2011**, *Green Chem*., 13, 2154.
[59] C. Branneby et al., **2002**, *J. Am. Chem. Soc.*, 125(4), 874-5.
[60] T. Kitazume et al., **1986**., *J. Chem. Soc. Chem. Commun.*, 1331.
[61] J.L. Arpigny & K.E. Jaeger, **1999**, *Biochem*. *J.*, 343, 177–83.
[62] M.T. Neves Petersen et al., **2001**, *J. Biotechnol.*, 85, 115–47.
[63] R. Verger, **1997**, *Trends Biotechnol.*, 15, 32–8.
[64] C. Carrasco-Lopez et al., **2009**, *J. Biol. Chem.*, 284, 4365–72.
[65] D. Ribitsch et al., **2012**, *Polymers*, 4, 617–29.
[66] S. Chen et al., **2010**, *J. Mol. Catal. B Enzym.*, 63, 121–7.
[67] E. Herrero Acero et al., **2011**, *Macromolecules*, 44, 4632–40.
[68] D. Ribitsch et al., **2012**, *Biocatal. Biotransfor.*, 30(1), 2-9.
[69] K. Dresler et al., **2006**, *Bioprocess Biosyst*. *Eng*., 29, 169–83.
[70] T. Oeser et al., **2010**, *J. Biotechnol.*, 146, 100–4.
[71] A. Eberl et al., **2009**, *J. Biotechnol.*, 143, 207–12.
[72] S. Kumar & R. Nussinov, **2001**, *Cell. Mol. Life Sci.*, 58, 1216–33.
[73] V. Perz et al., **2016**, *N. Biotechnol.*, 33, 295–304.
[74] A. Biundo et al., **2016**, *Appl*. *Microbiol*. *Biotechnol*., 100, 1753–64.
[75] V. Perz et al., **2016**, *Biotechnol*. *Bioeng*., 113, 1024–34.
[76] M. Dimarogona et al., **2015**, *Biochim*. *Biophys*. *Acta - Gen*. *Subj*., 1850 2308–17.
[77] K. Kasuya et al., *Int. J. Biol. Macromol.*, 33, 221–6.
[78] C. Silva et al., **2011**, *Biotechnol. J.*, 6, 1230–9.
[79] A. Eberl et al., **2008**, *J. Biotechnol.*, 135, 45–51.

[80] F. Kawai et al., **2014**, *Appl. Microbiol. Biotechnol.,* 98, 10053–64.
[81] R. Wei et al., **2014**, *AMB Express*., 4, 44.
[82] N. Sinsereekul et al., **2010**, *Appl*. *Microbiol*. *Biotechnol*., 86, 1775–84.
[83] F. Muroi et al., **2017**, *Polym*. *Degrad*. *Stab*..
[84] C.M. Silva et al., **2005**, *J. Polym. Sci. Part A Polym. Chem.*, 43, 2448–50.
[85] Z. Liu et al., **2009**, *J. Am. Chem. Soc.*, 131, 15711–6.
[86] P.J. Baker et al., **2012**, *Appl. Microbiol. Biotechnol.*, 93, 229–40.
[87] Å.M. Ronkvist et al., **2009**, *Macromolecules*, 42, 6086–97.
[88] Å.M. Ronkvist et al., **2009**, *Macromolecules*, 42, 5128–5138.
[89] A.N. Shirke et al., **2016**, *Appl. Microbiol. Biotechnol.*, 100, 4435–46.
[90] H. Kontkanen et al., **2006**, *Appl*. *Microbiol*. *Biotechnol*., 72, 696–704.
[91] C. Vieille& G.J. Zeikus, **2001**, *Microbiol*. *Mol*. *Biol*. *Rev*., 65, 1–43.
[92] A. Biundo et al., **2016**, *Appl*. *Microbiol*. *Biotechnol*., 100, 1753–64.
[93] V. Perz et al., **2016**, *Biotechnol*. *Bioeng*., 113, 1024–34.
[94] C. Carrasco-López et al., **2009**., *J. Biol. Chem.*, 284, 4365–72.
[95] M.S. Packer & D.R. Liu, **2015**, *Nat. Rev. Genet.*, 16, 379–94.
[96] D.W. Leung et al., **1989**, *Technique*, 1, 11-5.
[97] D.G. Gibson et al., **2009**, *Nat. Methods*, 6, 343–5.
[98] J.A. Wells et al., **1985**, *Gene*, 34, 315–23.
[99] U. Thumarat et al., **2012**, *Appl. Microbiol. Biotechnol.*, 95, 419–30.
[100] R. Araújo et al., **2007**, *J. Biotechnol.*, 128, 849–57.
[101] E. Krieger et al., **2002**, *Proteins*, 47, 393–402.
[102] A. Biundo et al., **2016**, *Biotechnol*. *J*.
[103] J.R. Whiteford & P.D. Spanu, **2002**, *Mol. Plant Pathol.*, 3, 391–400.
[104] H. Kontkanen et al., **2009**, *Appl. Environ. Microbiol.*, 75, 2148-57.
[105] T. Takahashi et al., **2005**, *Mol. Microbiol.*, 57, 1780–96.
[106] L. Espino-Ramme et al., **2013**, *Appl. Environ. Microbiol.*, 79, 4230–8.
[107] D. Ribitsch et al., **2015**, *Appl. Environ. Microbiol.*, 81, 3586–92.
[108] V. Perz et al., **2015**, *Biomacromolecules*, 16, 3889–96.
[109] D. Ribitsch et al., **2013**, *Biomacromolecules*, 14, 1769–76.
[110] R. Wei et al., **2016**, *Biotechnol*. *Bioeng*., 113, 1658–65.
[111] M. Marciello et al., *Catal*. *Sci*. *Technol*., 2, 1531.
[112] I. D. Prijambada et al., **1995**, *Appl. Environ. Microbiol.*, 61, 2020–2.
[113] T. Deguchi et al., **1998**, *Appl. Environ. Microbiol.*, 64, 1366–71.
[114] S. Kakudo et al., **1993**, *Appl. Environ. Microbiol.*, 59, 3978–80.
[115] Ö. D. Ekici et al., **2008**, *Protein Sci.*, 17, 2023–37.
[116] M. A. Phillips and R. J. Fletterick, **1992**, *Curr. Opin. Struct. Biol.*, 2, 713–20.
[117] K. Greimel et al., **2013**, *React. Funct. Polym.*, 73, 1335–39.
[118] P.-O. Syrén, **2013**, *FEBS J.*, 280, 3069–83.

[119] P.-O. Syrén and K. Hult, **2011**, *ChemCatChem*, 3, 853–60.

[120] L. Hedstrom, **2002**, *Chem. Rev.*, 102, 4501–24.

[121] B. Liu et al., **2006** *J. Biol. Chem.*, 2006, **281**, 24024–35.

[122] S. Chen et al., **2013**, *Biotechnol. Adv.*, 31, 1754–67.

[123] A. Wróbel et al., **1978**, *Polymer*, 19, 908-12.

[124] D. Carta et al., **2003**, *Environ. Sci. Pollut. Res. Int.*, 10, 390-4.

3

Characterization of a Poly(butylene adipate-*co*-terephthalate)-Hydrolyzing Lipase from *Pelosinus fermentans*

Abstract

Certain α/β hydrolases have the ability to hydrolyze synthetic polyesters. While their partial hydrolysis has a potential for surface functionalization, complete hydrolysis allows recycling of valuable building blocks. Although knowledge about biodegradation of these materials is important regarding their fate in the environment, it is currently limited to aerobic organisms. A lipase from the anaerobic groundwater organism *Pelosinus fermentans* DSM 17108 (PfL1) was cloned and expressed in *Escherichia coli* BL21-Gold(DE3) and purified from the cell extract. Biochemical characterization with small substrates showed thermoalkalophilic properties (T_{opt}=50 °C, pH_{opt}=7.5), and higher activity towards *para*-nitrophenyl octanoate (12.7 U mg^{-1}) compared to longer and shorter chain length (C14 0.7 U mg^{-1} and C2 4.3 U mg^{-1}, respectively). Crystallization and determination of the 3D structure displayed the presence of a lid structure and a zinc ion surrounded by an extra domain. These properties classify the enzyme into the I.5 lipase family. PfL1 is able

to hydrolyze poly(1,4-butylene adipate-*co*-terephthalate) (PBAT) polymeric substrates. The hydrolysis of PBAT showed the release of small building blocks as detected by liquid chromatography-mass spectrometry (LC-MS). Protein dynamics seem to be involved with lid opening for the hydrolysis of PBAT by PfL1.

3.1 Introduction

Polymers, especially polyesters, are ubiquitously present in our daily life. They can find different applications in various areas, such as tissue engineering [1], textile production [2], and food packaging [3]. Biodegradable polymers entered the market in the 1980s for the application in waste management, food packaging and agriculture. Since then, processes have been developed to increase the production and the properties of biodegradable polyesters.

Microorganisms in landfills where plastic waste is discarded can secrete enzymes able to cleave primarily aliphatic polyesters. However, for many applications aromatic polyesters are used due to their superior properties, like high strength and others [4]. Consequently aromatic/aliphatic copolyesters have been developed with interesting properties yet being biodegradable [5]. PBAT is one of the various aliphatic-aromatic copolyesters present in the market. This material finds application in food packaging (containers and lamination materials) and agricultural equipment (mulch films) [6], because of similar mechanical properties of low density polyethylene (LDPE) [7]. Different studies showed the microbial degradation of this polyester using soil bacteria, where enzymes are expressed for the hydrolysis [8].

Enzymes could play a role both in environmentally friendly processing and recycling of polymers. For polymer functionalization, enzymes can replace harsh chemicals and high energy processes, such as wet chemical and plasma treatment, respectively [9]. In contrast to these processes, enzymes can specifically introduce new functional groups on polymer surfaces without attacking the bulk of the polymer [10]. Conversely, bacterial enzymes can be used for the recycling of polymer building blocks avoiding by-products such as in thermo/chemical hydrolysis processes [11, 12]. Various enzymes have been reported to hydrolyze synthetic polymers, such as polyesters and polyamides [13-16], as previously described for two cutinases from *Thermobifida cellulosilytica* DSM 44535 TcC1 and TcC2 [17], an extracellular polyester hydrolase from *Thermomonospora fusca* [18], and an amidase from *Nocardia farcinica* [19]. Cutinases are grouped together with esterases and lipases in the carboxylesterase class of enzymes (EC 3.1.1). They possess a common catalytic triad consisting of a nucleophile (serine, aspartate or cysteine), a histidine and a catalytic acid (aspartate or glutamate) [20]. The Ser residue of the catalytic triad is usually found in the pentapeptide Gly-X-Ser-X-Gly, on the so called “nucleophile elbow”. In various members of the class EC 3.1.1 the first Gly residue is replaced

with an Ala residue, forming the Ala-X-Ser-X-Gly motif. These proteins show a very close structure called an α/β fold [21, 22]. Most lipases possess an extra domain known as “lid”. This structure can be found in two different positions, closed or open. The open position is visible only when the enzyme can recognize a surface (emulsions or particles), which leads to the mechanism of “interfacial activation”, by which the activity of the enzyme is increased in the presence of an interface, such as for hydrolysis of bulky substrates [23, 24]. This feature allows the enzyme to adsorb onto hydrophobic surfaces including hydrophobic polymers showing higher interfacial activation, as reported by Mateo et al [25]. Other features can improve the thermostability of the enzyme, the presence of a zinc ion, mainly found in the I.5 lipase family.

This study focuses on a new lipase from the anaerobic bacterium *Pelosinus fermentans* DSM 17108 [26, 27] (PfL1) and its application for hydrolysis of PBAT. Apart from the potential of this enzyme for polyester functionalization or recycling, this paper shows for the first time that anaerobic groundwater organisms [28] possess enzymes to hydrolyze polyesters.

3.2 Materials and Methods

Chemicals and Reagents

All chemicals and reagents used in this work were of analytical grade. Buffer components, acrylamide/bis-acrylamide 30% (v v^{-1}) solution, bovine serum albumin (BSA), *para*-nitrophenol (*p*-NP) and *para*-nitrophenyl esters (*p*-NPesters), and formic acid were purchased from Sigma-Aldrich (USA). Water and acetonitrile for mass spectrometric analysis were purchased from LabScan (Poland). LB-agar, dimethyl sulfoxide (DMSO), and ethanol (EtOH) were purchased from MerckMillipore (Germany). Yeast extract and peptone were from Fluka (Germany). PBAT (BASF, Germany), poly(3-hydroxybutyrate-*co*-hydroxyvalerate) (PHBV), gift from Dr. Manfred Zinn at HES-SO Valais/Wallis (Sion, Switzerland), poly(L-lactic acid) (PLA) and poly(ethylene terephthalate) (PET) (Goodfellow, UK) were used as polymeric substrates.

Bacterial Strains, Plasmids and Media

For efficient expression of PfL1, the pET26b(+) vector was used for subcloning of recombinant lipase in *E. coli* XL-10 and expression in *E. coli* BL21-Gold(DE3) (Agilent Technologies, USA), constructing pET26b(+)_*pfl1*. Both strains were grown in LB medium containing 40 µg mL^{-1} kanamycin sulfate (Sigma-Aldrich, USA). Cell density at OD_{600} was determined using a Hach DR3900 spectrophotometer (USA).

Sequencing, Database Searches and Alignments

Analysis of DNA and protein sequences was performed by CLC Main Workbench, version 7.0.3 (Qiagen, Netherlands). DNA sequencing was performed *via* LGC genomics (Germany) with Sanger sequencing.[29] The protein sequence from *Pelosinus fermentans* lipase 1 (PfL1) (protein accession number EIW29778.1, genome accession number AKVN01000044.1, complement 237910 to 239118) was analyzed by Compute pI/Mw (ExPASy, Switzerland) [30]. The resulting gene sequence was optimized against *E. coli* codon usage and purchased by GeneArt® (Life Technologies, USA). Alignment analysis was performed with NCBI-basic local alignment search tool (BLAST) (NCBI, USA) [31]. Multiple alignment analysis was

calculated with Multalin version 5.4.1 (CNRS, France).[32] Phylogenetic analysis was performed with Phylogeny (LIRMM, France).[33, 34] In order to detect the presence of α/β hydrolase fold, Motif Scan (ExPASy, Switzerland) was carried out. To investigate the appropriate lipase subfamily, the sequence was analyzed *via* the Lipase Engineering Database (LED, Germany).[35]

General Recombinant DNA Techniques

All DNA manipulations were performed by standard methods [36]. Digestion of DNA with restriction endonucleases (New England Biolabs, USA) and ligation with DNA Ligation kit, Mighty mix (Takara Bio Inc., Japan), were performed according to the manufacturer's instructions. Plasmid DNA was prepared using PureYield™ Plasmid Miniprep System and PureYield™ Plasmid Midiprep System (Promega GmbH, Germany). Agarose (Sigma-Aldrich, USA) was used to cast agarose gel for DNA electrophoresis. 100 bp and 1 kb DNA ladders (Peqlab, Germany) were used as markers.

Cloning of PfL1

The polymerase chain reaction (PCR) was performed to amplify the optimized gene of PfL1. The primers used were: 5´-GGA ATT CCA TAT GAA TAG CTA TCC GAT TGT G-3´ (forward primer) and 5´-CCG CTC GAG ATT GCT AAT GGT CA-3´ (reverse primer), allowing amplification with fusion of the 6xHis-tag at the C-terminus of the lipase. The restriction enzyme sites are *Nde*I and *Xho*I upstream and downstream of the gene, respectively. The amplification was carried out with Phusion® High-Fidelity DNA Polymerase (New England Biolabs, USA) with the following PCR conditions: an initial denaturation step at 98 °C for 3 min, 30 cycles at 98 °C for 10 sec, annealing at 70 °C for 30 sec, and extension at 72 °C for 35 sec, except for the final extension of 10 min. The PCR product was electrophoresed on a 0.8% (w v^{-1}) agarose gel and purified with a QIAQuick Gel Extraction Kit (Qiagen, Netherlands). The purified product and the pET26b(+) vector were digested, separately, with restriction enzymes *Xho*I and *Nde*I, following the manufacturer's protocol. The reaction was inactivated at 65 °C for 20 min. The digested amplification product was cloned into the linearized vector with DNA Ligation kit, Mighty mix (Takara Bio Inc., Japan). The ligation product was chemically transformed into

E. coli XL-10 competent cells, and screened on LB-agar plate (40 µg mL^{-1} kanamycin). Plasmid DNA was extracted from positive clones and analyzed by restriction enzymes and by sequencing (LGC Genomics, Germany) using the following primers, pET26.F: 5´-GAG CGG ATA ACA ATT CCC CTC TAG AA-3´ and pET26.R: 5´- CAG CTT CCT TTC GGG CTT TGT-3´.

Expression of PfL1 in *E. coli* and Purification by IMAC

The recombinant plasmid was chemically transformed into *E. coli* BL21-Gold(DE3) and plated on LB-agar plate. *E. coli* clones were grown in unbaffled Erlenmeyer flasks containing LB medium on a rotary shaker (160 rpm) at 37 °C. *E. coli* BL21-Gold(DE3) cells were induced with 0.08 mM isopropyl-*β*-D-thiogalactoside (IPTG) (Sigma-Aldrich, USA) at OD_{600} 0.8 for 20 h at 20 °C. Cultures (200 mL) were harvested by centrifugation at 4,000 rpm for 20 min at 4 °C.

For monitoring the protein expression, bacterial cells were harvested by centrifugation and the pellet resuspended with CelLytic™ B Cell Lysis reagent (Sigma-Aldrich, USA) following the manufacturer's protocol. 1 g wet cell pellet was resuspended in 5 mL buffer containing 20 mM $NaH_2PO_4 \cdot 2H_2O$, 500 mM NaCl and 10 mM imidazole, pH 7.4 (buffer A) and sonicated with three times 45 s pulse, with a 30 s pause, 70% duty cycle under ice cooling with BRANSON Digital Sonifier 250 (Branson Ultrasonic Corporation, USA). Cellular debris was removed by centrifugation at 18,000 rpm and 4 °C for 20 min. The supernatant was filtered through a 0.22 µm PES filter and used for purification.

Lipase purification was performed by immobilized metal ion affinity chromatography (IMAC) using HisTrap FF 5-mL columns coupled with ÄKTA purifier 900 (GE Healthcare, UK). For this reason a 6xHis-Tag was fused at the C-terminus of PfL1 through an Ala-Leu-Glu linker, for affinity towards nickel ions present in the column. The column was equilibrated with buffer A. Cell-free extract (50 mL) was loaded onto the column and eluted following the manufacturer's protocol. Fractions were pooled, and concentrated by Vivaspin-20 column with a molecular weight cut-off (MWCO) of 10,000 Da (Sartorius AG, Germany). The buffer was exchanged with 0.1 M Tris-HCl pH 7 by PD-10 desalting columns (GE Healthcare, UK).

Protein Analysis

Protein concentration was measured by Bradford assay [37] using Bio-Rad Protein Assay kit (Bio-Rad, USA). Bovine serum albumin (BSA) was used as protein standard. Sodium dodecyl sulfate-polyacrylamide gel electrophoresis (SDS-PAGE) was performed according to Laemmli [38] using 4% (v v^{-1}) stacking gels and 12% (v v^{-1}) separating gels, and run at 150 V. Prestained protein marker IV (Peqlab, Germany) was used as a molecular mass marker. Proteins were stained with Coomassie method.

The PfL1 intact mass was measured via LC-MS using an Agilent Infinity 1280 ultra high performance liquid chromatography (UHPLC) system coupled to an Agilent quadrupole-time-of-flight (QTOF) 6530 mass spectrometer with an Agilent Jet Stream electrospray ionisation (AJS ESI) source (Agilent Technologies, Waldbronn, Germany) (Supplementary Information, Protein analysis).

Characterization of PfL1

The purified enzyme was characterized using the assay according to Lehner and Verger [39], with slight modifications. The time course of the absorbance was measured at 400 nm for 5 min using a Hitachi U2900 spectrophotometer (Japan). The final assay mixture contained 100 µM substrate (*p*-NPesters in DMSO), 900 µL homogenization buffer (20 mM buffer, 150 mM NaCl, and 0.01% Triton X-100), and 100 µL purified enzyme. A blank was measured using buffer instead of enzyme. The optimal buffer and pH was determined at 25 °C with *para*-nitrophenyl butyrate (*p*-NPB), over a pH range of 6 to 9, using the following buffer systems: sodium phosphate buffer (pH 6 – 8), potassium phosphate buffer (pH 6 – 8), and Tris-HCl buffer (pH 7 – 9), molar extinction coefficient shown (Table S1). In order to determine the optimal temperature, the mixture was incubated with 100 µM *p*-NPB for 15 min at different temperatures in the range of 25 to 85 °C. Various compounds were tested to determine the enhancing or inhibition of the enzymatic activity on *p*-NPB at 25 °C. The substrate specificity was determined with different 100 µM aliphatic chain length *p*-NPesters, ranging from *p*-NPA (acetate), to *p*-NPM (myristate) at the same conditions as above. All experiments were performed in triplicate. One unit of enzyme activity (U) was defined as the amount of enzyme releasing 1 µmol of *p*-NP per min under the given experimental conditions. Specific activity was expressed as U mg^{-1} of protein.

Kinetics of PfL1

The apparent Michaelis-Menten parameters K_m^{app} and k_{cat}^{app} were determined by using *p*-NPB as substrate in the range of concentration of 0.3 to 16 mM at 25 °C in assay mixture containing 100 mM sodium phosphate buffer pH 7.5 [40]. The parameters were calculated by simple weighted non-linear regression of the Michaelis-Menten equation using the SigmaPlot software, version 12.5 (Systat Software Inc).

Enzyme Stability

To investigate the thermal stability in the range of the optimal temperature, the enzyme was incubated for up to 72 h at different temperatures, in the range of 45 to 55 °C. Time points were withdrawn and incubated with 100 µM *para*-nitrophenyl butyrate (*p*-NPB) to measure the residual specific activity.

Synthesis and hydrolysis of PBAT model substrates

In order to elucidate the mechanism of PBAT hydrolysis by PfL1, model substrates were kindly provided by BASF SE (Ludwigshafen, Germany). Hydrolysis experiments with PfL1 were carried out on three different model substrates as described in Perz at al (2015) (DaBTaBDa, TdaBTaBTda, and BaBTaBBA, with B as 1,4-butanediol, Ta as terephthalic acid, Da as decanoic acid, Tda as tetradecanoic acid, and Ba as benzoic acid) (Figure S1).

Purified PfL1 to a final concentration of 0.6 µM was used for the hydrolysis of 6.84 mM PBAT model substrates in 2 mL hydrolysis buffer (0.1 M sodium phosphate buffer pH 7.5). Time points were withdrawn after 24, 48, and 72 h of incubation at 50 °C and 100 rpm. The reaction was stopped by mixing 500 µL of 100% ice-cold methanol to 500 µL of solution and then acidified to pH 4. The enzyme was precipitated and the supernatant was analyzed by LC-MS system consisting of a Dionex Ultimate 3000 pump (Dionex Cooperation, Sunnyvale, USA). The samples were eluted from the column using a non-linear gradient (Table S2). The release products were detected *via* UV absorbance at 241 nm.

Hydrolysis of Polyesters

Hydrolysis of PBAT

In order to test the possible cleavage of PBAT by PfL1, pieces of film of 0.05 mm thickness were cut in pieces of 5 x 10 mm and washed first with a solution of 5 g L^{-1} Triton X-100, with a 100 mM sodium carbonate in the second step and finally with MilliQ water. The washed PBAT films were incubated with 0.6 µM PfL1 in hydrolysis buffer and samples were withdrawn every 24 h for 72 h. The reactions were stopped as above and the supernatants were analyzed by LC-MS to detect the released molecules. The hydrolysis reaction of PBAT was also performed with 10 mg milled substrate.[56] Reactions were incubated at 50 °C and 100 rpm and time points were taken and analyzed by LC-MS, as above. To investigate the ability of commercially available lipase to hydrolyze the polymer, *Candida antarctica* lipase B (CaLB) was used at the same concentration and in the same buffer to identify the release of smaller building blocks out of PBAT after 72 h. The release products were analyzed as described above.

Hydrolysis of Various Polyesters

PfL1 (0.6 µM) was incubated with different polyesters, namely PHBV, PLA, and PET (Figure S2) in a total volume of 2 ml. For PET and PLA films, pieces of 5 x 10 mm (0.05 mm thickness), were incubated with the enzyme for 72 h at 50 °C and 100 rpm in hydrolysis buffer and time points were taken every 24 h. PfL1 was also incubated with 10 mg of PHBV milled and tested as described above for milled PBAT. Reactions with PHBV and PLA were stopped by precipitation with Carrez method [41], and the supernatant was filtered through a 0.22 µm nylon filter. Filtered solutions were analyzed by LC using refrective index detection (Nucleogel Sugars 810 H, Macherey-Nagel, Switzerland, and 1100 Series, Agilent Technologies, CA, respectively) of 300 mm by 7.8 mm and 7 µm particle diameter. Column temperature was kept at 37 °C and 45 °C, respectively. PHBV samples were analyzed by isocratic elution with 5 mM H_2SO_4 for 30 min at 0.45 mL min^{-1}. PLA samples were analyzed as decribed in Pellis et al. (2015). Reactions for the hydrolysis of PET films were stopped and analyzed as described above for PBAT.

Crystal structure determination

Crystallization experiments were performed by the sitting-drop method using a SwissCl Triple Drop Plate from Molecular Dimensions. Different formulations based on commercial crystallization screens were tested including those from Hampton Research (Index), Molecular Dimensions (Morpheus Screen), and Qiagen (PACT). Drops were prepared by mixing 0.5 µL of the protein solution (7.5 mg mL^{-1}) with an equal volume of mother liquor which were pipetted using an ORYX 8 pipetting robot from Douglas Instruments. Crystallization plates were incubated at 20 °C. First crystal clusters were observed after approximately 48 h. Well diffracting crystals of PfL1 were obtained with 0.8 M potassium sodium tartrate tetrahydrate, 0.1 M Tris, pH 8.5 and 0.5% (w v^{-1}) polyethylene glycol monomethyl ether 5000 from the Index Screen.

X-ray diffraction data were collected on beamline BM30A (λ=0.97242 Å) at the European synchrotron radiation facility (ESRF) Grenoble (France). A complete data set was collected to a maximum resolution of 2.5 Å. The crystals were tetragonal (space group $P4_12_12$) with unit-cell parameters a=b=91.8 Å and c=215.9 Å. Data were processed using the X-ray detector software (XDS) package.[42] 5% of the reflections were randomly chosen and set aside for the calculation of R_{free} values [43]. The structure was solved by molecular replacement using the structure of the lipase L1 from *Geobacillus stearothermophilus* (GsL1) (PDB code: 1KU0, sequence identity: 46%). The initial model was built using the mr-Rosetta module of PHENIX yielding two molecules of PfL1 in the asymmetric unit consistent with the calculated Matthews coefficient from CCP4 program suite [44, 45]. Structure rebuilding and refinement were performed using the programs Coot and PHENIX [46]. Clear electron density was observed for the majority of the amino acids except for the 2 C-terminal residues in chain B. Residual density was interpreted as zinc ions and polyethylene glycol (PEG) fragments in both chains. An additional metal binding site was observed in chain B and was modeled to be occupied by a potassium ion, which was a component of the crystallization condition. 31 water molecules were added manually. Non-crystallographic symmetry restraints were applied throughout the refinement. In the later stages two TLS groups (one per chain) were defined and used in the refinement. The final structure was validated using the program *MolProbity* [47]. Detailed statistics pertaining to data processing and structure

refinement are summarized (Table S3). The atomic coordinates and structure factors have been deposited in the Protein Data Bank under the code 5AH0.

Nucleotide Sequence Accession Number.

The nucleotide sequence codon usage optimized for *E. coli* was deposited in the GenBank database via the National Center for Biotechnological Information (NCBI, USA), and the accession number KM377649 was assigned.

3.3 Results

Cloning, Heterologous Expression, and Sequence Analysis of the Lipase from Pelosinus fermentans PfL1.

The DNA sequence of PfL1, on the basis of the genome sequence from *Pelosinus fermentans* DSM 17108 strain R7 ctg4 (NZ_AKVN01000044.1), was optimized against the *E. coli* codon usage and purchased by GeneArt® (Life Technologies, USA). The DNA sequence of PfL1 was already assigned to produce a putative lipase. The obtained PCR product (1,174 bp) was cloned over the *Nde*I/*Xho*I restriction sites into the vector pET26b(+) containing the T7 lac promoter for tight regulation of expression. *Xho*I restriction site was used for fusion of a 6xHis coding sequence at the C-terminus of PfL1.

A BLAST search for the deduced amino acid sequence grouped PfL1 to the α/β hydrolase fold enzymes, revealing high identity to lipases especially from the bacteria *Clostridium novyi* NT (CnL) (YP_879096.1) (53%), *C. botulinum* (CbL) (WP_003356624.1) (55%), *C. tetani* E88 (CtL) (NP_781602.1) (55%), *Bacillus thuringensis* serovar. kurstaki strain HD73 (BtL) (AGE78976.1) (54%), and GsL1 (AAC12257.1) (46%). The catalytic triad formed by Ser129, His372 and Asp330 in PfL1, is conserved within the family. However, the conserved motif of the pentapeptide Gly-X-Ser-X-Gly in serine hydrolases possesses a substitution leading the Ala-X-Ser-X-Gly motif (residues 112 to 116) already found in GsL1 (Figure 1).

A phylogenetic tree was constructed showing the potential evolutionary relationship of PfL1 with other bacterial lipases. Although PfL1 shows special features present in GsL1, the lipase is most similar to lipases from *Clostridium* sp. and least similar to the lipase from *G. stearothermophilus* (Figure S3).

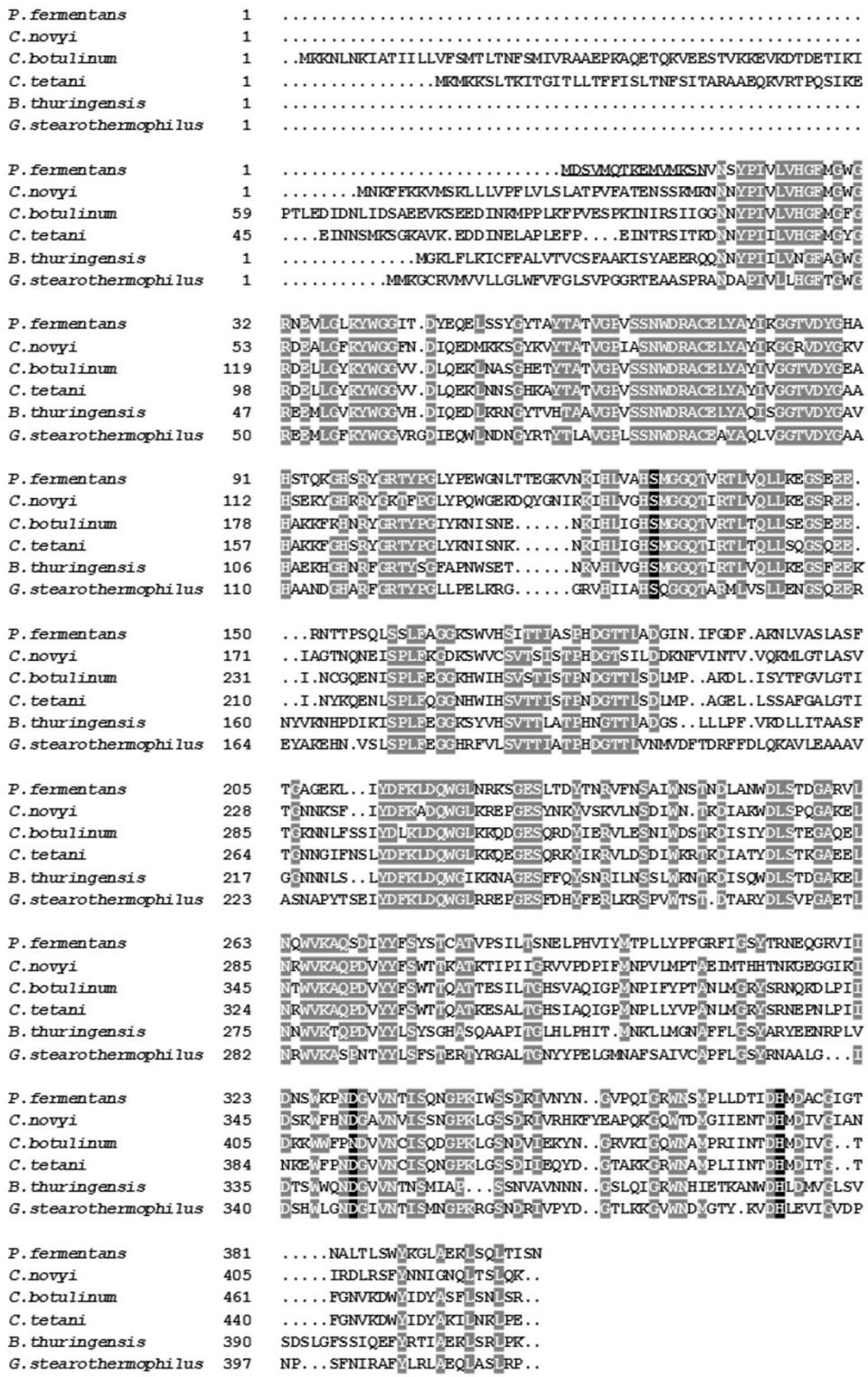

Figure 1. Alignment of the consensus of PfL1 from *P. fermentans* and lipases belonging to the abH15.01 superfamily. Protein sequence alignment was carried out using the Multalin version 5.4.1 (multiple sequence alignment with hierarchical clustering [http://www-archbac.u-psud.fr/]). Accession numbers are as follow: WP_007937185 (PfL1), YP_879096.1 (CnL), WP_003356624.1 (CbL), NP_781602. 1 (CtL), AGE78976.1 (BtL), and AAC12257.1 (GsL1). Identical sequences are marked by *grey background*. Three amino acids belonging to the catalytic triad are marked by *black background*.

According to the LED, PfL1 belongs to the homologous abH15 *Burkholderia* lipases superfamily, subfamily abH15.01 *Staphylococcus aureus* lipase like, also known as lipase family I.5. This lipase family comprises mostly lipases from Gram-positive bacteria showing thermoalkalophilic properties and high molecular weight resulting from an extra domain where a zinc ion is coordinatively bound to the enzyme, which is assumed in GsL1 to cause thermal stability.[48, 49] The amplified DNA sequence of PfL1 contains 52.9% of GC. The lipase was expressed in *E. coli* BL21-Gold(DE3) and the plasmid-carrying cells were induced at 20 °C with 0.08 mM IPTG showing a strong protein band after 20 h of incubation around 40 kDa as revealed by SDS-PAGE analysis of the soluble fraction (Figure 2). The band corresponded well to the calculated mass of 43.9 kDa for the His-tagged lipase. The molecular weight was confirmed by UHPLC-QTOF MS, as described above, revealing a mass of 43922.0 Da (which corresponds to the theoretical value of 23 ppm, Figure S4). The lipase was purified by Immobilized Metal Affinity Chromatography (IMAC) through the 6xHis-tag to high purity (ca. 95%). Approximately 1 to 1.5 mg of protein could be purified from 200 mL bacterial culture.

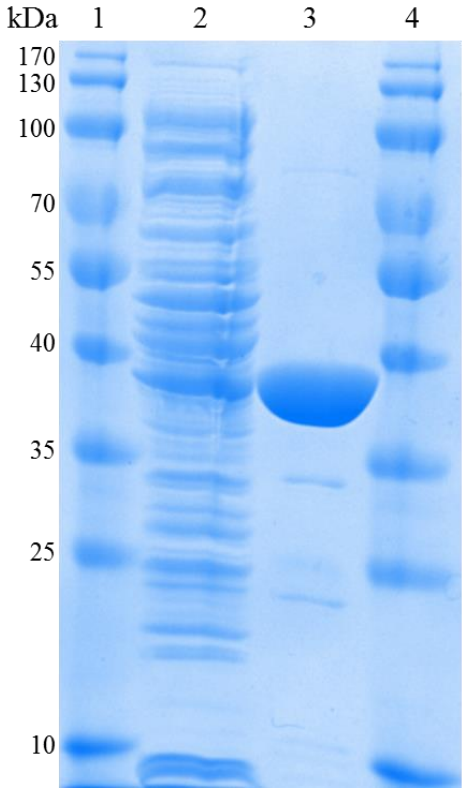

Figure 2. SDS-PAGE analysis (4–12 %) of PfL1 expressed in *E. coli* BL21-Gold(DE3) with 0.08 mM IPTG and purified by IMAC. Samples were taken after 20 h of induction at 20 °C. Lane 1, prestained protein molecular ladder Protein Marker IV (Peqlab, Germany); lane 2, soluble cell fraction; and lane 3, purified PfL1.

Biochemical Characterization and Kinetics of PfL1

The purified PfL1 showed a temperature optimum at 50 °C (Figure S5) and pH optimum at 7.5. PfL1 revealed a half time of 6 h at 45 °C, and the activity strongly decreased with increasing temperatures (data not shown). The substrate specificity was determined on *p*-NPesters with different chain length varying from 2 (*p*-NPA) to 14 carbon atoms (*p*-NPM) (Figure 3). Out of the *p*-NPesters tested, PfL1 revealed higher specificity for shorter acid moieties from C2 to C8 but much less activity for longer chain length.

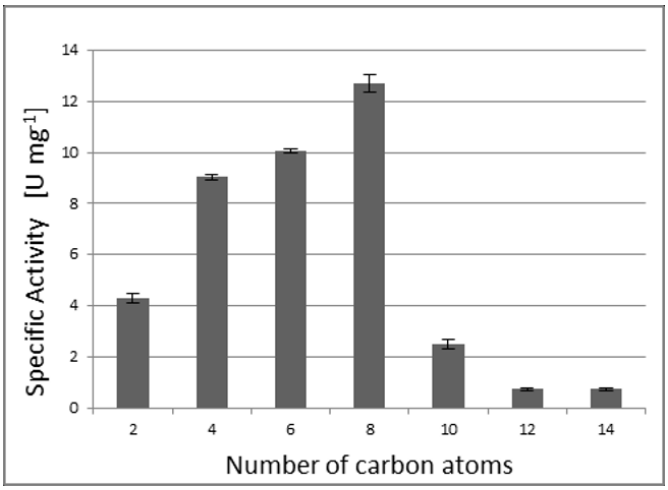

Figure 3. Substrate specificity of PfL1 on *para*-nitrophenyl (*p*-NP)-esters with fatty acids of different chain length (100 µM). Data are mean values of three different measurements, and bars represent the standard deviation.

The effect of metal ions and inhibitors was determined using *p*-NPB as substrate. Out of the metal ions tested, Ca^{2+} was the only one that led to a slightly higher activity (107%) on *p*-NPB when compared to the reference. K^{+}, Co^{2+}, Zn^{2+} and Fe^{3+} strongly reduced activity (< 25% residual activity) whereas Ni^{2+} resulted in a complete loss of activity. Addition of PMSF or EDTA led to inhibition of the enzyme. Similar results were obtained from tests on inhibitors and detergents at different concentrations. The apparent kinetic parameters of the enzyme were determined against the substrate *p*-NPB at pH 7.5. The K_m^{app} was 6.67 mM while the k_{cat}^{app} was 5 s^{-1}. The small substrate was chosen to allow comparison with other hydrolases, *e.g.* CaLB which showed a K_m^{app} of 4.53 mM, more affine to the substrate compared to PfL1, but a k_{cat}^{app} of 0.45 s^{-1}, much smaller than k_{cat}^{app} of the enzyme of interest.

Hydrolysis of polyesters and oligomers

PBAT model substrates

The substrate specificity of PfL1 was studied on PBAT model substrates with terminal benzoic acid (BaBTaBBa) and terminal aliphatic acids with different chain length (DaBTaBDa and TdaBTaBTda). Similar as for *p*-NPesters, the substrate with C10 terminal acid DaBTaBDa was preferably hydrolyzed when compared to the C14 derivative (Figure 4). When the terminal aliphatic acids were replaced by benzoic acid in BaBTaBBa, a lower hydrolysis rate was seen. Generally, the terminal acids seem to be liberated first resulting in higher concentration of BTaB initially which is subsequently hydrolyzed to yield BTa and finally Ta.

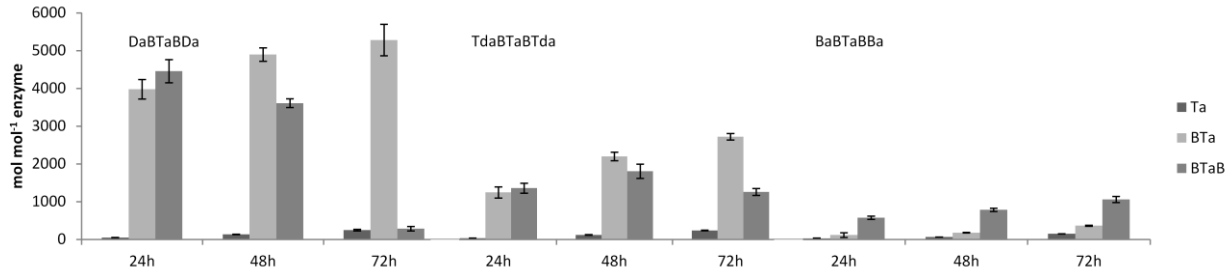

Figure 4. Hydrolysis of PBAT model substrates with different chain length terminal aliphatic acids (C10 DaBTaBDa and C14 TdaBTaBTda) or terminal benzoic acid (BaBTaBBa) by PfL1. Data are mean values of three different measurements, and bars represent the standard deviation

Polyesters

Two different forms of PBAT, milled PBAT and films, were incubated with PfL1 and CaLB. Higher concentration of released products was detected when PfL1 was incubated with the milled form than with the film most likely due to a higher accessible surface area (Figure 5). Nevertheless, the pattern of released molecules was similar. CaLB was only able to release small amount of release products, showing a little higher amount for the milled form of the polymer, as shown for PfL1 with 1000 times more of detected release products (Figure S6).

Hydrolysis of various further polyesters, both of aromatic and/or aliphatic building blocks by PfL1 was studied. However, no hydrolysis was detected of PET, PLA and PHBV.

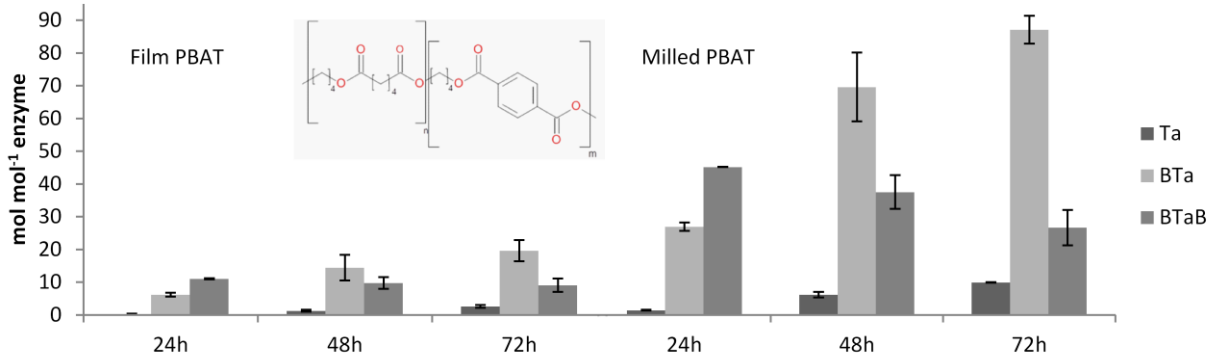

Figure 5. Time course of the hydrolysis of the polymeric PBAT with PfL1. PBAT film and milled. Data are mean values of three different measurements, and bars represent the standard deviation.

Crystal structure of PfL1

The crystal structure of PfL1 was determined using X-ray crystallography at 2.5 Å resolution (Table S3). The crystal was tetragonal (space group $P4_12_12$) and contained two lipase molecules in the asymmetric unit. According to an analysis of intermolecular interactions in the crystal using the PDBePISA server, PfL1 is most likely present as a monomer in solution [50]. The overall structure consists of a central *β*-sheet consisting of seven strands surrounded by *α*-helices indicating that PfL1 belongs to the family of α/β-hydrolases. The two lipase molecules in the asymmetric unit are very similar to each other with a root-mean-square-deviation (RMSD) of 0.13 Å calculated after the superposition of 353 out of 385 Cα-atoms using the program PyMol [51].

Cap domain

Two insertions into the α/β-hydrolase core (residues 178 to 255 inserted after *β*-strand 4 and residues 282 to 328 inserted after *β*-strand 5) form a cap domain and cover the active site and the catalytic triad. A similar cap or lid has been described for GsL1 [52]. This cap prevents access to the active site indicating that PfL1 adopts a closed conformation in the present crystal structure. Hydrolysis of polymeric substrates definitely requires large conformational changes (i.e. opening of the lid) (Figure 6A and Figure 6B).

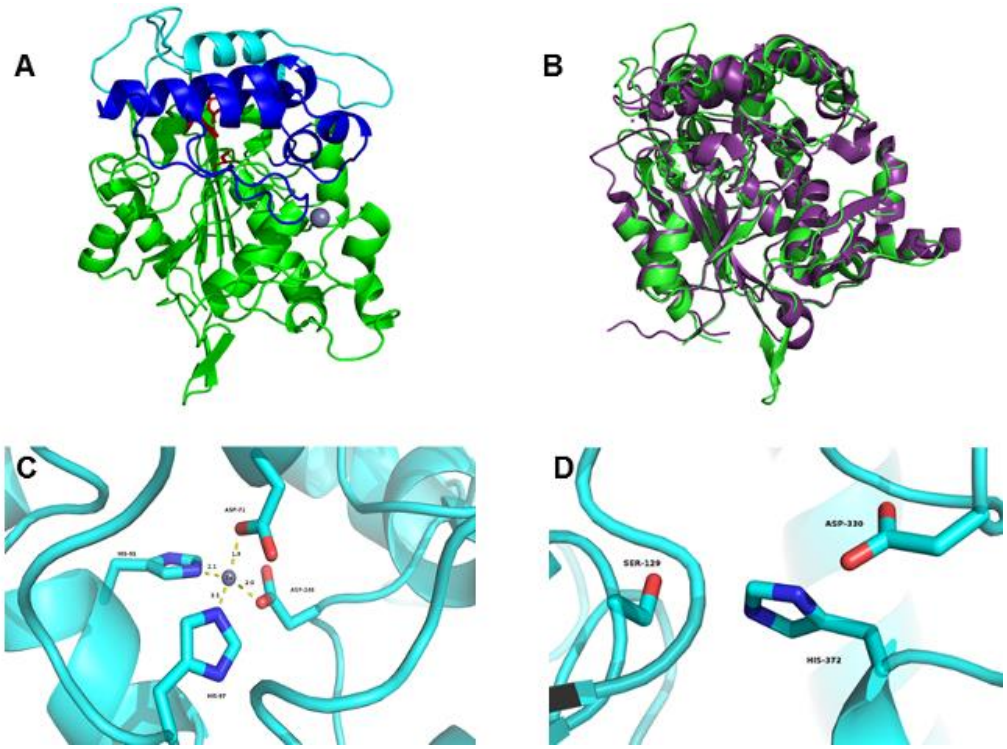

Figure 6. Crystal structure of PfL1. (**A**) Cartoon representation of the overall structure of PfL1 showing the α/β-hydrolase core in green and the two insertions forming the cap domain in cyan and blue. The catalytic triad is shown as stick (red). The zinc ion is shown as a gray sphere. (**B**) Superposition of the structures of PfL1 (green) and of GsL1 (violet; PDB code 1KU0). (**c**) Close-up view of the Zn-binding site. (**d**) Close-up view of the catalytic triad.

Zinc binding site

We identified a metal binding site in PfL1 in which we placed a zinc ion. This ion is tetragonally coordinated by the side chains of Asp71, His91, His97 and Asp248. The metal ligand distances are in range of 1.94 to 2.08 Å consistent with zinc as the central ion (Figure 6C). This zinc binding site is located close to the surface of the enzyme at a distance of 18.5 Å from the catalytic serine residue. A very similar site was observed at the equivalent position in the structure of GsL1. In that case, metal coordination was discussed as one important factor for the thermostability of the protein and was also ascribed an important role in the regulation of the lid opening. Consistent with the latter hypothesis one of the coordinating residue (Asp248) is part of the cap domain described above. As in GsL1 additional interactions exist between residues in the vicinity of the metal binding site and a long loop region in the cap domain [52].

Active site

A BLAST search against the Protein Data Bank (PDB) yielded GsL1 (PDB code: 1KU0) as the most similar hit (46% sequence identity and 49% similarity). Based on the structural alignment with this lipase (RMSD of 0.76 Å for 268 superimposed Cα-atoms), the catalytic triad in PfL1 consists of Ser129, His372 and Asp330 with the serine located on the top of the “nucleophile elbow” (Figure 6D). Most lipases have the conserved Gly-X-Ser-X-Gly motif including the catalytic serine residue. However, some lipases, like GsL1, have a glycine to alanine substitution resulting in the new Ala-X-Ser-X-Gly motif. Also PfL1 has an alanine at this position (Ala127) which points toward the hydrophobic core of the protein and could play a role in the stabilization of the loop conformation. This could contribute to increased thermostability of PfL1 as also discussed for GsL1. The region around the catalytic triad serine is occupied by mostly non-polar residues contributing to the hydrophobicity of the substrate binding site [52].

3.4 Discussion

Different α/β hydrolases have been previously studied for the hydrolysis of polyesters, mostly from microorganisms present in the soil of landfills. However, little is known about polyesterases from anaerobic sources [53, 54] Nonetheless, these materials could be present in biogas plants (food packaging) or end up in other anaerobic environments such as groundwater as microplastics. In this study, the lipase PfL1 from the anaerobic strain *P. fermentans* DSM 17108 present in groundwater[26] was studied. Thermoalkalophic properties of the enzyme and sequence analysis and alignment with other bacterial lipases confirmed that PfL1 belongs to the I.5 lipase family. This family of enzymes possesses unique features, for instance high activity at increased temperature and alkaline environments. These characteristics were shown already in different lipases mainly from thermophilic strains belonging to the *Bacillus* genus. GsL1 was reported to have higher activity at alkaline pH and high temperature (60 – 65 C) [55]. PfL1 showed higher activity at milder conditions (50 °C and pH 7.5), compared to other members of the I.5 lipase family, such as GsL1 and *G. thermocatenulatus* lipase 2 (BTL2). Structural analysis of PfL1 showed properties also existing in GsL1. Both enzymes showed a substitution of the pentapeptide Gly-X-Ser-X-Gly towards the Ala-X-Ser-X-Gly motif. The presence of a zinc ion in different members of the I.5 lipase family was demonstrated for GsL1 to provide thermophilic and folding properties to the enzyme [49]. The extra domain surrounding the metal ion conferred higher molecular weight to the member of the family. As shown for different lipases, in the close structure of PfL1 a lid domain blocks the active site. Dynamics of the enzyme have to be involved in the hydrolysis of bulky substrates, as already reported for the hydrolysis of triacylglycerol by BTL2, where the conformational change of approximately 70 amino acids takes place [56]. Kinetic parameters calculated for PfL1 on small substrates like *p*-NPB showed a lower affinity to the tested substrates and a lower k_{cat} when compared to polyester-hydrolase TcC from *Thermobifida* (k_{cat} of 5 and 195 s^{-1} and K_m of 6.67 and 1.48 mM, respectively) (Gouda et al. 2002). Investigation of the substrate specificity of PfL1 on PBAT model substrate with terminal benzoic acid and terminal aliphatic acids with different chain length indicated a preference for aliphatic acids in general and specifically for the shorter chain-length C10 derivative. Likewise, the C10 fatty acid *p*-NPesters was preferred to the C14 derivative while a shorter chain *p*-NPesters from C2 to C8 were hydrolyzed even faster with an optimum for the C8

derivative. The low activity on the PBAT model substrate with an aromatic terminal acid is in agreement with the fact that PfL1 did not show any activity on PET. PLA and PHBV on the other hand possess side groups which probably sterically prevent entrance to the active site and consequently hydrolysis.

In conclusion, in the present study we have cloned and expressed the first lipase from a risk 1 anaerobic strain which is able to hydrolyze PBAT. At slightly thermoalkalophilic conditions, PfL1 led to the hydrolysis of PBAT model and polymeric substrates. Engineering of the active site by site-directed mutagenesis focused on specific residues has the potential to increase the range of polymeric substrates to be hydrolyzed or could improve the hydrolysis of PBAT itself with applications for monomer recovery or surface functionalization. For industrial application, immobilization of the enzyme would improve the stability, with its reusability. In order to permit the possible sorption of the enzyme on the hydrophobic surface of the polymer, immobilization on magnetic nanoparticles or smart polymers seem to be the most promising immobilization techniques [57-59]. Furthermore, we demonstrate here for the first time that anaerobic ground-water organisms possess enzymes for PBAT degradation.

ACKNOWLEDGEMENT

This project (Antonino Biundo) has received funding from the European Union's Seventh Framework Programme for research, technological development and demonstration under grant agreement N° 289253. This work (Altijana Hromic) has also been supported by the Federal Ministry of Science, Research and Economy (BMWFW), the federal Ministry of Traffic, Innovation and Technology (bmvit), the Styrian Business Promotion Agency SFG, the Standortagentur Tirol and ZIT - Technology Agency of the City of Vienna through the COMET-Funding Program managed by the Austrian Research Promotion Agency FFG. We highly appreciate the support of the beamline staff at the ESRF in Grenoble, France during diffraction data collection. We acknowledge Stephanie Follonier at HES-SO Valais (Sion, Switzerland) for help during the experiments with PHBV.

Conflict of Interest

The authors declare no financial or commercial conflict of interest.

3.5 References

[1] A. Asti & L. Gioglio **2014**, *Int. J. Artif. Organs*, 37(3), 187-205.

[2] J. Pal et al. **2013**, *Mater. Sci. Eng. C Mater. Biol. Appl.*,33(7), 4213-20.

[3] S.V. Vijayendra & T.R. Shamala,**2014**, *Crit. Rev. Biotechnol.*, 34(4), 338-57.

[4] U. Witt et al. **1995**, *J. Environ. Polym. Degrad.*, 3(4), 215-223.

[5] U. Witt et al. **2001**, *Chemosphere*, 44(2), 289-299.

[6] A.A. Shah et al. **2014**, *Appl. Microbiol. Biotechnol.*, 98(8), 3437-47.

[7] T. Kijchavengkul et al. **2008**, *Chemosphere*, 71(5), 942-953.

[8] T. Kijchavengkul et al. **2010**, *Polym. Degrad. Stabil.*, 95(12), 2641-2647.

[9] A. Eberl et al. **2009**, *J. Biotechnol.*, 143(3), 207-212.

[10] M. Vertommen et al. **2005**, *J. Biotechnol.*, 120(4), 376–386.

[11] D. Carta et al. **2003**, *Environ. Sci. Pollut. R.*, 10(6), 390-394.

[12] G.P. Karayannidis et al. **2007**, *Macromol. Mater. Eng.*, 292(2), 128-146.

[13] G.M. Guebitz & A. Cavaco-Paulo **2008**, *Trends Biotechnol.*, 26(1), 32-38.

[14] K. Suzuki et al. **2014**, *Appl. Microbiol. Biotechnol.*, 98(10), 4457-65.

[15] C.A. Murphy et al. **1996**, *Appl. Environ. Microbiol.*, 62(2), 456-60.

[16] S. Yang et al. **2013**, *J. Ind. Microbiol. Biotechnol.*, 40(2), 217-26.

[17] E.H. Acero et al. **2011**, *Macromolecules*, 44, 4632-4640.

[18] M.K. Gouda et al. **2002**, *Biotechnol. Progr.*, 18, 927-934.

[19] S. Heumann et al. **2009**, *Biotechnol. Bioeng.*, 102(4), 1003-11.

[20] H. Jochens et al. **2011**, *Chembiochem*, 12(10), 1508-17.

[21] M. Nardini et al. **1999**, *Curr. Opin. Struct. Biol.* 9(6), 732-7.

[22] H. Wong & M.C. Schotz **2002**, *J. Lipid Res.*, 43(7), 993-9.

[23] A.M. Brzozowski et al. **1991**, *Nature*, 351(6326), 491-4.

[24] R. Verger **1997**, *Trends Biotechnol.*, 15(1), 32-38.

[25] C. Mateo **2007**, *Enzyme Microb. Technol.*, 40(6), 1451–1463.

[26] E.S. Shelobolina et al. **2007**, *Int. J. Syst. Evol. Microbiol.*, 57(Pt 1), 126-35.

[27] S.D. Brown et al. **2012**, *J. Bacteriol.*, 194(18), 5147-8.

[28] W.M. Moe et al. **2012**, *Int. J. Syst. Evol. Microbiol.*, 62(Pt 6), 1369-76.

[29] F. Sanger et al. **1977**, *Proc. Natl. Acad. Sci. U. S. A.*, 74(12), 5463-7.

[30] E. Gasteiger et al. **2003**, *Nucleic Acids Res.*, 31(13), 3784-8.

[31] S.F. Altschul **1990**, *J. Mol. Biol.*, 215(3), 403-10.

[32] F. Corpet **1988**, *Nucleic Acids Res.*, 16(22), 10881-90.

[33] A. Dereeper et al. **2008**, *Nucleic Acids Res.*, 36 465-9.

[34] A. Dereeper et al. **2010**, *BMC Evol. Biol.*, 10, 8.

[35] M. Fischer et al. **2003**, *Nucleic Acids Res.*, 31(1), 319-21.

[36] J.E. Sambrook **1989**, *Cold Spring Harbor*, New York.

[37] M. Bradford **1976**, *Anal. Biochem.*, 72, 248-254.

[38] U.K. Laemmli **1970**, *Nature*, 227, 680-685.

[39] R. Lehner & R. Verger **1997**, *Biochemistry*, 36(7), 1861-8.

[40] D. Ribitsch et al. **2011**, *Biotechnol*. *Prog*., 27.

[41] Y. Sterr et al. **2009**, *Int. J. Food Microbiol.*, 136(1), 75-82.
[42] W. Kabsch **2010**, *Acta Crystallogr. D Biol. Crystallogr.*, 66(Pt 2), 125-32.
[43] G.J. Kleywegt & A.T. Brunger **1996**, *Structure*, 4(8), 897-904.
[44] P.D. Adams et al. **2010**, *Acta Crystallogr. D Biol. Crystallogr.*, 66(Pt 2), 213-21.
[45] M.D. Winn et al. **2011**, *Acta Crystallogr. D Biol. Crystallogr.*, 67(Pt 4), 235-42.
[46] P. Emsley et al. **2010**, *Acta Crystallogr. D*, 66(4), 486-501.
[47] V.B. Chen et al. **2010**, *Acta Crystallogr. D Biol. Crystallogr.*, 66(Pt 1), 12-21.
[48] J.L. Arpigny & K.E. Jaeger **1999**, *Biochem. J.*, 343 (Pt 1), 177-83.
[49] W.C. Choi et al. **2007**, *J. Mol. Biol.*, 372(3), 774-97.
[51] W.L. Delano, The PyMOL Molecular Graphics System, (2002) (2005).
[52] S.T. Jeong et al. **2002**, *J. Biol. Chem.*, 277(19), 17041-7.
[53] A.A. Shah et al. **2013**, Polym. Degrad. Stabil., 98(2), 609-618.
[54] A.A. Shah et al. **2013**, Polym. Degrad. Stabil., 98(12), 2722-2729.
[55] H.K. Kim et al. **1998*,*** *Biosci. Biotechnol. Biochem.*, 62(1), 66-71.
[56] C. Carrasco-Lope et al. **2009**, *J. Biol. Chem.*, 284(7), 4365-72.
[57] S.A. Ansari & Q. Husain **2012**, *Biotechnol. Adv.*, 30(3), 512-23.
[58] R.A. Sheldon **2007**, Adv. Synth. Catal., 349(8-9), 1289-1307.
[59] C. Mateo etal. **2007,** *Biochem. Soc. Trans.*, 35(Pt 6), 1593-601

4

Engineering of the zinc-binding domain of an esterase from *Clostridium botulinum* towards increased activity on polyesters

Abstract

The carboxylesterase from *Clostridium botulinum* (Cbotu_EstA) has been shown to hydrolyze the surface of the polyester poly(butylene adipate-*co*-terephthalate) (PBAT) releasing the monomeric building blocks. Cbotu_EstA contains a zinc ion, tetrahedrally coordinated by two histidine and two aspartic acid residues, which is buried inside an extra domain typical for members of the I.5 lipase family. To elucidate the role of this extra domain with regard to polyester hydrolysis, variants of the zinc-binding domain were constructed and expressed in *E. coli* BL21-Gold(DE3). These enzyme variants were characterized with respect to their specific activity, kinetic parameters and thermostability on soluble substrates as well as on PBAT. All the variants exhibited a similar affinity towards the small substrate *para*-nitrophenyl butyrate (*p*NPB), with K_M values between 0.4 and 1.2 mM, while the catalytic efficiency decreased approximately 1000-fold for the zinc-binding variants and 5-fold for the zinc cavity variants. Moreover, all four variants of the zinc-coordination site (D130L, H150F, H156F, and D302L) showed a loss in thermostability. However, H156F and D302L revealed a drastic loss of thermostability compared to D130L and H150F. Novertheless, compared to Cbotu_EstA, variants carrying substitutions of

amino acids in the zinc-binding domain were able to release up to 10 times more soluble products from the polymeric substrate PBAT. The thermostability at 50 °C was increased in the case of F154Y and W274H, carrying more hydrophilic residues. These data clearly demonstrate the importance of different regions of the zinc-binding domain for the hydrolysis of polyesters like PBAT.

Published in: *Catalysis Science & Technology*, 2017, DOI: 10.1039/C7CY00168A

4.1 Introduction

Polymers are present in our daily life and find applications in different areas ranging from food packaging [1-3] to tissue engineering [4]. Polyesters possess specific properties, such as strength and resistance to chemicals, which make them suitable for a large variety of applications including textile manufacture [5], packaging [6,7] and matrices for microarrays [8]. Most of the polyesters present on the market display a hydrophobic and inert surface. Hence surface modification is used to introduce anchor groups for covalent attachment of functional molecules. Nowadays, wet chemistry and high energy methods, such as alkaline and plasma treatment, are used for the surface functionalization of polyesters. These methods can release by-products directly in wastewater and can negatively affect the material bulk properties which has been shown to lead to a material loss of up to 15 % in case of polyethylene terephthalate (PET) [9,10]. In order to produce a more environmentally friendly method for polyester functionalization, enzymes have been studied for this purpose [11] mainly focusing on PET, the most widely used polyester with an annual global market of 50 million tons [12].

Limited enzymatic polymer hydrolysis results in the generation of functional groups specifically on the surface allowing targeted coupling of functional compounds [13]. On the other hand, complete enzymatic hydrolysis represents a mild and environmentally friendly strategy to recover the polyester building blocks for recycling. Mainly, enzymes belonging to the carboxylesterase superfamily (EC 3.1.1) have shown the ability to hydrolyze polyesters. Among this enzyme family, esterases (EC 3.1.1.1), lipases (EC 3.1.1.3) and cutinases (EC 3.1.1.74) have been reported to be able to act on synthetic aromatic polyesters including PET and the biodegradable polyester poly(butylene adipate-*co*-terephthalate) (PBAT) [14-23]. PBAT has shown complete biodegradability in the presence of soil bacteria [24] but also under anaerobic conditions, as recently reported by our group [19].

Members of the carboxylesterase family share a similar core, named *α/β*-hydrolase fold, which can also be found in other members of serine proteases. A common active site is present in the structure and composed of serine nucleophile, a histidine and an acidic residue, usually an aspartic or a glutamic acid [25,26]. Besides of the common structural features of *α/β*-hydrolases, lipases are well known to contain a lid structure covering the hydrophobic cavity of the active site. The lid structure occurs in two different conformations, namely closed and open. The closed conformation is

predominant in water with a basal activity of the enzyme. By contrast, lid opening occurs at hydrophobic interfaces, termed “interfacial activation” [27,28] and allows access of substrates to the active site.

Lipases are classified into various families [29] while members of the I.5 lipase family show very attractive features. Lipases from this family are thermoalkalophilic showing increased thermostability and higher activities at elevated temperatures due to the presence of an additional domain containing a zinc ion. The existence of this extra domain leads to higher molecular weights (40-45 kDa) compared to classical microbial lipases (ca. 30 kDa). As expected, most of the thermoalkalophilic lipases can be found in thermophiles, where the enzymes need to withstand and work at high temperatures of the respective environments [30].

The lipase L1 from the thermophile *Geobacillus stearothermophilus* was the first lipase reported related to thermostability displaying best activities at temperatures ranging from 50 to 60 °C [31,32]. Thereafter, another thermophile *G. thermocatenulatus* has been reported to produce two lipases, BTL1 and BTL2 [33,34]. After the recombinant expression in *E. coli* and a biochemical characterization of the BTL2 lipase [35], its structure has been determined in an open conformation, showing a dramatic rearrangement, compared to the activation mechanism of lipases lacking a zinc ion, for instance *Candida rugose* lipase, where the lid is formed by an amphiphilic helix which moves from the closed to the open conformation [36]. The zinc-binding domain has been shown to play a crucial role in the rearrangements of the lid structure of the enzyme [37].

The zinc ion-binding domain, present in BTL2, has been found also in enzymes expressed from mesophilic microorganisms. These enzymes are resistant to higher temperatures above the organism’s optimum growth temperatures [38]. Two anaerobic mesophilic bacteria, *Clostridium botulinum* ATCC 3502 and *Pelosinus fermentans* DSM 17108, have been reported by our group to produce lipases with specific features of the I.5 lipase family, namely Cbotu_EstA and PfL1, respectively [19,23]. Cbotu_EstA and PfL1 have also been reported to be able to hydrolyze biodegradable polyesters, especially the copolyester PBAT, which finds application in food packaging and mulch for agriculture. Hydrolysis of the polymer by these two enzymes (Cbotu_EstA and PfL1) has been shown to be possible at 50 °C, which is indicative of the high thermostability of these two enzymes.

In the current study, the 3D structure of the enzyme Cbotu_EstA was analyzed and mutagenesis experiments involving the four residues of the zinc-binding site, two residues present on the surface and three in the core of the zinc-binding domain were carried out. The resulting enzymes were compared in terms of hydrolysis activity on PBAT in order to investigate whether substitutions of residues of the zinc-binding domain could improve the activity on polymeric substrates.

4.2 Materials and methods

Polymers and reagents

Films of poly(1, 4-butylene adipate-*co*-terephthalate) (PBAT), with a thickness of 0.05 mm, were kindly provided by BASF SE (Germany). HPLC-grade methanol, *para*-nitrophenyl butyrate (*p*NPB) and all other analytical-grade chemicals and reagents used in this work were purchased from Sigma (Germany).

General recombinant DNA techniques

All DNA manipulations were performed by standard methods (Sambrook et al. 1989). *Dpn*I restriction enzyme was purchased by New England Biolabs (USA). The PCR was performed in a peqSTAR 96 Universal Gradient (Peqlab Biotechnologie GmbH, Austria) to amplify the gene of Cbotu_EstA using *Pfu* DNA polymerase (Promega, Germany) with dNPTs purchased from MBI Fermentas (Germany). The vector DNA was prepared using Promega miniprep and midiprep kits (USA).

Site-directed mutagenesis of Cbotu_EstA

Site-directed mutagenesis of the gene of Cbotu_EstA was performed by the QuickChange multi site-directed mutagenesis kit (Stratagene) using pET26b(+)_*Cbotu_EstA* as template [19] and megaprimers carrying the specific mutation (Table 1), with the following PCR conditions: for the first step an initial denaturation at 95 °C for 1 min was performed, 4 cycles at 95 °C for 50 s, annealing at 58 °C for 30 s, and extension at 72 °C for 9 min, except for the final extension of 5 min. For the second step of PCR 21 cycles instead of 4 were used. After PCR, the amplified products were transformed into chemically competent *E. coli* XL-10 cells, and subsequently the sequences confirmed by commercial sequencing (LGC Genomics, Germany) [39]. PCR products cloned into the pET26b(+) vector were transformed in *E. coli* BL21-Gold(DE3) for further expression.

Protein expression and purification

Freshly transformed *E. coli* BL21-Gold(DE3) cells were inoculated in 30 mL of Lysogenic broth (LB)-medium containing 40 µg mL^{-1} kanamycin and were cultivated overnight at 37 °C and 150 rpm. The culture was used to inoculate 200 mL of the

same medium to OD_{600}=0.1 and incubated at 37 °C until an OD_{600} = 0.6-0.8 was reached. Induction was carried out for 20 h at 20 °C and 150 rpm using 0.05 mM isopropyl-β-D-thiogalactoside (IPTG) (Sigma, Germany). Cells were harvested by centrifugation at 4000 rpm for 20 min at 4 °C. Purification was carried out by Immobilized Metal Affinity Chromatography (IMAC) using the C-terminal His-Tag as described previously [40].

Protein analysis

Protein concentration was measured by the Bio-Rad Protein Assay Kit (USA) [41] using bovine serum albumin (BSA) as protein standard. Sodium dodecylsulfate - polyacrylamide gel electrophoresis (SDS-PAGE) was performed according to Laemmli, using 4% stacking gel and 15% separating gels. Prestained protein marker IV was purchased from Peqlab (Germany) and used as molecular mass marker. Proteins were stained using Coomassie Brilliant Blue.

Esterase and stability assay

Esterase activity was measured using *para*-nitrophenyl butyrate (*p*NPB) as a substrate [42]. Kinetic constants were determined in 100 mM potassium phosphate buffer pH 7 at 25 °C using substrate concentrations in the range of 0.3 to 16 mM following the release of *p*NP with absorbance at 405 nm (ε_{pNP}=8.31 M^{-1} cm^{-1}) in a Tecan plate reader Infinite M200 PRO (Switzerland). Parameters were calculated by simple weighted non-linear regression of the Michaelis-Menten equation using the SigmaPlot software, version 12.5, using the Michaelis-Menten model (Systat Software Inc, Germany). Determination of thermostability was performed at the optimal temperature of the enzyme of 50 °C [43] for up to 48 h with 0.6 µM enzyme in 100 mM potassium phosphate buffer pH 7. Aliquots were withdrawn at different time points and tested with 100 µM *p*-NPB to measure the residual specific activity, according to Lehner and Verger [44]. One unit of enzyme activity (U) was defined as the amount of enzyme releasing 1 µmol of *p*NP per minute under the given experimental conditions. Specific activity was expressed as U mg^{-1} of protein.

Hydrolysis of Poly(butylene adipate-*co*-terephthalate) films

PBAT films (thickness 0.05 mm) were cut into pieces of 0.5 cm × 1 cm and washed as previously described [40]. Hydrolysis experiments were carried out using 0.6 µM enzyme in 1 mL 0.1 M potassium phosphate buffer pH 7 and addition of one piece of polymer. Hydrolysis of 72 h at 50 °C and 100 rpm was performed. The reactions were stopped by 100% ice cold methanol as previously described [40]. The supernatant containing terephthalic acid (Ta) and mono(4-hydroxybutyl) terephthalate (BTa) as release products was filtered through a 0.45 µm nylon filter and analyzed by high performance liquid chromatography (HPLC) in a Hewlett Packard series 1050 system, equipped with an Agilent Poroschell 120 EC-C18, 3.0 x 5.0 mm, 2.7 µm, using a UHPLC guard column (Agilent Technologies, USA) heated at 40 °C and a fluorescence detector. The samples were eluted from the column using a non-linear gradient with a constant flow rate of 0.85 mL min^{-1}. Concentration of formic acid (A) was kept at 10 %. The gradient started with 10 % methanol (B) and 80 % water (C) at 1 min, 50 % B and 40 % C at 8 min, 90 % B and 0 % C at 10 min. The injection volume of the sample was 10 µL. The release products were detected *via* UV spectroscopy at 241 nm. A calibration curve of the products was used to calculate the amount of release products

.

4.3 Results and discussion

Selection of residues and site-directed mutagenesis of Cbotu_EstA

In our previous work, the crystal structure of Cbotu_EstA was solved to a resolution of 1.2 Å (PDB code: 5AH1) [43]. The structure displayed an extra domain containing a zinc ion and a lid structure and hence the enzyme was grouped to the I.5 lipase family.

It is known that the extra domain surrounding the I.5 lipase family enzymes stabilizes the changes of the lid conformation during interfacial activation at high temperatures. A lipase from *G. thermocatenulatus* (BTL2) was the first member of the I.5 lipase family whose open conformation has been solved [45]. Comparison of the structure of BTL2 and Cbotu_EstA showed the presence of conserved residues involved in the interfacial activation. Two helices, so called α6 and α7, were shown to be important for the opening of the lid to perform interfacial activation.

In the structure of Cbotu_EstA, the residues Asp-302 and Gln-273 (Asp-239 and Gln-211 in BTL2, respectively) form the molecular hinge for the α7 helix. Since Asp-302 is involved in the zinc-binding site, modification of the side chain could change the interaction and the stability of the open conformation of the lid, decreasing the thermostability of the enzyme. The second residue Gln-273, as shown for BTL2, is not involved in the zinc-binding site, but interacts through a H-bond with the Zn-coordinating residue Asp-130 (Asp-62 in BTL2). Four other amino acids act as a molecular hinge for the α6 helix in Cbotu_EstA, namely Lys-270 and Asp-272 (Lys-208 and Asp-210 in BTL2, respectively) forming salt bridges to Glu-93 and Arg-161, respectively, (Glu-24 and Asp-93 in BTL2, respectively) and connecting the lid region to the inner core of the enzyme. In order to destroy the binding in the zinc-coordination site and to investigate their effect on stability, four residues involved in the binding were replaced by side chains without the native functional group, leading to design of the variants D130L, H150F, H156F, and D302L. Furthermore, investigation of the possible effect of the zinc-binding domain on the hydrolysis of the bulky substrate PBAT was focused on residues with a distance cut-off of 4.5 Å from the zinc ion in the extra domain. Substitutions of residues surrounding the metal ion in the cavity of the extra domain produced variants S127A, F154Y, and W274H. The variant S127A might improve the adsorption on the PBAT surface, while the variants F154Y and W274H were designed to have a higher hydrophilicity which could increase the solubility and stability of the enzyme at higher temperatures.

Finally, analysis of the crystal structure of Cbotu_EstA showed a cavity entrance to the zinc-coordination site. The cavity entrance was analyzed in order to understand the possible involvement of this region to the enzymatic hydrolysis of PBAT.

Replacement with Ala residues was carried out to improve the dynamics of the enzyme for PBAT hydrolysis, forming variants W129A and S199A. In the case of the latter variant, the substitution from hydrophilic to hydrophobic residue could also improve adsorption of the enzyme to the hydrophobic polymer surface as previously demonstrated for PET hydrolysis by cutinases carrying hydrophobic binding modules [46,47].

In summary, in order to test the differences in expression, thermostability and hydrolysis of the bulky polymer PBAT, four amino acids of the metal ion binding site, two of the residues at the entrance of the cavity, and three amino acids surrounding the zinc ion were substituted by site-directed mutagenesis. Expression, kinetic parameters, thermostability, and hydrolysis of the polymeric substrate PBAT of the variants were compared to the native Cbotu_EstA (Fig. 1).

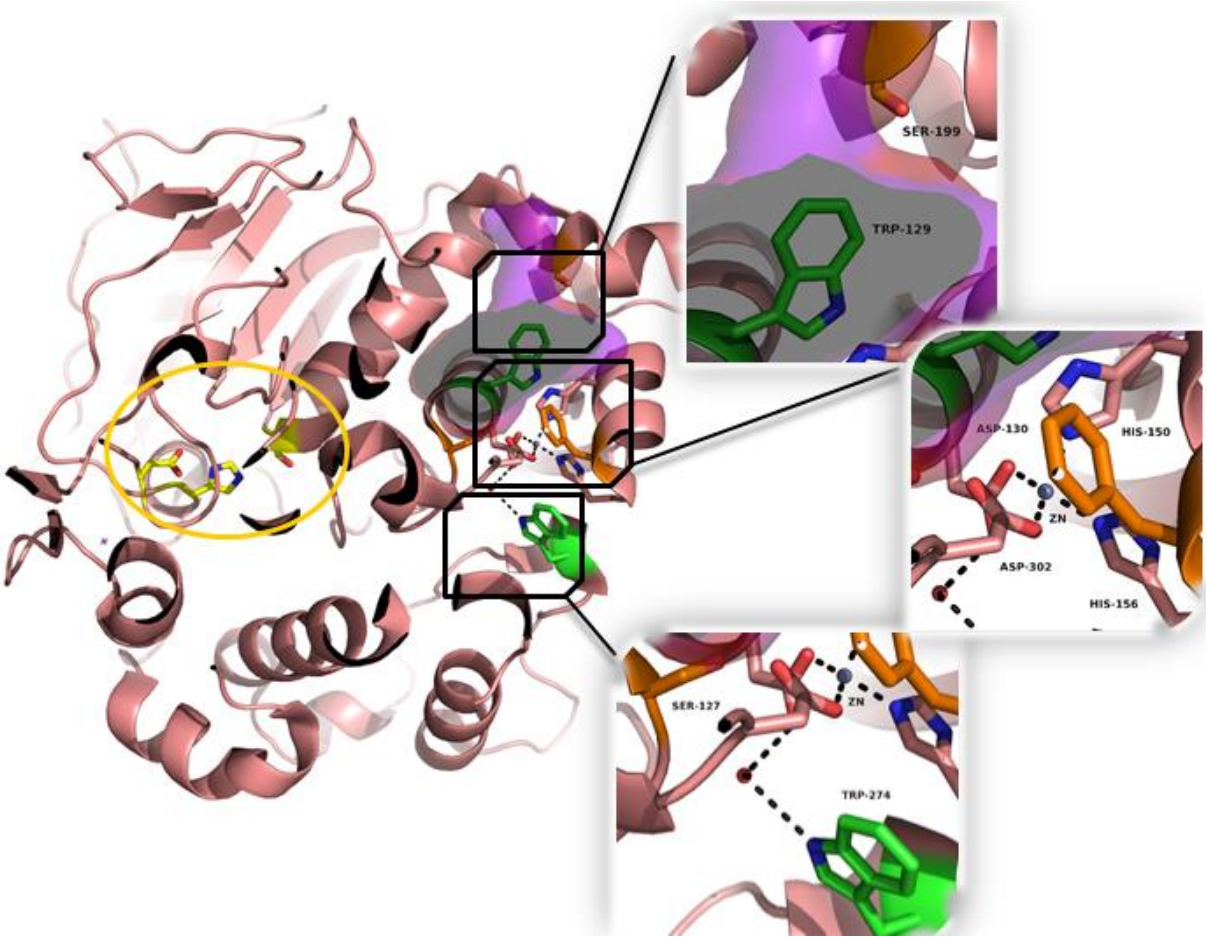

Figure 1. Overview of mutation locations of Cbotu_EstA (PDB-Code 5AH1). Important and mutated residues are highlighted as sticks. The active site (Asp-384, Ser-182, His-426) is marked with a yellow circle. The location of the zinc-binding site and mutated residues are highlighted with black rectangles. A possible entrance to the zinc-binding site is depicted as transparent cavity surface. Mutated residues are labeled in the close-ups. (top: Ser-199, Trp-129; middle: zinc-binding site with Asp-130, Asp-302, His156, His-150; bottom: Ser-127, Trp-274). The representation was created using PyMOL v. 1.7.0 [50].

Expression and purification of Cbotu_EstA variants

Plasmids encoding the Cbotu_EstA variants were transformed into *E. coli* BL21-Gold(DE3) and expressed at 20 °C with 0.05 mM IPTG to avoid the formation of inclusion bodies [48,49]. After 20 h of incubation, the expression level of the variants was analyzed by SDS-PAGE of the cleared cell lysate and cell pellets in comparison to the wild-type enzyme in order to investigate differences in the expression level indicated by the specific protein band at around 55 kDa. The four variants of the zinc-coordination site (D130L, H150F, H156F, and D302L) were expressed in lower amounts, both in the cell-lysate and in the cell pellet (Fig. S1). Obviously, the lack of functional groups weakens the binding between the zinc ion and each of the four residues, leading to lower expression of the proteins compared to the wild-type enzyme, and higher presence of inclusion bodies compared to the soluble fraction.

SDS-PAGE analysis of the zinc cavity variants displayed overexpression of the F154Y variant in a soluble form. The other two variants, S127A and W274H, exhibited a comparable expression level of the soluble form to the wild-type enzyme (Fig. S2) showing no effect of the substitutions on the expression of the enzyme. However, substitution of the two residues placed on the entrance of the cavity of the zinc-binding domain, W129A and S199A, showed different levels of expression (Fig. S2). A decrease of expression both in soluble and insoluble fractions was seen for W129A. In contrast, the S199A variant showed overexpression both as soluble and insoluble forms, confirming the effect of the substitutions on the expression of the enzyme.

In order to purify the proteins from the cell-extract, fusion of the 6xHisTag to the C-terminus of the enzymes was performed for rapid purification. The cell pellet of cultures after 20 h of induction was disrupted by sonication and cleared by centrifugation and filtration to remove cell debris. The soluble protein was purified by IMAC (Fig. S3).

Kinetic parameters with *para*-nitrophenyl butyrate

In order to determine the kinetic parameters of the different variants, the substrate *p*NPB was used in the range of concentration of 0.3-15.75 mM at 25 °C and pH 7 in 0.1 M Tris-HCl (Table 1) and no substrate inhibition in this range of concentrations was shown (Fig. S4). The K_M values for Cbotu_EstA wild-type and variants were in a similar range between 0.45 and 1.16 mM, which suggested that the affinity of substrates to enzymes were not affected dramatically by the single substitutions. A drastic decrease by a factor of 1000 of the turn over number k_{cat} was found for the mutant D130L which carried out a substitution in one of the four residues of the zinc-binding site. Out of all enzymes, Cbotu_EstA wild-type converted the soluble substrate *p*NPB with the highest catalytic efficiency (k_{cat}/K_M).

The variants carrying substitutions both at the entrance of the cavity and in the zinc cavity of Cbotu_EstA did not affect drastically both the turn over number (k_{cat}) and the catalytic efficiency (k_{cat}/K_M), showing values between 3 and 7 times lower for both constants compared to Cbotu_EstA. Only the S199A variant presented a 14-fold decrease in both k_{cat} and k_{cat}/K_M. These results point at the S199 residue as a possible hot spot for the stability of the enzyme.

Table 1. Kinetic parameters of Cbotu_EstA wild-type and variants on the soluble substrate *p*NPB.

	V_{max} [µmol min^{-1} mg^{-1}]	K_M [mM]	k_{cat} [sec^{-1}]	k_{cat}/K_M [sec^{-1} mM^{-1}]
Wild-type	88.10±1.22	1.16±0.13	74.15	63.93
D130L	0.088±0.004	0.455±0.129	0.074	0.163
H150F	0.438±0.009	0.627±0.071	0.369	0.588
H156F	0.065±0.007	0.914±0.427	0.054	0.059
D302L	0.56±0.02	1.128±0.165	0.471	0.416
S127A	23.87±1.38	0.853±0.143	20.09	23.56
W129A	12.52±0.44	0.60±0.12	10.54	17.64
F154Y	13.29±0.82	1.094±0.413	11.18	10.22
S199A	6.19±0.53	1.156±0.441	5.21	4.51
W274H	17.91±0.50	0.782±0.112	15.07	19.26

Thermostability of Cbotu_EstA variants

In order to understand whether the thermostability is affected by different substitutions, 0.6 µM of the enzymes were incubated for up to 48 h at 50 °C. Esterase activity assays were carried out to measure the residual activity [45]. Lower solubility of proteins, especially for unstable proteins, can lead to agglomeration and precipitation. In order to prevent possible agglomeration and precipitation of the enzyme at high concentration, the same concentration of 0.6 µM was used for each variant.

Interestingly, as for the variants of the zinc-coordination site H156F and D302L showed a loss in the thermostability while residual activity of the variants D130L and H150F was only slightly lower compared to Cbotu_EstA (Fig. 2A). This suggests that H156 and/or D302 are necessary to hold zinc while D130 and H150 are less important in this respect. Likewise, it was shown for a zinc-containing ferredoxin that only one histidine residue was necessary for the binding of the zinc ion [51].

As for the zinc cavity variants, substitutions with more hydrophilic amino acids, F154Y and W274H, led to higher thermostability (Fig. 3B). Besides the hydrophilic effect of the His residues, the substitution W274H could cause a stabilization of the zinc ion in place by the aromatic ring, which can form a shield for water molecules as already reported for the Trp-212 in BTL2 [52], conserved in Cbotu_EstA (Trp-274). The latter amino acid is involved in the position of the zinc ion, creating a hurdle for solvent molecules to solvate the zinc ion [52].

Substitutions of residues present at the entrance of the zinc cavity of the zinc-binding domain showed different results (Fig. 2B). W129A exhibited a negative effect on thermostability of the enzyme, which is probably due to a loss of a cation-π interaction from the tryptophan residue [53]. S199A displayed higher residual activity compared to the wild-type enzyme, which showed better stabilization of the structure influencing positively the behavior of the enzyme at high temperatures, maintaining intact the presence of intramolecular bonds.

S127A revealed a decrease of residual activity as shown in Fig. 2B, probably due to the hydrophobic effect. Hydrophobic substitution can lead to intermolecular hydrophobic bonds formation, causing agglomeration and further precipitation of the proteins, or misfolding of the surrounding structure of the protein permitting accommodation of the poorly hydrophilic residues in solvent-free regions as previously reported for the irreversible thermal inactivation of *Bacillus* α-amylases [54].

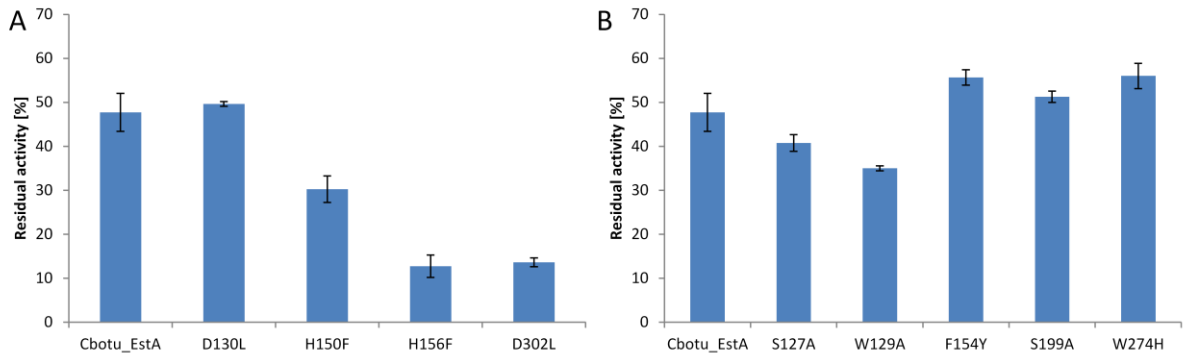

Figure 2. Temperature stability of Cbotu_EstA wild-type and variants analyzed by *p*NPB. (**A**) Zinc-binding variants; (**B**) zinc-cavity variants. The columns represent residual activities of purified enzymes after 48 h incubation at 50 °C.

Hydrolysis of Poly(butylene adipate-*co*-terephthalate) Films

In order to test the ability of the variants of the extra domain of Cbotu_EstA to hydrolyze the polymeric substrate PBAT, following possible enzymatic pattern previously described [43] (Fig. S5), incubation of 0.6 µM of each enzyme at 50 °C for 72 h was performed. As expected, the variants for the zinc-coordination site did not show any release of soluble products (data not shown).

In contrast, although the variants of five different residues of the extra domain of Cbotu_EstA showed a higher product inhibition by terephthalic acid (Ta) (Fig. S6), a larger amount of soluble products Ta and BTa from the polymeric substrate was

released [55-57]. This is interesting since these mutants showed lower V_{max} on the soluble substrate *p*NPB when compared to the wild-type enzyme (Table 1). Hydrophobic residues on the surface of the enzyme could play an important role in the adsorption of the enzyme onto the hydrophobic surface of polymeric substrates as previously shown for PET hydrolysis [46,47,58,59]. The equilibrium between adsorption and solubility of the variants can lead to active and stable variants for polyester surface hydrolysis. In this case all five variants carrying a single substitution showed higher release of soluble products compared to the wild-type enzyme (Fig. 3).

The highest activity on PBAT was measured for the two variants W129A and S199A carrying more hydrophobic residues at the entrance of the cavity of the zinc-binding domain. These results allow a better understanding of the function of the cavity entrance displayed in the crystal structure of Cbotu_EstA in terms of polyester hydrolysis. Hydrolysis of PBAT performed with F154Y and W274H led to high amount of release products, nonetheless lower compared to the two variants, W129A and S199A. S127A showed the least amount of release products which, however, was still higher compared to the Cbotu_EstA wild-type enzyme.

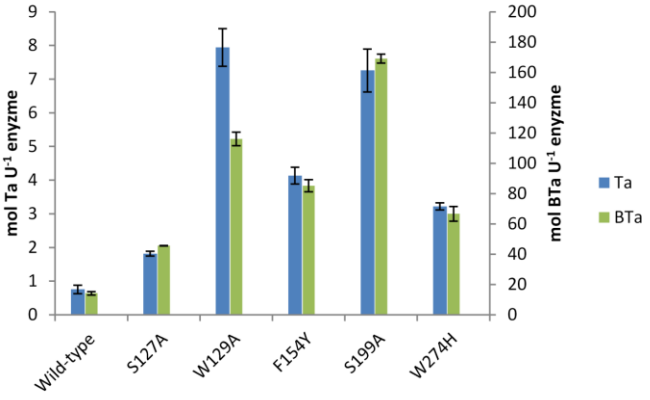

Figure 3. PBAT hydrolysis of Cbotu_EstA variants compared to the wild-type. Released products Ta and BTa are measured. Data are mean value of three different measurements and bars represent standard deviation.

4.4 Conclusions

In this study, we have successfully demonstrated that residues present in the zinc-binding domain of Cbotu_EstA play an important role in the hydrolysis of the polymeric substrate PBAT. Nine different variants were constructed and expressed in *E. coli* to analyze differences in expression, kinetics on the soluble substrate *p*NPB and thermostability at 50 °C. Zinc-coordination variants showed an overall decrease of expression and thermostability. Although, the substitution of each of the four amino acids did not show any release of soluble products after incubation of PBAT, they behaved differently in terms of thermostability and kinetics, probably caused by the dissimilarity in properties of each of the four residues**.** The presence of the cavity entrance was identified at the surface of the zinc-binding domain and led to the production of the variants W129A and S199A. Both variants W129A and S199A showed a decrease in catalytic efficiency on *p*NPB. Although, W129A appeared to be expressed to a lower extend compared to S199A, which showed an improved expression of the soluble form of the enzyme. In terms of thermostability, W129A showed a decreased residual activity while S199A appeared to be more stable at 50 °C. Both variants hydrolyzed the bulky substrate PBAT releasing higher building blocks compared to Cbotu_EstA, whereas S199A showed a 1.6-fold higher activity compared to W129A.

Side chains of residues surrounding the zinc ion, with a distance cut-off of 4.5 Å, were exchanged in order to identify their influence to the metal ion. Either enhanced or similar expression was shown for the variants S127A, F154Y, and W274H. A decrease in the catalytic efficiency of the three variants was observed in a similar range. Improved thermostability of the enzyme was shown in the presence of more hydrophilic residues, as in the case of F154Y and W274H. In case of variant S127A, a decrease of thermostability was measured. Activity on the polymeric substrate PBAT exhibited an increased amount of release of hydrolysis products Ta and BTa for all variants. Both variants from the entrance to the zinc-binding site (W127A and S199A) produced the highest amount of release products. The other three variants (W127A, F154Y, and W274H) displayed a similar release of soluble products from PBAT.

Further analysis of the 3D structure of industrially important enzymes, for instance, members of the I.5 lipase family, can identify possible hot spots which can enhance the activity of the enzyme on “difficult” polymeric substrates. The combination of

mutations in the gene of Cbotu_EstA by site-directed mutagenesis could point to the formation of variants carrying substitutions of residues and/or deletions of specific domain of the enzyme. The combination could probably increase specific properties of the enzyme or introduce new features to upgrade the enzyme for industrial applications.

Acknowledgement

This work has received further support by the Federal Ministry of Science, Research and Economy (BMWFW), the Federal Ministry of Traffic, Innovation and Technology (bmvit), the Styrian Business Promotion Agency SFG, the Standortagentur Tirol, the Government of Lower Austria and ZIT - Technology Agency of the City of Vienna through the COMET-Funding Program managed by the Austrian Research Promotion Agency FFG.

4.5 References

[1] C. Silvestre et al. **2011**, *Prog. Polym. Sci.*, 36, 1766–1782.

[2] S. V. N. Vijayendra and T. R. Shamala **2014**, *Crit. Rev. Biotechnol.*, 34, 338–357.

[3] V. Siracusa et al. **2008**, *Trends Food Sci. Technol.*, 19, 634–643.

[4] A. Asti and L. Gioglio, **2014**, *Int. J. Artif. Organs*, 37, 187–205.

[5] J. Pal et al. **2013**, *Mater. Sci. Eng. C*, 33, 4213–4220.

[6] D. Cava et al. **2006**, *J. Plast. Film Sheeting*, 22, 265–274.

[7] M. D. Sanchez-Garcia et al. **2007**, *J. Plast. Film Sheeting*, 23, 133–148.

[8] D. G. Anderson et al. **2005** *Biomaterials*, 26, 4892–4897.

[9] A. Wróbel et al. **1978**, *Polymer (Guildf).*, 19, 908–912.

[10] D. Carta et al. **2003**, *Environ. Sci. Pollut. Res. Int.*, 10, 390–4.

[11] G. M. Guebitz and A. Cavaco-Paulo, **2008**, *Trends Biotechnol.*, 26, 32–38.

[12] A. Pellis et al. **2016**, *Trends Biotechnol.*, 34, 316–328.

[13] A. Pellis et al. **2015**, *Biotechnol. J.*, 10, 1739–1749.

[14] I. Donelli et al. **2009**, *Biotechnol. Bioeng.*, 103, 845–856.

[15] K. Dresler et al. **2006**, *Bioprocess Biosyst. Eng.*, 29, 169–83.

[16] M. K. Gouda et al. **2002**, *Biotechnol. Prog.*, 18, 927–934.

[17] K. Greimel et al. **2013**, *React. Funct. Polym.*, 73, 1335–1339.

[18] Y.-L. Hsieh and L. A. Cram, **1998**, *Text. Res. J.*, 68, 311–319.

[19] V. Perz et al. **2016**, *Biotechnol. Bioeng.*, 113, 1024–1034.

[20] D. Ribitsch et al. **2012**, *Polymers (Basel).*, 4, 617–629.

[21] A. Biundo et al. **2016** *Biotechnol. J.*,.

[22] E. Herrero Acero et al. **2011**, *Macromolecules*, 44, 4632–4640.

[23] A. Biundo et al. **2016** *Appl. Microbiol. Biotechnol.*, 100, 1753–1764.

[24] T. Kijchavengkul et al. **2008**, *Chemosphere*, 71, 1607–1616.

[25] H. Jochens et al. **2011**, *ChemBioChem*, 12, 1508–1517.

[26] M. Nardini and B. W. Dijkstra, **1999**, *Curr. Opin. Struct. Biol.*, 9, 732–7.

[27] A. M. Brzozowski et al. **1991** *Nature*, 351, 491–4.

[28] R. Verger, **1997**, *Trends Biotechnol.*, 15, 32–38.

[29] J. L. Arpigny and K. E. Jaeger, **1999**, *Biochem. J.*, 343 Pt 1, 177–83.

[30] W.-C. Choi et al. **2005**, *FEBS Lett.*, 579, 3461–6.

[31] S.-T. Jeong et al. **2002**, *J. Biol. Chem.*, 277, 17041–7.

[32] H. K. Kim et al. **1998**, *Biosci. Biotechnol. Biochem.*, 62, 66–71.

[33] C. Schmidt-Dannert et al. **1994**, *Biochim. Biophys. Acta*, 1214, 43–53.

[34] M. L. Rúa et al. **1997**, *J. Biotechnol.*, 56, 89–102.

[35] C. Schmidt-Dannert et al. **1996**, *Biochim. Biophys. Acta*, 1301, 105–14.

[36] S. Brocca et al. **2003**, *Protein Sci.*, 12, 2312–9.

[37] C. Carrasco-López et al. **2009**, *J. Biol. Chem.*, 284, 4365–72.

[38] C. Vieille and G. J. Zeikus, **2001**, *Microbiol. Mol. Biol. Rev.*, 65, 1–43.

[39] F. Sanger et al. **1977**, *Proc. Natl. Acad. Sci. U. S. A.*, 74, 5463–7.

[40] A. Biundo et al. **2016**, *Appl. Microbiol. Biotechnol.*, 100, 1753–64.

[41] M. M. Bradford, **1976**, *Anal. Biochem.*, 72, 248–54.
[42] D. Ribitsch et al. **2011**, *Biotechnol. Prog.*, 27, 951–960.
[43] V. Perz et al. **2016**, *Biotechnol. Bioeng.*, 113, 1024–1034.
[44] R. Lehner and R. Verger, **1997**, *Biochemistry*, 36, 1861–1868.
[45] C. Carrasco-Lopez et al. **2009**, *J. Biol. Chem.*, 284, 4365–4372.
[46] D. Ribitsch et al. **2015**, *Appl. Environ. Microbiol.*, 81, 3586–92.
[47] D. Ribitsch et al. **2013**, *Biomacromolecules*, 14, 1769–1776.
[48] Schrodinger LLC, **2015**.
[49] A. Correa and P. Oppezzo, **2011**, *Biotechnol. J.*, 6, 715–730.
[50] C.-J. Huang et al. **2012**, *J. Ind. Microbiol. Biotechnol.*, 39, 383–399.
[51] K. Kojoh et al **1999**, *Eur. J. Biochem.*, 264, 85–91.
[52] E. Timucin et al. **2016**, *Proteins Struct. Funct. Bioinforma.*, 84, 129–142.
[53] D. A. Dougherty, **1996**, *Science (80-.).*, , 271.
[54] S. J. Tomazic and A. M. Klibanov, **1988**, *J. Biol. Chem.*, 263, 3086–91.
[55] A. Scozzafava et al. **2015**, *J. Enzyme Inhib. Med. Chem.*, 30, 941-6
[56] J. Zhao et al. **2013**, *J. Phys. Chem. B*, 117,14615-24.
[57] M. Hajighasemi et al. **2016**
[58] A. Biundo et al. **2016**, *Biotechnol. J.*
[59] E. Herrero Acero et al. **2013**, *Biotechnol. Bioeng.*, 110, 2581–2590

5

Polyester hydrolysis is enhanced by a truncated esterase: Less is more

Abstract

An esterase from *Clostridium botulinum* (Cbotu_EstA) previously reported to hydrolyze the biodegradable polyester poly(butylene adipate-*co*-terephthalate) was redesigned to improve the hydrolysis of synthetic polyesters. Increased activity was indeed observed for del71Cbotu_EstA variant, which performed activity on the widespread polyester polyethylene terephthalate, which was not able to be attacked by the wild-type enzyme Cbotu_EstA. Analysis of the 3D structure of the enzyme showed that removing 71 residues at the N-terminus of the enzyme exposed a hydrophobic patch on the surface and improved sorption of hydrophobic polyesters concomitantly facilitating the access of the polymer to the active site. These results show a new route for enhancing enzyme activity for hydrolysis and modification of polyesters.

Published in: *Biotechnology Journal*, 2016, DOI: 10.1002/biot.201600450

5.1 Introduction

Polyesters, and especially polyethylene terephthalate (PET) which has an estimated global market of 50 million tons per year [1], are present in our everyday life and they are applied in many different areas [2-4].

It is known that with regard to hydrolyzing polyesters, chemical treatments aimed at producing the desired level of hydrophilicity can lead to a material loss of up to 15% and to changes in bulk properties. Moreover, current recycling strategies only allow partial recovery of the materials. By contrast, enzymatic hydrolysis can both render processing more efficient and environmentally friendly, and allow the recycling of valuable building blocks [5]. Nonetheless, although microbial degradation of PET has recently been reported in Science [6], enzymes are not designed by Nature to hydrolyze synthetic PET.

Hence, site-directed mutagenesis was carried out on esterases to enhance their hydrolytic activity on non-natural synthetic polyesters [7]. These strategies were directed towards increased thermostability [8-10] towards an enlargement of the active site [7, 11], and, more recently, towards tuning of the hydrophobicity of the enzymes surface to improve sorption processes [11, 12]. The latter 'hydrophobicity tuning' was also achieved by fusing the hydrophobic polymer-binding module (PBM) of the polyhydroxyalkanoate depolymerase from *Alcaligenes faecalis* onto a cutinase from *Thermobifida cellulosilytica* which indeed led to faster hydrolysis [13]. Similarly, amphiphilic peptides, specifically fungal hydrophobins from *Aspergillus* sp. and *Trichoderma* sp. were successfully used to enhance enzymatic hydrolysis of polybutylene succinate-*co*-adipate (PBSA) [14] and PET, respectively, both in combination and as fusion constructs with the enzyme [15, 16]. Nevertheless, with respect to the production costs, one would rather "minimize" an enzyme than enlarge the protein with additional domains.

To achieve the above, a polyesterase from *Clostridium botulinum* (Cbotu_EstA) was engineered based on its recently solved 3D structure [23]. The native enzyme showed high activity on the aliphatic/aromatic copolyester polybutylene adipate-*co*-terephthalate (PBAT), but it was considerably less active on polyethylene terephthalate (PET), which is the most widely used polyester. Moreover, the 3D structure of Cbotu_EstA showed two uncommon features. The first feature was an extra domain containing a zinc ion coordinated by four amino acids (D130, H150, H156, and D302) conserved among different lipases. This feature has been reported

in various enzymes of the I.5 lipase family, which shows stability at high temperatures [17, 18]. The second feature, which other esterases lack, was an extended N-terminal domain between the helices of the lid domain that closes the active site, obviously influencing the accessibility of the active site by larger substrates. Moreover, this domain covers two hydrophobic surface patches, which may become accessible upon removal of the domain, thereby improving the sorption of the enzyme on hydrophobic surfaces. In this work, the construction of the truncated gene was performed for the expression of the del71Cbotu_EstA, which carried hydrophobic patches and performs high dynamics during the interaction with the polymeric substrate.

5.2 Materials and methods

Model Construction

A model for del71Cbotu_EstA was generated based on the recently determined crystal structure of Cbotu_EstA (protein accession number: A5I055;PDB code: 5AH1) using YASARA Structure (v. 14.12.2) [19] by deleting the residues (Ile-28 to Ser-71) of the N-terminal part of the structure. Residues Met-1 to Thr-27 are not present in the structure of Cbotu_EstA. The hydrophobic surface representations of Cbotu_EstA and of the truncated model (del71Cbotu_EstA) were calculated and analyzed using VASCo [20, 21] and they were visually compared using the VASCo plug-in and PyMOL [22].

Construction of Truncated Gene-Carrying Vector

The gene encoding for del71Cbotu_EstA optimized for the *Escherichia coli* codon usage was purchased from GeneArt® (Life Technologies, USA). The gene and the vector pET26b(+) were digested separately with *Nde*I and *Hind*III restriction enzymes (New England Biolabs, USA) following the manufacturer's protocol. Digested DNA was recovered after agarose gel electrophoresis with 0.8% agarose and purified using a QIAQuick Gel Extraction Kit (Qiagen, Netherlands). The digested gene was cloned into the linearized vector with DNA Ligation kit, Mighty mix (Takara Bio Inc., Japan), following the manufacturer's protocol. The ligation product was chemically transformed into *E. coli* XL10 competent cells, and screened on LB-agar plate containing 40 µg mL^{-1} kanamycin. PureYield™ Plasmid Miniprep System (Promega GmbH, Germany) was carried out to extract plasmid DNA from the positive clones and further sequencing was performed as customer at LGC genomics (Germany) using the following primers, pET26.F: 5´-GAG CGG ATA ACA ATT CCC CTC TAG AA-3´ and pET26.R: 5´- CAG CTT CCT TTC GGG CTT TGT-3´.

Recombinant Expression of Cbotu_EstA and del71Cbotu_EstA in *E. coli*

Plasmids carrying the gene for Cbotu_EstA and for del71Cbotu_EstA were separately transformed into *E. coli* BL21-Gold(DE3) competent cells and plated on LB-agar plate. Freshly transformed colonies were grown in flasks containing LB-medium supplemented with 40 µg mL^{-1} kanamycin at 37 °C. The enzyme expression

was induced as described by Perz et al. [23] and purity confirmed by Coomassie SDS-PAGE. The wild-type and truncated version of the enzyme were concentrated by Vivaspin-20 column with a molecular weight cut-off (MWCO) of 10,000 Da (Sartorius AG, Germany). The buffer was exchanged with 0.1 M Tris-HCl pH 7 by PD-10 desalting columns (GE Healthcare, UK). Enzymes were quantified by Bradford assay [24] using Bio-Rad Protein Assay kit (Bio-Rad, USA). Bovine serum albumin (BSA) was used as protein standard.

Characterization of Enzymes

In order to test substrate specificities, del71Cbotu_EstA and the wild-type enzyme were incubated at 25 °C with 100 µM aliphatic *para*-nitrophenyl(*p*NP)-esters with chain length ranging from 2 (*p*NP-acetate) to 14 (*p*NP-myristate) carbon atoms. Each substrate was first dissolved in dimethyl sulfoxide (DMSO) and then diluted into a final volume of 200 µL containing homogenization buffer (20 mM potassium phosphate buffer, 150 mM NaCl, 0.01% Triton X-100, pH 7) and 20 µL of enzyme solution. The absorbance of the released *para*-nitrophenol was measured at 405 nm for 5 min using a Tecan plate reader infinite pro M200 (Switzerland). One unit of enzyme activity (U) was defined as the amount of enzyme releasing 1 µmol of *para*-nitrophenol per min under the given experimental conditions. Specific activity was expressed as U mg^{-1} of enzyme. Michaelis-Menten parameters (K_M and k_{cat} and their ratio) were measured for the two forms of the enzyme as already reported [25], using 0.1 M potassium phosphate buffer pH 7 at 25 °C (ε_{pNP} = 8.4375 M^{-1} cm^{-1}). The parameters were calculated by a simple weighted non-linear regression of the Michaelis-Menten equation using the SigmaPlot software, version 12.5 (Systat Software Inc).

Interaction with Polyesters

To investigate hydrolysis of polyesters, del71Cbotu_EstA and the wild-type enzyme were incubated with amorphous PET (Goodfellow, UK). Pieces of 0.5 x 1 cm of the film were first washed at 50 °C and 100 rpm, each step for 30 min, with 5 g L^{-1}Triton X-100, secondly with 100 mM sodium carbonate and finally with MilliQ water. Dried pieces of PET films were incubated with 2 µM of enzymes at 50 °C and 100 rpm for

120 h, in 0.1 M potassium phosphate buffer pH 7. Reactions were stopped by mixing 1:1 ice-cold methanol to the supernatant for protein precipitation and were then acidified to pH 4. After centrifugation at 14,000 x *g* for 15 min at 0 °C, the supernatant was filtered through a 0.45 µm nylon filter and analyzed by high performance liquid chromatography (HPLC) in a Hewlett Packard series 1050 system, equipped with an Agilent Poroshell 120 EC-C18, 30 x 50 mm, 2.7 µm column with a precolumn Poroshell 120 EC-C18, 3.0 x 5.0 mm, 2.7 µm, UHPLC guard column (Agilent Technologies, USA) heated at 40 °C and a fluorescence detector. The samples were eluted from the column using a non-linear gradient with a constant flow rate of 0.75 mL min^{-1}. Concentration of formic acid (A) was always kept at 0.01%. The gradient started with 10% methanol (B) and 80% water (C) at 1 min, 50% B and 40% C at 8 min, 90% B and 0% C at 11 min. The injection volume of the sample was 10 µL. The release products were detected via UV spectroscopy at 241 nm and the amount was calculated through a calibration curve of the compounds. A modified western blotting method was used to investigate adsorption of del71Cbotu_EstA and the wild-type enzyme onto PET. 20 µM of the enzymes were incubated for 2 h at 28 °C and 150 rpm with PET films and then washed by dipping twice into Tris buffered saline supplemented with Tween 20 (TBST) solution (50 mM Tris, 150 mM NaCl, 0.05% Tween-20). The washed PET films were incubated with a solution containing a monoclonal anti-polyhistidine-peroxidase labelled antibody produced in mouse (1:2000 dilution) (Sigma-Aldrich, USA) for 40 min at 20 °C and 100 rpm. The films were washed three times by dipping into TBST solution and then incubated in Lumilight western blotting substrates (Roche, Switzerland). Imaging was carried out using with a ChemiDoc XRS+ with Image Lab software (Bio-Rad, USA). Chemiluminescence was quantified with a Colorlite sph 850 (Colorlite, Germany).

5.3 Results and discussion

Modeling and design of the del71Cbotu_EstA for a better sorption

Enzymes have been studied and used in the hydrolysis of polyesters in order to improve methods for surface modification [1, 2]. Carboxylesterases have shown the ability to hydrolyze different polyesters [12, 26]. Enzymes belonging to the I.5 lipase family have also shown activity on the hydrolysis of polyesters, especially on the biodegradable polyester PBAT [23, 25]. Molecular modeling techniques have been carried out to identify specific hotspot for site-directed mutagenesis to enhance the activity of the enzyme on the polymeric substrate [7, 8]. In order to improve the adsorption of the enzyme to the substrate, fusion of different domains has been carried out which led to an enhancement of the release products from the polymer (Supporting information, Fig. S1) [13]. Surface analysis of Cbotu_EstA revealed a hydrophobic patch, which is hidden under an extra domain of the enzyme, which also covers the lid structure (Fig. 1). Analysis of the 3D structure of the enzyme revealed that the extra domain is formed by the N-terminal 71 amino acids of Cbotu_EstA.

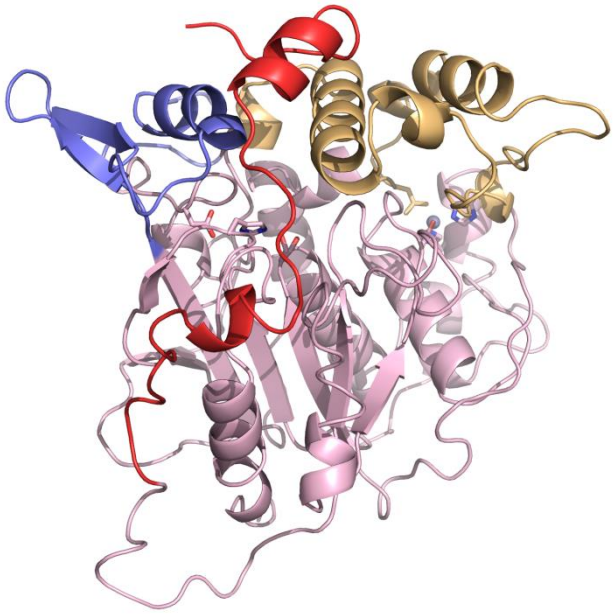

Figure 1. Cartoon representation of the overall structure of Cbotu_EstA showing the α/β-hydrolase core in *pink*, the two insertions forming the lid domains in *purple* and *sand*.The extra N-terminal domain missing in the truncated variant is shown in *red*. The position of the active site is indicated by an *orange* circle. The catalytic triad as well as well as the zinc coordinating residues are drawn as *stick.*

Consequently, a truncated variant of Cbotu_EstA was constructed missing these 71 amino acids in order to increase surface hydrophobicity of the enzyme which might improve the adsorption onto the hydrophobic polymer surface (Fig. 2A) [23].

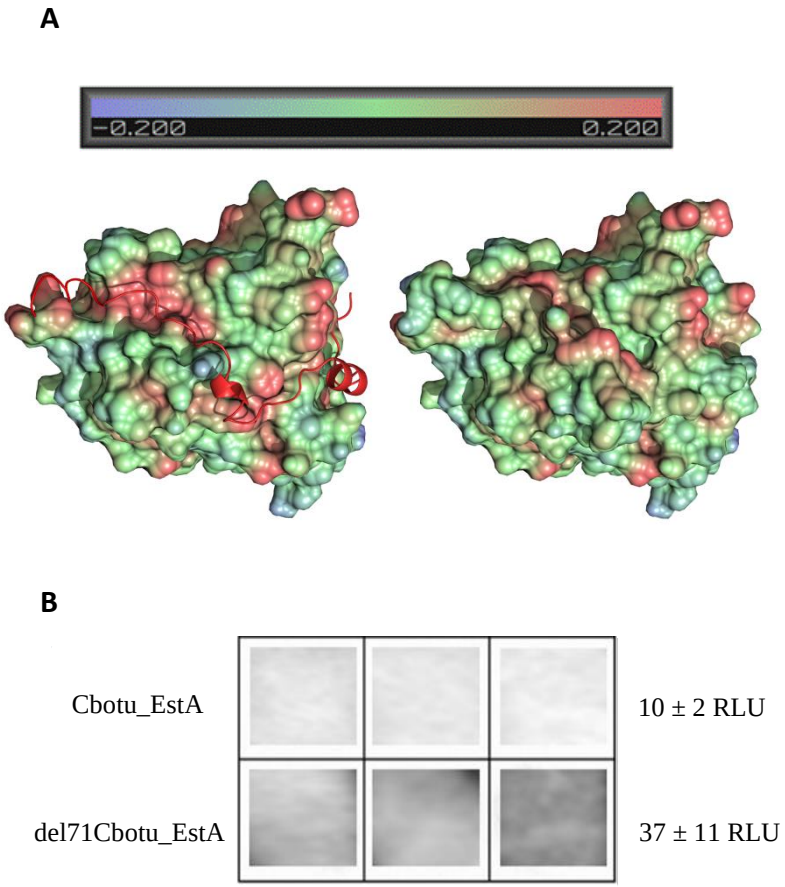

Figure 2. (**A**) Comparison of surface hydrophobicity of del71Cbotu_EstA (left) and Cbotu_EstA (right) calculated from the model and the X-ray crystal structure, respectively. Hydrophilic areas are marked in blue and hydrophobic areas in red. The N-terminal domain which is absent in the del71Cbotu_EstA is shown in red in cartoon representation (bottom). (**B**) Adsorption of Cbotu_EstA (top) and del71Cbotu_EstA (bottom) onto PET film based on chemiluminescence measurements. The adsorbed proteins were detected using a murine monoclonal anti-polyhistidine-peroxidase antibody. RLU: relative light units obtained using a modified western blot protocol [13].

Expression and characterization of Cbotu_EstA and del71Cbotu_EstA

The truncated enzyme (del71Cbotu_EstA) was expressed in *E. coli* and purified by affinity chromatography (Supporting information, Fig. S2). Although del71Cbotu_Est8 showed higher specific activity (21.58 U mg^{-1}) on the soluble substrate *para*-nitrophenyl butyrate (*p*NPB) compared to the native enzyme Cbotu_EstA (2.82 U mg^{-1}), the two enzymes showed similar substrate specificity on *para*-nitrophenyl (*p*NP)-

esters with chain lengths ranging from C2 to C14 except for a more pronounced preference for *p*NP-acetate (Supporting information, Fig. S3). Analysis of the kinetic parameters of Cbotu_EstA and del71Cbotu_EstA, using *p*NPB as substrate in 0.1 M potassium phosphate buffer pH 7 at 25 °C, led to K_M values of 2.48 ± 0.38 mM and 0.64 ± 0.14 mM, respectively, showing almost four times higher affinity of the truncated enzyme towards *p*NPB. The turnover number k_{cat} values were 123 s^{-1} and 194 s^{-1} and V_{max} were 144 ± 7 U mg^{-1} and 268 ± 10 U mg^{-1}, respectively, displaying together an almost two times higher velocity of del71Cbotu_EstA in the hydrolysis of *p*NPB. k_{cat}/K_M values were 50 M^{-1} s^{-1} and 304 M^{-1} s^{-1}, respectively, showing more than six times higher efficiency of the truncated enzyme on the substrate.

Enzyme - Polymer interaction

Finally, the measurement of chemiluminescence indicated enhanced adsorption on PET (Fig. 2B). Indeed, on the polymeric substrate PET, a dramatic improvement of release product was seen, where del71Cbotu_EstA showed more than eight times higher activity compared to the wild-type enzyme in total release-products. When Cbotu_EstA was incubated with PET films it did not show any release of terephthalic acid (Ta), while in the presence of the truncated variant, the Ta level reached almost 0.5 mol mol^{-1} of enzyme. Similar results were found for the oligomer mono-(2-hydroxyethyl) terephthalate (MHET) with almost seven times higher amounts released by del71Cbotu_EstA; this is probably due to the enzyme cleaving faster to the polymer because of improved adsorption (Fig. 3). The data strongly suggest that the improved sorption properties of del71Cbotu_EstA with a more hydrophobic surface also improve the activity of the enzyme.

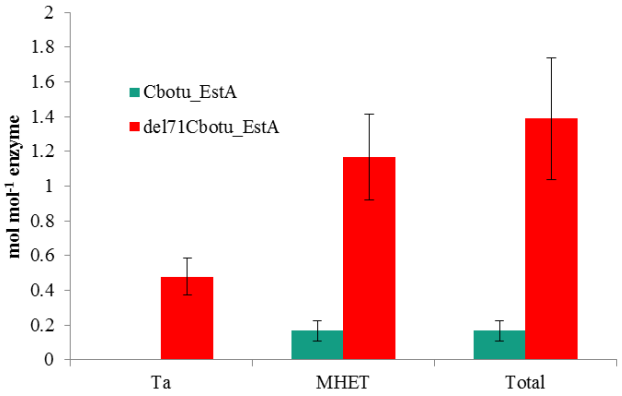

Figure 3. Hydrolysis of PET by esterases from *Clostridium botulinum*. Released Ta (terephthalic acid), MHET (mono-(2-hydroxyethyl) terephthalate) and their sum, after incubation with 2 µM Cbotu_EstA and del71Cbotu_EstA for 120 h at 50 °C. Data are mean values of three independent experiments and the bars represent the respective standard deviations.

5.4 Concluding Remarks

In summary, we have demonstrated that surface engineering is a successful approach to adapt esterases to non-natural polymeric substrates. For instance, the truncation of the N-terminal domain of Cbotu_EstA improved the adsorption of the enzyme on hydrophobic polymeric surfaces and enhanced their hydrolysis releasing higher amount of products compared to the wild-type enzyme. This work suggests another path for enzyme development important for industrial purposes.

Acknowledgement

The authors (Antonino Biundo) acknowledge the European Union's Seventh Framework Programme for research, technological development and demonstration for funding under grant agreement N° 289253, for funding from the European Union's Horizon 2020 research and innovation programme under grant agreement N° 641942. This work (Georg Steinkellner) has received further support by the Federal Ministry of Science, Research and Economy (BMWFW), the Federal Ministry of Traffic, Innovation and Technology (bmvit), the Styrian Business Promotion Agency SFG, the Standortagentur Tirol, the Government of Lower Austria and ZIT - Technology Agency of the City of Vienna through the COMET-Funding Program managed by the Austrian Research Promotion Agency FFG.

Conflict of interest

The authors declare no financial or commercial conflict of interest

5.5 References

[1] A. Pellis et al. **2016**, *Trends Biotechnol., 34*(4), 316-28.

[2] A. Asti & L. Gioglio **2014**, *Int. J. Artif. Organs*, *37*(3), 187-205.

[3] J. Pal et al. **2013**, *Mater*. *Sci. Eng. C. Mater. Biol. Appl., 33*(7), 4213-20.

[4] S. V. Vijayendra & T. R. Shamala **2014**, *Crit. Rev. Biotechnol., 34*(4), 338-57.

[5] A. Cavaco-Paulo & G. M. Guebitz, G. M. **2008**, *Trends Biotechnol*., *26*(1), 32-38.

[6] S. Yoshida et al. **2016**, *Science*, 351(6278), 1196-1199.

[7] R. Araujo et al. **2007**, *J. Biotechnol*., 128(4), 849-857.

[8] C. Roth et al. **2014*,*** *Appl. Microbiol. Biotechnol.,* 98(18), 7815-23.

[9] K. Kitadokoro et al. **2012**, *Polym. Degrad. Stabil.,* 97(5), 771-775.

[10] U. Thumarat et al. **2012**, *Appl. Microbiol. Biotechnol*., 95(2), 419-30.

[11] R. Wei et al.**2016**, *Biotechnol. Bioeng.,* 113(8), 1658-65.

[12] E. Herrero Acero et al. **2013**, *Biotechnol. Bioeng.,* 110(10), 2581-90.

[13] D. Ribitsch et al. **2013**, *Biomacromolecules,* 14, 1769-1776.

[14] T. Takahashi et al. **2005**, *Mol. Microbiol*., 57(6), 1780-1796.

[15] D. Ribitsch et al. **2015**, *Appl. Environ. Microbiol.,* 81(11), 3586-3592.

[16] L. Espino-Rammer et al. **2013**, *Appl. Environ. Microbiol.,* 79(14), 4230-8.

[17] W. Choi et al. **2005**, *FEBS Lett.*, 579(16), 3461-6.

[18] S. T. Jeong et al. **2002**, *J. Biol. Chem.,* 277(19), 17041-7.

[19] E. Krieger et al. **2002**, *Proteins: Struct., Funct., Bioinf.,* 47(3), 393-402.

[20] G. Steinkellner et al. **2009**, *BMC Bioinformatics,* 10, 32.

[21] M. F. Sanner et al. **1996**, *Biopolymers*, 38(3), 305-320.

[22] L. L. C. Schrödinger, The PyMOL Molecular Graphics System, Version~1.41. 2011.

[23] V. Perz et al. **2016**, *Biotechnol. Bioeng.,* 113(5), 1024-34.

[24] M. Bradford **1976**, *Anal. Biochem.*, 72, 248-254.

[25] A. Biundo et al. **2016**, *Appl. Microbiol. Biotechnol.*, 100(4),1753-1764.

[26] A. Pellis et al. **2015**, *Biotechnol. J.*, 10, 1739-1749.

6

Nylonidases by Redesign of Water Networks

Abstract

Recalcitrance of plastics like Nylon and other polyamides contributes to environmental problems (e.g. microplastics in oceans) and restricts possibilities for recycling. The fact that hitherto discovered amidases (EC 3.5.1. and 3.5.2.) only show no, or low, activity on long-chain polyamides currently obstructs biotechnological-assisted depolymerization of man-made materials. To overcome this major bottleneck, we capitalized on enzyme engineering to afford a reallocated water network adapted to synthetic polyamide backbones in the polyester-hydrolyzing biocatalysts *Humicola insolens* cutinase (HiC) and *Thermobifida cellulosilytica* cutinase 1 (TcC). Using this novel concept enabled efficient transition state stabilization for hydrolysis of the industrial polymer Nylon 6,6. Specifically, the presence of a favorable water-molecule network in a double variant of HiC resulted in abolished PET-activity and high Nylonidase activity, as confirmed by increased surface hydrophilicity, mass spectrometry and FTIR. Thus we envision that Nylonidases will find important applications as versatile and specific biocatalysts in material science, circular fashion and biotechnology.

Submitted in: *Science*

Polymers are extensively used in packaging, in the manufacturing of vehicles, airplanes and advanced medicinal and electronic devices and are indispensable for our everyday life. Although the proportion of bio-based monomers in the annual 300 Megaton production of synthetic polymers is increasing (*1*) (currently representing 1%), many man-made polymers are non-biodegradable (*2*). Disposed polymers get fragmented through abiotic mechanisms into smaller and inert pieces (≤ 1 mm) referred to as microplastics (*3*). As only 1-2% of all plastics are recycled in Europe and in the US (*4*) and up to 43% of the plastic used worldwide is disposed of in landfills (*5*), the impact of post-consumer polymer waste on our environment and health can be tremendous (*6*, *7*). Innovative approaches to valorize this source of secondary raw material and minimize our impact (*6*, *7*) on the environment are urgently needed. One approach consists of capitalizing on mild enzymatic hydrolysis to depolymerize macromolecular architectures (*8*). Due to the high specificity of enzymes this would allow for step-wise recovery of pure hydrolysis products even from polymer mixtures or composite materials.

Enzymatic hydrolysis of the surface of polymers by extracellular hydrolases was reported to be the first step of the biotic degradation of polyesters by microorganisms (*8*). Thus, several studies have focused on the enzymatic hydrolysis of polyesters using proteases and members of the *α/β*-hydrolase superfamily, including cutinases and lipases, in order to increase wettability and dye staining, and to decrease pilling and hydrophobicity (*9*–*11*). Recently, it was reported that the bacterium *Ideonella sakaiensis* is able to degrade and assimilate the polyester polyethylene terephthalate (PET) (*12*). In contrast to ester bonds, due to resonance stabilization, chemical hydrolysis of an amide bond proceeds three orders of magnitude slower than that of an ester bond (*13*). Moreover, even if amide and peptide bonds share the same features, amide bonds in polyamides (PA) are separated by extended carbon chains (fig. S1), which permit the formation of a more rigid and crystalline structure. Thus, mild enzymatic depolymerization of inert polyamide backbones is challenging. Although some enzymes have been reported to hydrolyze Nylon oligomers which are by-products of Nylon production (*15*–*17*), efficient enzymatic hydrolysis of polyamides seems to be considerably more difficult (*18*). Since Nylon is used in fashion and as light-weight metal-replacements it has been found to significantly contribute (*3*) to the ~10-20 Megatons of plastics that end up in the oceans each year (*5*). Therefore, “nylonidases” would constitute one important class of designer enzymes allowing

recycling of wastes to valuable building blocks. To meet this formidable challenge, enzyme engineering and design tools are greatly needed as evolution did not yet have had sufficient time to develop enzymes efficient towards hydrolysis of Nylon.

Protein design is the key for depolymerization by biocatalysts

Enlarging the cavity of the active site of biocatalysts that hydrolyze natural polyesters like cutin, for a better fitting of the polymer chain, is a common design method to improve enzymatic activity on bulky, insoluble hydrophobic substrates (*19*, *20*). Structural analysis is used to identify specific residues, which when replaced by enzyme engineering, can lead to improved affinity and accelerated biocatalysis (*21*). In this study, we developed a novel approach for which a water network in the enzyme is adapted to the synthetic polymer to enable specific and catalytically favorable interactions. With their solvent exposed active site, we reasoned that cutinases would constitute suitable starting templates to achieve optimized transition state (TS) stabilization by water-restructuring mutations (*22*) to afford polyamide plastic hydrolysis. Cutinases are extracellular serine hydrolases produced by bacteria and fungi to attack the plant cuticle and especially to degrade the natural polyester cutin (*23*, *24*). Cutinases and lipases have been extensively analyzed in order to increase their activity on bulky substrates (*25*, *26*). The ability of cutinases to adsorb onto hydrophobic surfaces has been widely used to hydrolyze biodegradable and non-biodegradable polyesters (*27*, *28*), such as poly(lactic acid) (PLA) and PET, respectively, which results in surface functionalization (*29*, *30*). However, introducing the missing key hydrogen bond acceptor in (poly)esterases, required for facilitated nitrogen inversion (*31*), and thus efficient (poly)amidase activity, by traditional enzyme engineering constitutes a bottleneck (*32*). Thus, herein we hypothesized that our alternative enzyme design strategy centered on redesigning a water network in the enzyme active site to afford efficient transition state stabilization would be favorable (*33*) to unlock the chemistry and spatial constraints dictated by protein side chains (*34*). Nylon 6 (fig. S1B, left) forms intermolecular H-bonds which are longer and therefore weaker, while Nylon 6,6 (fig. S1B, right) contains short H-bonds which yield a strong and dense molecular architecture with a high melting temperature (255-265 °C in comparison with 210-220 °C for Nylon 6). Nylon 6,6 thus represents an excellent model system of a “tough” man-made polymer. We aimed for introducing

Nylon 6,6 hydrolytic activity (herein referred to as “nylonidase” activity), in two model cutinases, namely *Humicola insolens* cutinase (HiC) and cutinase 1 from *Thermobifida cellulosilytica* (TcC, formerly known as TcC) (*27*, *28*). In order to identify “hot-spot” positions that could be important in dictating interactions between water and the transition state (TS), molecular dynamics (MD) simulations were performed using 3PA 6,6 as model substrate (*i.e.* representing an oligomer of Nylon 6,6, fig. 1C). The second tetrahedral intermediate formed during acylation represented the TS for nitrogen inversion (*31*). We hypothesized that de-shielding the protein backbone to afford enhanced polarity and reduced steric hindrance at identified key sites (fig. S2) would be beneficial in providing enhanced water access of “spectator” water molecules (i.e. non-nucleophilic) to the TS, as previously discussed in the context of protein unfolding (*18*). Thus, the impact of a small set of water-restructuring mutations (TcC I179A/N/Q, HiC I167Q, HiC L64H/I167Q, table S2) on catalysis was evaluated *in silico* and experimentally.

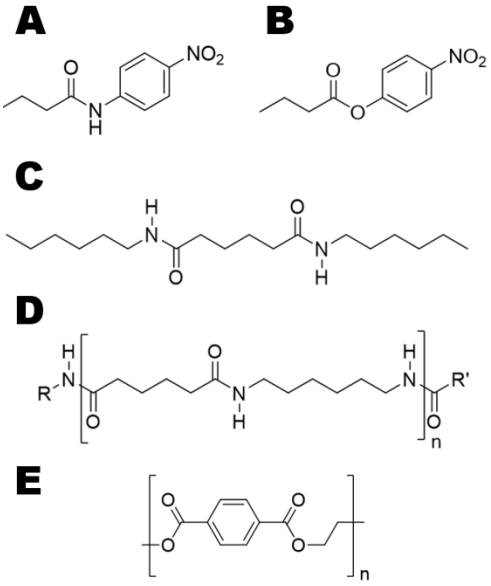

Fig. 1. Chemical structures of the investigated molecules used to study transformation of polyesterases into polyamidases. Substrates ranged from a small aliphatic amide (**A,** *p*-nitrobutyranilide), ester (**B**, *p*-nitrophenyl butyrate) and a representative amide oligomer (**C**, N^1,N^6-dihexyladipamide (3PA 6,6)) to model polyamides (**D**, polyhexamethylene adipamide (Nylon 6,6)) and polyesters (**E**, polyethylene terephthalate (PET)).

The expression of the corresponding codon-optimized genes in *Escherichia coli* BL21-Gold(DE3) was first assayed in shake flasks revealing that TcC wild type and

variants were expressed in high amounts (fig. 2A). In contrast, HiC wild type and designed variants did not show overexpression notwithstanding codon optimization and thus expression by fed-batch bioreactors was required to reach sufficient amounts of enzyme to be used for downstream processing (fig. 2A). Initial experimental analysis on the selected small aliphatic substrates revealed a general trend: variants targeted for redesigned water networks (fig. S2) displayed enhanced specificity for amides and decreased specificity for esters (fig. 2B). The most prominent effect was observed for HiC L64H/I167Q that showed increased catalytic efficiency towards *p*NBA (5-fold increase in k_{cat}/K_M) and a significant decrease in esterase activity (13-fold) as compared to that of wild-type HiC, which together resulted in a 66-fold change in relative reaction specificity in favor of amide bond hydrolysis. For TcC, only variant I179Q displayed a higher catalytic efficiency for amide bond hydrolysis as compared to that of wild-type (fig. 2B).

A

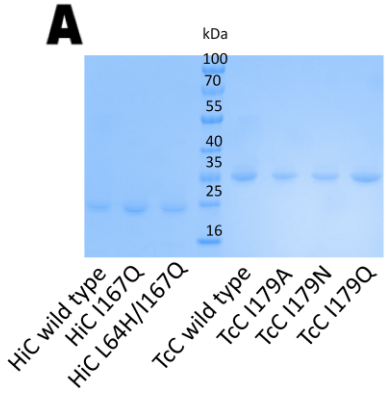

B

Substrate	*p*NPB	*p*NBA	Relative reaction specificity
kinetic parameter unit	k_{cat}/K_M (s^{-1} mM^{-1})	k_{cat}/K_M (s^{-1} mM^{-1} * 10^3)	(k_{cat}/K_M, amide/k_{cat}/K_M, ester)
***H. insolens* cutinase**			
HiC wild type	141.8	0.2	1
HiC I167Q	102.0	0.6	4.2
HiC L64H/I167Q	10.8	1.0	65.7
***T. cellulosilytica* cutinase**			
TcC wild type	22.46	0.06	1
TcC I179A	3.93	0.06	5.7
TcC I179N	2.13	0.07	12.3
TcC I179Q	4.87	0.5	38.4

Fig. 2. Biochemical analysis of HiC and TcC wild type and variants with enhanced amidase activity. (**A**) SDS-PAGE analysis of HiC and TcC enzymes (purification level > 90%, 23 and 30 kDa, respectively) after immobilized metal ion affinity chromatography. (**B**) Kinetic analysis of wild-type enzymes and variants in the hydrolysis of a small aliphatic ester and amide (fig. S3). Values of relative reaction specificities were compared and normalized against each wild-type enzyme.

De-polymerization enabled by water-restructuring mutations are backbone specific

Encouraged by the observed change in relative reaction specificity using the most soluble substrates, hydrolysis of 3PA 6,6 (fig. 1C), was analyzed computationally and experimentally (fig. 3A, S5, table S2). Indeed, it was found that the relative abundance of weak hydrogen bonds (see Materials and Methods for details) to the

reacting amide group in the modeled TS correlated with the experimentally determined hydrolytic activity (fig. 3A, table S4), which points towards an important role for chemistry in contributing to the rate-limiting step. MD analysis confirmed that the preferred hydrogen bond acceptor in the modeled TS of the variants was a water molecule network (fig. S4A, tables S5-S7), in line with our hypothesis that water-restructuring mutations (fig. S2) dictate interactions between water and the TS for oligomer hydrolysis. In fact, for HiC a water network was 120-fold more likely to act as hydrogen bond acceptor compared to the engineered side chain(s) (table S4 bottom, fig. S4A). Moreover, the introduced mutations were found to impact the density of water around the TS for 3PA 6,6 hydrolysis (table S7). TcC wild type and designed variants, with the highest activity towards 3PA 6,6, were evaluated in the biocatalytic depolymerization of Nylon 6,6 (see Materials and Methods for details). To our great surprise, significant depolymerization of Nylon 6,6 could not be confirmed experimentally (fig. S6). Thus, in order to investigate the impact on the active site water network of additional hydrophilic amide links in the oligomer chain of 3PA 6,6 (fig. 1C), which would better correspond to the actual backbone of Nylon 6,6 (fig. 1D), additional MD-simulations were performed using R = Me, R' = Me in fig. 1D (see Materials and Methods for details). For TcC, the relative *in silico* probabilities of forming a hydrogen bond to the reacting amide group in TS for the hydrolysis of the dimeric oligomer backbone with such increase in polarity (corresponding to log P = -0.21 compared to log P = 3.52 for 3PA 6,6), were analogous to those of 3PA 6,6 (fig. 3B, left). In contrast, HiC wild type and variants displayed a significantly elevated TS stabilization for the more polar oligomer backbone (fig. 3B, right). Double mutant HiC L64H/I167Q displayed a relative probability of hydrogen bond formation that was one order of magnitude higher than that of any of the other enzyme variants investigated (fig. 3B). The hydrogen bond stabilization for the better resembling backbone of Nylon 6,6 was found to be provided by a favorable water network rather than by the engineered side chains (fig. S4B, tables S8-S10). A detailed analysis of all possible networks of water providing a weak hydrogen bond to the modeled TS showed how short chains of water clusters, that favorably solvated the TS, progressively became more favorable (HiC wild type fig. 3C, I167Q fig. 3D, and the L64H/I167Q double variant fig. 3E. In particular, the HiC L64H/I167Q double mutant displayed a relatively high-abundance of short water clusters and was capable of accommodating a water molecule in a favorable position (fig. 3F). In contrast, the

total solvation of the active site as measured by the number of water molecules within 8 Å of the reacting nitrogen atom in TS for TcC and HiC L64/H167Q were similar (table S11).

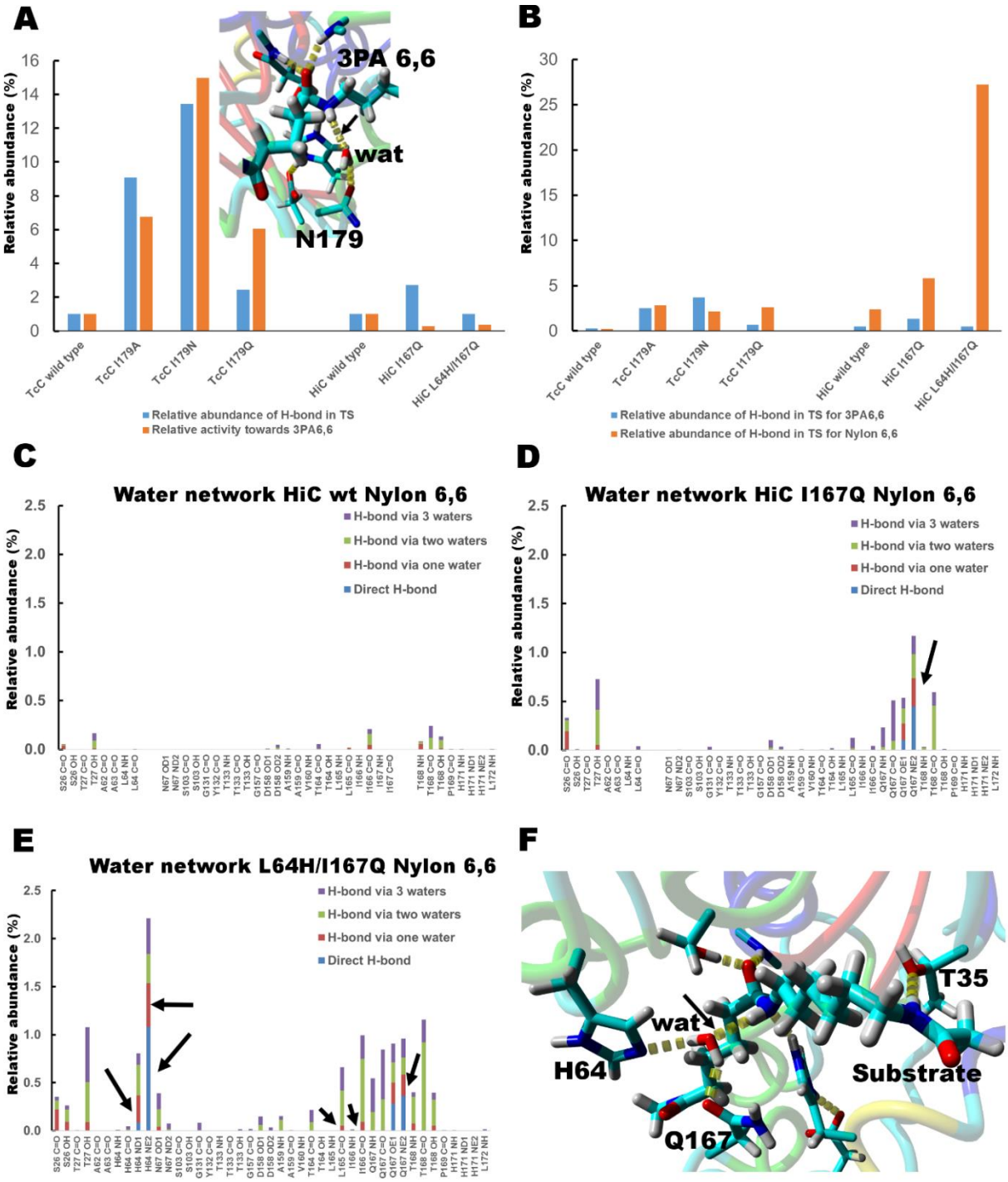

Fig. 3. *In silico* evaluation of nylonidases with altered water networks capable of accepting a H-bond donated by the reacting NH-group in the TS. (**A**) Variants of TcC (left) were capable of weak hydrogen bond formation accepted by water in the modeled TS of 3PA 6,6 hydrolysis, which was associated with higher experimentally determined relative hydrolysis activity (see also fig. S4). The

inset shows a snapshot from an MD-simulation of the TcC I179N variant with the key hydrogen bond indicated by the arrow. In contrast, HiC variants (right) did not display significantly higher abundances of productive water clusters. For reference, the experimentally determined hydrolysis activities are normalized to wild type in each case (see table S4). (**B**) *In silico* analysis of the model compound with a more polar oligomer backbone representing hydrolysis of Nylon 6,6 (fig. 1D) reveals HiC variants displaying significantly elevated relative abundances of weak hydrogen bond formation in the TS accepted by water. For comparison, the relative abundancies of productive hydrogen bond formation for 3PA 6,6 are given. The modeled oligomer corresponds to R = Me, R' = Me in fig. 1D. (**C-E**) Detailed *in silico* analysis of the spatial organization of water clusters in HiC wild-type (**C**) and the evolution of water clusters in variants (**D, E**) capable of hydrogen bond formation to the reacting NH-group of the model substrate representing Nylon 6,6 (R = Me, R' = Me in fig. 1D). For visual clarity, only water clusters accepting a strong hydrogen bond (see Supporting Information) are shown. The arrows illuminate emerging and short water clusters consisting of up to two water molecules. (**F**) Snapshot of the HiC L64H/I167Q double mutant high-lighting the redesigned water cluster comprising one water molecule held in place by H64 and Q167. The key hydrogen bond to the model compound representing polyamide hydrolysis is shown (arrow).

Hydrolysis of Nylon 6,6 yields carboxylic and amine groups increasing surface hydrophilicity. The hydrophilicity of the surface was reported to be explanatory in the analysis of polyester hydrolysis (*35*). The water contact angle (WCA) technique can be used to analyze the presence of polar functional groups on polymeric surfaces. On the other hand, the increased number of carboxylic groups as a result of surface hydrolysis can be detected by FTIR. Hydrolysis of Nylon 6,6 by TcC single variants indeed resulted in an increased surface hydrophilicity when compared to the wild-type enzyme. Moreover, the fact that no increase of hydrophilicity was found with a loss-of-function variant (S131A) confirmed the impact of the mutations onto amide bond hydrolysis (fig. S6A). However, FTIR analysis did not give a clear signal related to an expected increase of carboxylic acid groups on the Nylon 6,6 surface (fig. S6B), presumably due to insufficient activity. Moreover, using GC-MS analysis no significant amounts of possible released products during PA depolymerization were detected (fig. S7, S8) for the wild-type and the single variants of TcC (fig. S6C).

In contrast, in agreement with the MD-simulations (fig. 3B-F), experimental characterization confirmed high activity of the L64H/I167Q double variant in the hydrolysis of Nylon 6,6 (fig. 4). Activity could readily be detected by i) contact angle measurement (fig. 4A), ii) a clear FTIR peak at 1715 cm^{-1} corresponding to carboxylic acid groups formed on the PA surface (fig. 4B) and iii) significant release of

hydrolysis products (fig. 4C). The presence of these hydrolysis products, namely hexane-1,6-diamine, adipic acid and 1,8-diazacyclotetradecane-2,7-dione (fig. S7), was revealed by GC-MS analysis of the derivatized diamine (fig. S8A and C), diacid (fig. S8B) and cyclization of a dimer (fig. S8D).

From polyesterase to polyamidase

HiC wild type showed a high activity on PET, corresponding to the release of almost 200 moles of products per mol biocatalyst (fig. 4D), while TcC wild type was less active in the release of polyester hydrolysis products (25 times less efficiently, fig. S6D). Remarkably, the HiC L64H/I167Q double variant showed a complete loss of activity on PET, while HiC I167Q showed a striking decrease in activity of almost 94%.

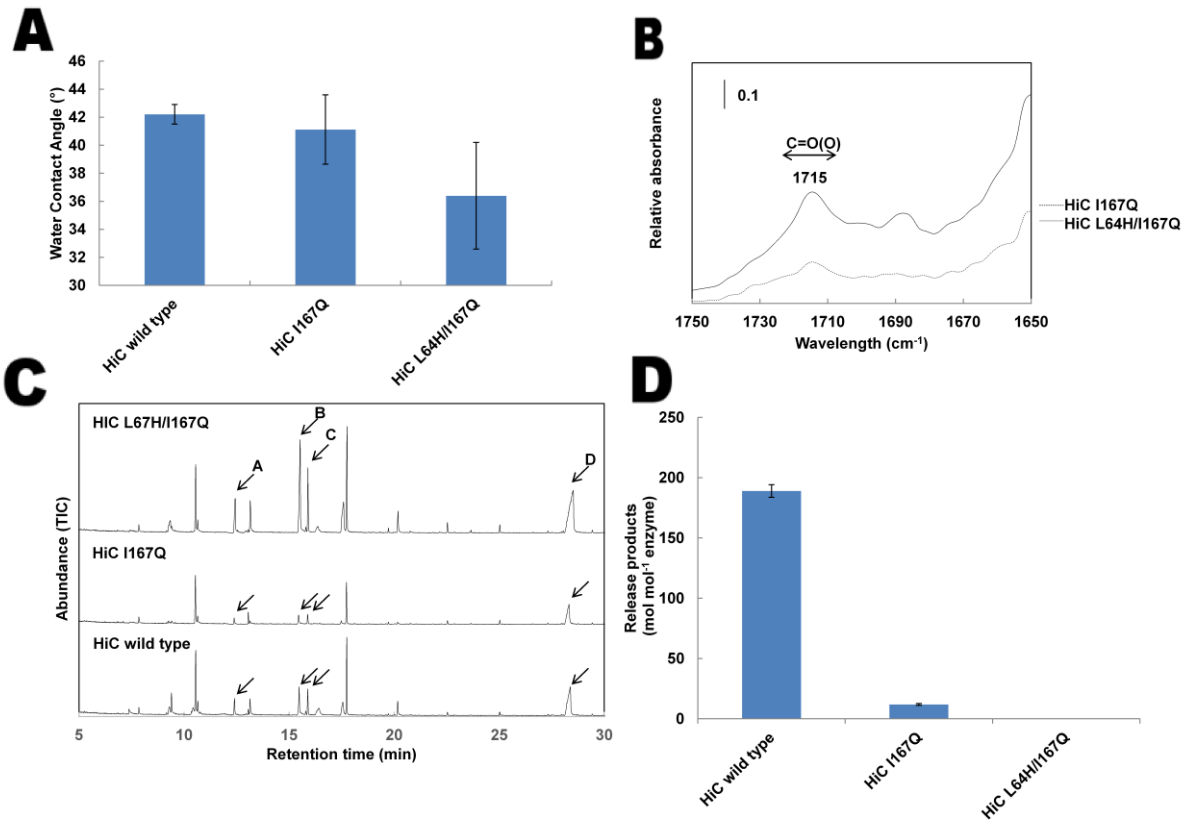

Fig. 4. HiC L64H/I167Q is a nylonidase with switched specificity from polyesterase to polyamidase. (**A**) The variant HiC L64H/I167Q increases the hydrophilicity of the Nylon 6,6 surface after treatment of the polymer for 72 h at 50 °C. Values are average measurements from three reactions, ± standard deviations are shown. (**B**) The enhanced number of carboxylic groups present

on the surface of Nylon 6,6 was analyzed by FTIR spectra from 4000 to 650 cm^{-1} (fig. S9), focusing on 1715 cm^{-1} for carboxylic residues. The relative intensities of HiC wild type have been subtracted from the shown data. (**C**) Release of hydrolysis products was determined through gas chromatography coupled to mass spectrometry (GC-MS). Derivatized compounds were identified through comparison of the respective fragmentation pattern with data in the NIST library (details on identification are described in the Materials and Methods section). The labeled arrows represent the compounds identified (spectra and structure are described in fig. S7-8). (*A*) *N*-(6aminohexyl)acetamide; (*B*) 6-ethoxy-6-oxohexanoic acid; (*C*) *N,N'*-(hexane-1,5-diyl)diacetamide; (*D*) 1,8-diazacyclotetradecane-2,7-dione (**D**) The characteristics of the HiC L64H/I167Q double variant to hydrolyze the polyamide Nylon 6,6 was associated with abolished polyesterase activity. Analysis of released products from PET films was carried out by high-performance liquid chromatography and via UV-spectroscopy at 241 nm (fig. S10). The amount was calculated through a calibration curve of release products (see Materials and Methods for details). Data are means of three reactions, ± standard deviations are shown.

To our knowledge, no microorganism has been identified so far, which is able to degrade the industrial bulk polymer Nylon 6,6. Here we have shown that a reconfigured water network adapted to the synthetic polymer backbone and obtained by enzyme design can turn polyesterases into polyamidases hydrolyzing recalcitrant synthetic polymers like Nylon by providing efficient transition state stabilization. In particular, the complete shift in specificity from polyesterase to polyamidase displayed by the “nylonidases” could pave the way towards recovery of valuable polyamide building blocks from complex plastic mixtures, composites and blends (*36*) through selective depolymerization of the polyamide constituents.

6.1 Materials and Methods

Chemicals, film and reagents

All chemicals and reagents used in this work were of analytical grade. The model substrate N^1,N^6-dihexylhexanediamide (3PA 6,6) was produced according to Heumann et al (*37*). Films of Nylon 6,6 and polyethylene terephthalate (PET) were purchased from Goodfellow (UK) (thickness 50 µm). Buffer components, bovine serum albumin (BSA), *para*-nitrophenol (*p*NP), *para*-nitrophenyl butyrate (*p*NPB), *para*-nitroaniline (*p*NA) and methanol were purchased from Sigma-Aldrich (USA). The substrate for amidase activity assay *para*-nitrobutyranilide (*p*NBA) was purchased from AKoS GmbH (Germany).

Sequence analysis and sequencing

DNA and protein sequences were analyzed by CLC Main Workbench, version 7.0.3 (Qiagen, Netherlands). DNA sequencing was performed as a customer at LGC genomics (Germany) using Sanger sequencing (*38*) (fig. S11).

Preparation of variants

All DNA manipulations described in this work were performed by standard methods (*39*). Megaprimers for the TcC variants, possessing the specific mutation (Table S1) were purchased from Microsynth AG (Switzerland) and used in two-stage PCR reactions to introduce mutations using *Pfu* DNA Polymerase (Promega GmbH, Germany) and pET26b(+)_*TcC* as template. Restriction enzymes were purchased from New England Biolabs and used following the manufacturer's protocol. Plasmid DNA was prepared using PureYield™ Plasmid Miniprep and Plasmid Midiprep system (Promega GmbH, Germany). The amplified products were chemically transformed in *Escherichia coli* XL-10.

For HiC codon-optimized genes (*i.e. E. coli* codon usage) of wild-type, I167Q and L64H/I167Q variants were purchased from GeneArt® (Life Technologies, USA). The genes were cloned into the vector pET26b(+) and chemically transformed by heat shock into *E. coli* XL-10.

Bacterial strains, Plasmid and Media

E. coli XL-10 and *E. coli* BL21-Gold(DE3) (Agilent Technologies, USA) strains were used for subcloning and expression, respectively. The vector pET26b(+) (Novagen, Germany) was used for expression of HiC and TcC wild type and variants. Luria-Bertani (LB) media, supplemented by 40 µg mL^{-1} kanamycin as a selective agent, was used to culture the plasmid-carrying cells. In order to determine the cell density at OD_{600}, a Hach DR3900 Spectrophotometer (USA) was used.

Enzyme Expression and Purification

HiC wild type and variants

The fermentation of *E. coli* cells carrying the vector containing the genes for HiC wild type and variants was constituted by two phases, the overnight batch phase limited by nutrient availability and the fed batch phase for which induction of recombinant protein expression was performed. Cultivations were done in 5-L bioreactors (Minifors, Switzerland). The pH was controlled at pH 7.0 ± 0.2 by addition of 25 % NH_4OH, oxygen saturation was maintained at pO_2>30%, the temperature was set at 37.0 °C ± 0.5 °C and 5% w/w Glanapon 2000 (Bussetti, Austria) was used as antifoam solution. For the batch phase, 1.75 L batch medium (*40*) was sterile filtered into the bioreactor and supplemented with 40 µg mL^{-1} kanamycin. The trace element solution was prepared in 5 N HCl and included 40 g L^{-1} $FeSO_4 \cdot 7\ H_2O$, 10 g L^{-1} $MnSO_4 \cdot H_2O$, 10 g L^{-1} $AlCl_3 \cdot 6\ H_2O$, 4 g L^{-1} $CoCl_2$, 2 g L^{-1} $ZnSO_4 \cdot 7\ H_2O$, 2 g L^{-1} $Na_2MoO_2 \cdot 2\ H_2O$, 1 g L^{-1} $CuCl_2 \cdot 2\ H_2O$, and 0.5 g L^{-1} H_3BO_3. The batch was inoculated with the desired *E. coli* strains, carrying the vector for HiC wild type or variants, directly from the 1.5 mL cryo-stock and grown overnight. After complete consumption of nutrient defining the end of the batch phase, an exponential fed batch cultivation, which maintained a constant specific growth rate of 0.1 h^{-1}, was initiated. The substrate feed (3 g L^{-1} KH_2PO_4, 4 g L^{-1} K_2HPO_4, 113 g L^{-1} glucose monohydrate, 10 g L^{-1} $Na_3C_6H_5O_7 \cdot 2\ H_2O$, 4 g L^{-1} $MgSO_4 \cdot 7\ H_2O$, 0.8 g L^{-1} $CaCl_2 \cdot 2\ H_2O$, 2 mL L^{-1} and Trace elements) was maintained by feedback control of feed flask weight loss and last for 3 generations (approximately 23 h). Recombinant protein expression was induced by addition of isopropyl-*β*-D-1-thiogalactoside (IPTG) to the reactor at the beginning of the fed-batch phase with 0.9 µmol IPTG per g calculated cell-dry matter (5.6 g CDM). A final volume of 3.2 L was reached. Aliquots were taken frequently and stored at -20 °C until further analysis.

TcC wild type and variants

Freshly transformed single colonies were picked from agar plates containing 40 µg mL^{-1} kanamycin and inoculated in 20 mL LB-medium supplemented with 40 µg mL^{-1} kanamycin and incubated overnight at 37 °C and 150 rpm. This culture was diluted in 200 mL LB -medium containing 40 µg mL^{-1} kanamycin to an OD_{600} of 0.1 and incubated at 37 °C and 150 rpm until an OD_{600} of 0.6-0.8 was reached. The culture was induced with 0.05 mM isopropyl-*β*-D-1-thiogalactoside (IPTG) (Sigma-

Aldrich, USA) for 20 h at 20 °C. The inactive variant TcC_Ser131Ala was expressed and purified as previously described (*41*).

Purification of His-tagged enzymes

Cell lysis and purification by nickel-immobilized metal ion affinity chromatography (Ni-IMAC) were carried out as previously described by Herrero et al (*27*). The buffer was exchanged to 0.1 M Tris-HCl pH 7 by PD-10 desalting columns (GE Healthcare, USA) and the solution was concentrated by Vivaspin 20, 10,000 Da MWCO (Sartorius AG, Germany).

Protein analysis

Bradford assay (*42*) using Bio-Rad Protein Assay kit was carried out to measure the protein concentration using bovine serum albumin (BSA) (Sigma-Aldrich, USA) as standard. Sodium dodecyl sulfate-polyacrylamide gel electrophoresis (SDS-PAGE) was performed according to Laemmli using precast gels purchased from Bio-Rad (USA), and by using 200 V and a running time of 30 min. Pre-stained protein marker IV (Peqlab, Germany) was used as a molecular mass marker. Coomassie method was used to stain the protein bands.

Enzyme activity assay

Esterase activity

Esterase activity was measured using *p*NPB as substrate, as previously described (*43*) in 0.1 M potassium phosphate buffer pH 7 at 25 °C following the reaction at 405 nm for 5 min using a Tecan Infinite M200 (Tecan Austria GmbH) (*44*). A blank reaction was carried out containing buffer instead of enzyme solution. The molar extinction coefficient (ε_{405}) for *p*NP was calculated as 8.31 M^{-1} cm^{-1} in 0.1 M potassium phosphate buffer pH 7. One unit of enzyme activity (U) was defined as the amount of enzyme releasing 1 µmol of *p*NP per minute under the given experimental conditions. Specific activity was expressed as U mg^{-1} of protein. Substrate specificity (k_{cat}/K_M) was calculated in a substrate range of 0.3 to 6.3 mM *p*NPB. Kinetic data were calculated by simple weighted non-linear regression of the Michaelis-Menten equation using the SigmaPlot software, version 12.5 (Systat Software Inc).

Amidase activity

Amidase activity was measured using *p*NBA. The substrate was first dissolved in 100% DMSO, to a final concentration of 100 mM. Thereafter this solution was diluted in 0.1 M potassium phosphate buffer pH 7 to a final concentration of 2.25 mM. The amidase activity was measured at 405 nm and 25 °C for 4 hours using a substrate range of 0.1 to 2.04 mM *p*NBA and compared to the wild type enzyme. The molar extinction coefficient (ε_{405}) for *para*-nitroaniline (*p*NA) was calculated as 15.9 M^{-1} cm^{-1}. One unit of enzyme activity (U) was defined as the amount of enzyme releasing 1 µmol of *p*NA per minute under the given experimental conditions. Specific activity, substrate specificity and kinetic data were carried out as reported above.

Hydrolysis of polyethylene terephthalate (PET)

In order to determine the reducing activity towards bulky PE, 5 µM HiC and TcC wild type and variants were incubated with 0.5x1 cm amorphous PET films (50 µm thickness) in 0.1 M potassium phosphate buffer pH 7 for 72 h at 50 °C and 100 rpm. In order to remove impurities prior to enzymatic treatment, PET films were washed with three different washing steps at 50 °C and 100 rpm, each step for 30 min, firstly with 5 g L^{-1} Triton X-100, then with 0.1 M sodium carbonate and finally with MQ water. After incubation with enzyme, the supernatant was treated to precipitate off the enzyme by adding ice-cold methanol in a ratio of 1:1. The sample was then acidified with 6M HCl to a pH 4 and then centrifuged at 14000 x *g* at 0 °C for 15 min. Finally the supernatant was filtered through a 0.22 µm filter and analyzed by high-performance liquid chromatography (HPLC) in a Hewlett Packard series 1050 system, coupled with an Agilent Poroshell 120 Ec-C18, 30 x 50 mm, 2.7 µm column, a Poroshell 120 Ec-C18, 3.0 x 5.0 mm, 2.7 µm precolumn, and with an UHPLC guard column (Agilent Technologies, USA), heated at 40 °C using a fluorescence detector. The samples were eluted using a non-linear gradient with a constant flow rate of 0.75 mL min^{-1}. Concentration of formic acid (A) was always kept at 0.01 %. The gradient starting with 10 % methanol (B) and 80 % water (C) at 1 min, 50 % B and 40 % B at 8 min, 90 % B and 0 % C at 11 min. The injection volume of the sample was 10 µL. The release products were detected via UV spectroscopy at 241 nm.

Hydrolysis of 3PA 6,6

To investigate the activity of the variants towards amide bonds, 10 mg 3PA 6,6 model substrate were incubated in the presence of 5 µM enzyme in 0.1 M potassium phosphate buffer pH 7 at 50°C and 100 rpm. After hydrolysis, the samples were frozen and lyophilized for 48 h, until complete removal of water was achieved. The powder was resuspended in 100% methanol. After centrifugation at 14,000 rpm the solution was filtered through a 0.2 µm PSTF filter and placed in a glass vial. Calibration standards of 3PA 6,6 in methanol for gas chromatography–flame-ionization detection (GC–FID) were prepared in a range of 1 to 250 mg L^{-1}. The GC–FID analyses were performed using a Hewlett-Packard (Palo Alto, CA). A J&W Scientific (Folson, CA) DB-17MS capillary column (30 m x 250 µm x 0.25 µm) was used with nitrogen as the carrier gas. A splitless injection mode (1 µL) was used with the following GC temperatures and method: injection port, 300 °C; initial column temperature, 40 °C; initial hold time, 0.5 min; first temperature ramp, 20 °C min^{-1}; second column temperature, 70 °C; second hold time, 1 min; second temperature ramp, 30 °C min^{-1}; final column temperature, 340 °C; final hold time, 2 min. The total GC-FID run time was 14 min.

Hydrophilicity measurements

Nylon 6,6 surfaces treated with wild-type enzyme and variants were analyzed by Water Contact Angle (WCA) to analyze their hydrophilicity. In order to remove impurities from the surface of 2 x 2 cm Nylon 6,6 film (50 µm thickness) (Goodfellow, UK), three consecutive washing steps were carried out, as explained above for the PET hydrolysis. After 7 days of incubation in 10 mL at 50 °C and 100 rpm, in the presence of 5 µM of enzyme, the film was washed again to remove the adsorbed enzyme on the surface, as above. The inactive variant TcC_Ser131Ala, was designed to avoid artifacts measured due to adsorbed enzyme, which may contribute to hydrophilicity changes. Drop Shape Analysis system DSA 100 (Krüss GmbH, Hamburg, Germany) was used to analyze Nylon 6,6 films using ddH_2O as test liquid with a drop size of 2 µL, deposition speed 100 µL min^{-1}. WCAs were measured in static sessile drop method after 5 sec. Measurements were carried out from three sample surfaces with at least six different drops.

Fourier transform infrared spectroscopy analysis (FT-IR)

The surfaces of Nylon 6,6 films after hydrolysis of wild-type enzymes and variants were analyzed on a PerkinElmer Spectrum 100 spectrophotometer (PerkinElmer Inc., Germany) in Attenuated Total Reflectance (ATR) mode using a diamond crystal. Infrared spectra were collected in the range of 650-4000 cm^{-1} at 2 cm^{-1} optical resolution and 2 scan repetitions per analysis. The band at 1715 cm^{-1} was assigned as (C=O(O)).

Gas Chromatography-Mass Spectrometry (GC-MS)

In order to determine possible release of hydrolysis products from the bulky substrate Nylon 6,6, after incubation of the enzyme with the polymer, the supernatant of the reactions was lyophilized using a Christ Freeze dryer Beta 1-16, 220 V, 50 Hz, 1.2 kW. The lyophilized samples were resuspended in ethyl acetate (Sigma-Aldrich, USA) and filtered through a 0.2 µm PSTF filter and placed in a glass vial. The GC-MS analyses of the supernatant were performed using an Agilent 7890A (Santa Clara, CA) equipped with a mass selective detector 5975C VL MSD with triple axis. The system was equipped with a PAL-xt autosampler (CTC Analytics AG, Switzerland). A J&W Scientific (Folson, CA) DB-17MS capillary column (30 m x 250 µm x 0.25 µm) was used with nitrogen as the carrier gas. A deactivated glass wool tapered bleed temperature optimized (BTO) septawas used as an inlet liner. Splitless injection mode (1 µL) was used with the following GC temperatures and method: injection port, 300 °C; initial column temperature, 50 °C; initial hold time, 2 min; first temperature ramp, 7 °C min^{-1}; second column temperature 100 °C; second hold time, 1 min; second temperature ramp, 6 °C min^{-1}; third column temperature 220 °C; third hold time, 2 min; third temperature ramp, 20 °C min^{-1}; final column temperature, 340 °C; final hold time, 5 min; total run time, 43 min. The MSD source was kept at 230 °C, the quadrupole at 190 °C, the transfer line at 300 °C with a scan range between 25 and 500 AMU with a gain factor of 5. The solvent was delayed for 2.8 min.

Molecular dynamic (MD) simulations

Molecular dynamics simulations on *Humicola insolens* cutinase was based on the PDB file 4OYY (*45*) using YASARA (*46*) version 14.5.21. For *Thermobifida cellulosilytica* cutinase 1, the PDB file 5LUI was used. For both enzyme structures, missing hydrogens were added and the corresponding hydrogen network was optimized by using Amber03 force field, keeping all heavy atoms fixed. Crystallographic waters were kept. For the Van der Waals interactions, a cut-off of 7.86 Å was used and PME accounted for long-range electrostatics (*47*). The structures were minimized through repeated steps of short molecular dynamics and energy minimizations, initially by releasing fixed waters and then on all atoms. The thus obtained structures were finally subjected to simulated annealing. The second tetrahedral intermediate formed during acylation of the catalytic serine (S131 for TcC and S103 for HiC, respectively) represented the TS for nitrogen inversion (*31*). The tetrahedral intermediate was constructed by covalent attachment of the PA oligomer (3PA 6,6 and oligomer displaying a backbone of enhanced polarity more reminiscent of Nylon 6,6 R = Me, R' = Me in fig. 1D). For HiC, the construction of the tetrahedral intermediate was guided by a previously generated homology model (*32*) for acylation of the ester methyl methacrylate. Force field parameterization for the tetrahedral intermediate was obtained by the AUTOSMILES methodology (*48*) as implemented in YASARA. All simulations were performed in a water box that contained approximately 4000 (for HiC) and 5000 for (TcC) explicit water molecules. The pH was set to 7.4 and corresponding protonation states of enzyme side chains was predicted by the built-in empirical method (*49*) in YASARA. The introduced His in the HiC L64H/I167Q variant was kept unprotonated throughout the MD simulation (predicted pK_a 7.2). The simulation cell was neutralized through the addition of 0.9% NaCl. All simulations were performed under standard conditions under the canonical ensemble at 298 K using a Berendsen thermostat (and the Amber03 force field). For both investigated substrates (*i.e.* 3PA 6,6 and the oligomer displaying a backbone with enhanced polarity), MD-simulations were performed for 120 ns in duplicate, with a 20 ns equilibration phase and 100 ns production phase. Different initial random seeds were obtained by a slight change in the simulation temperature (by 0.0012 K). All possible water networks in proximity of the reacting amide group of the substrate were analyzed. A weak hydrogen bond was defined as an interaction

between donor and acceptor with a hydrogen bond distance of ≤3 Å, and angle ≥120°.

6.2 References and Notes

[1] Y. Zhu et al. 2016, *Nature*, *540*, 354–362.

[2] L. Shen et al. 2010, *Biofuels, Bioprod. Biorefining*, *4*, 25–40.

[3] M. Claessens et al. 2011, *Mar. Pollut. Bull.*, *62*, 2199–2204.

[4]. E. Huerta Lwanga et al., 2016, *Environ. Sci. Technol.*, *50*, 2685–91.

[5] J. Raynaud et al., 2014, *UNEP*, http://wedocs.unep.org/handle/20.500.11822/9238).

[6] R. Sussarellu et al., 2016, *Proc. Natl. Acad. Sci. U. S. A.*, *113*, 2430–5.

[7] M. Bergmann et al., 2017, *Nature*, *544*, 297–297.

[8] R.-J. Mueller 2006, *Process Biochem.*, *41*, 2124–2128.

[9] G. Fischer-Colbrie et al. 2004, *Biocatal. Biotransformation*., *22*, 341–346.

[10] A. Eberl et al. 2009, *J. Biotechnol.*, *143*, 207–212.

[11] M. A. M. E. Vertommen et al. 2005, *J. Biotechnol.*, *120*, 376–386.

[12] S. Yoshida et al. 2016, *Science (80-.). 351*, 1196–1199.

[13] B. Zerner et al. 1964, *J. Am. Chem. Soc.*, *86*, 3674–3679.

[14] S. Heumann et al. 2009, *Biotechnol. Bioeng.*, *102*, 1003–1011.

[15] S. Kakudo et al. 1993, *Appl. Environ. Microbiol.*, *59*, 3978–80.

[16] I. D. Prijambada et al. 1995, *Appl. Environ. Microbiol.*, *61*, 2020–2.

[17] T. Deguchi et al. 1998, *Appl. Environ. Microbiol.*, *64*, 1366–71.

[18] Z. E. Reinert et al. 2013, *J. Am. Chem. Soc.*, *135*, 12528–12531.

[19] R. Araújo et al. 2007, *J. Biotechnol.*, *128*, 849–857.

[20] E. Herrero Acero et al. 2013, *Biotechnol. Bioeng.*, *110*, 2581–2590.

[21] C. Silva et al. 2007, *Enzyme Microb. Technol.*, *40*, 1678–1685.

[22] J. M. Fox et al. 2017, *Angew. Chemie Int. Ed.*, *56*, 3833–3837.

[23] C. M. L. Carvalho et al. 1998, *Electron. J. Biotechnol.*, 1, 160–173.

[24] S. Chen et al. 2013, *Biotechnol. Adv.*, *31*, 1754–1767.

[25] D. Ribitsch et al. 2015, *Appl. Environ. Microbiol.*, *81*, 3586–92.

[26] A. Biundo et al. 2016, *Biotechnol. J.* doi:10.1002/biot.201600450.

[27] E. Herrero Acero et al. 2011, *Macromolecules*., *44*, 4632–4640.

[28] D. Ribitsch et al., 2012 doi:10.3109/10242422.2012.644435.

[29] A. Pellis et al. 2016, *Process Biochem.* doi:10.1016/j.procbio.2016.10.014.

[30] A. Ortner et al. 2017 *Green Chem.* doi:10.1039/C6GC03150A.

[31] P.-O. Syrén, 2013, *FEBS J. 280*, 3069–3083.

[32] P.-O. Syrén et al. 2012, *ChemBioChem*., *13*, 645–648.

[33] M. J. Fink, P.-O. Syrén 2017, *Curr. Opin. Chem. Biol.*, *37*, 107–114.

[34] P.-S. Huang et al. 2014, *Science*, *346*, 481–5.

[35] D. Ribitsch et al. 2011, *Biotechnol. Prog.*, *27*, 951–960.

[36] J. M. Eagan et al. 2017, *Science (80-.). 355*

[37] S. Heumann et al. 2006, *J. Biochem. Biophys. Methods*. *69*, 89–99.

[38] F. Sanger et al. 1977, *Proc. Natl. Acad. Sci. U. S. A.*, *74*, 5463–7.

[39] J. Sambrook et al. 1989, *Molecular cloning : a laboratory manual*.

[40] K. Marisch et al. 2013, *Microb. Cell Fact.*, *12*, 58.

[41] V. Perz et al. 2015, *Biomacromolecules, 16*, 3889–3896.

[42] M. M. Bradford 1976, *Anal. Biochem.*, *72*, 248–54.

[43] D. Ribitsch et al. 2011, *Biotechnol. Prog.*, *27*, 951–960.

[44] A. Biundo et al. 2016, *Appl. Microbiol. Biotechnol.*, *100*, 1753–1764.

[45] D. Kold et al. 2014, *Protein Sci. 23*, 1023–1035.

[46] E. Krieger et al. 2004, *Proteins*., *57*, 678–83.

[47] U. Essmann et al. 1995 *J. Chem. Phys.*, *103*, 8577–8593.

[48] A. Jakalian et al. 2002, *J. Comput. Chem.*, *23*, 1623–41.

[49] E. Krieger et al. 2006, *J. Mol. Graph. Model.*, *25*, 481–6.

[50] D. Ribitsch et al. 2013, *Biomacromolecules*, *14*, 1769–1776.

[51] A. Biundo et al. 2016, *Biotechnol. J.*, doi:10.1002/biot.201600450.

Acknowledgements

This project has received funding from the European Union's Horizon 2020 research and innovation program under the grant agreement 641942 (Resyntex project). It has also been supported by the Federal Ministry of Science, Research and Economy (BMWFW), the federal Ministry of Traffic, Innovation and Technology (bmvit), the Styrian Business Promotion Agency SFG, the Standortagentur Tirol and ZIT°-°Technology Agency of the City of Vienna through the COMET-Funding Program managed by the Austrian Research Promotion Agency FFG.

Supplementary Materials:

Materials and Methods

Figures S1-S11

Tables S1-S11

References (*27, 37-55*)

7

General Conclusion

This thesis was part of the FP7 REFINE project which aimed at the development of new skills and expertise in sustainable green materials manufacturing, technologies and applications for the development of a greener and more sustainable society. The general aim of the project was the enzymatic modification and functionalization of polyesters as well as the enzymatic production of bio-based polyesters for a more environmentally friendly approach. Basically, the production of bio-based polyesters can be achieved by means of biocatalytic reaction with the use of renewable feedstock, while high energy and harsh chemicals methods for the modification and functionalization of fossil-based polyesters can be avoided and replaced by recombinant wild-type or modified enzymes to improve their activity on polyesters, as investigated in this thesis.

Lipases that belong to the I.5 family, also known as thermoalkalophilic lipase family, expressed mainly by thermophilic bacteria, can act at the interface between two faces (i.e. interfacial activation). Interfacial activation is performed by a structural rearrangement of the enzyme conformation, which is carried out by a structure called lid. Moreover, the presence of a zinc-binding domain leads to the higher thermal stability of these biocatalysts.

Thermal stability and improved activity on the interface can allow the enzyme to hydrolyze the surface of polyester films. As a first step, in order to determine whether this family of enzymes could hydrolyze polyesters, the codon optimized gene of *Pelosinus fermentans* lipase 1 (PfL1) was expressed in *Escherichia coli* BL21-

Gold(DE3) and purified through Immobilized Metal Affinity Chromatography (IMAC) (44 kDa). The alignment of the primary structure confirmed the presence of the lid and of the zinc-binding domain, which are characteristic of the I.5 lipase family. The crystal structure, solved at 2.5 Å resolution, revealed the presence of a lid domain, covering the catalytic triad, Ser129/His372/Asp330, and a zinc-binding domain, which is important for the thermostability of the protein and for the interfacial activation in order to regulate the lid opening.

The optimal hydrolysis conditions were shown at pH 7.5 and 50 °C on the substrate *para*-nitrophenyl butyrate (*p*NPB), which confirmed the thermoalkaliphilic features of the enzyme. Furthermore, out of the *p*NP-esters tested for substrate specificity, chain length moieties from C2 to C8 revealed higher specificity. The enzyme was assayed for their apparent kinetic parameters, showing K_m^{app} of 6.67 and k_{cat}^{app} of 5 s^{-1}.

The ability of PfL1 to hydrolyze the aliphatic/aromatic copolyester PBAT and its oligomers (BaBTaBBa, DaBTaBDa and TdaBTaBTda) was further tested. The activity on PBAT was shown by the release of the building blocks, namely Ta, BTa, and BTaB. A higher release of building blocks was shown in the presence of the milled form of PBAT as compared to the film. Tests on different polyesters, such as PET, PLA, and PHBV, revealed high specificity of PfL1 to the copolyester PBAT. According to the chain length specificity for PfL1 for small-medium chain length, the substrate with smaller acid chain DaBTaBDa was preferably hydrolyzed, followed by the longer aliphatic TdaBTaBTda and by the aromatic BaBTaBBa. A general mechanism for the release of the final carboxylic acid was activated in the first step, followed by the complete hydrolysis of the oligomer BTaB.

After exploring wild-type enzymes as polyesterases, we investigated the potential of improving the activity of biocatalysts for the PBAT hydrolysis to enhance surface functionalization. In this part of the work, site-directed mutagenesis of residues present in the zinc-binding domain of the enzyme *Clostridium botulinum* EstA (Cbotu_EstA) was carried out. The enzyme Cbotu_EstA is another member of the I.5 lipase family which possesses a lid and a zinc-binding domain. Cbotu_EstA was previously reported to be able to hydrolyze PBAT. Four residues in the zinc-coordination site, three in the zinc cavity at a distance of 4.5 Å from the zinc ion and two which are present at the entrance of the cavity of the zinc-coordination site were substituted in order to study the thermostability of the enzyme and its activity on PBAT.

Expression of the enzymes in *E. coli* displayed a different production of soluble and insoluble fractions. Out of all the variants, the zinc-binding site variants were expressed in lower amounts with higher presence of inclusion bodies. Moreover, overexpression was also shown but only in the cases of F154Y and S199A. The soluble fraction of the other variants showed expression that was comparable to that of the wild type.

The purified enzymes were assayed for their kinetic properties, showing a similar affinity to all the enzymes towards *p*NPB. A drop in catalytic efficiency affected all the variants, showing higher values only in the case of the wild-type enzyme. However zinc-coordination variants were the most negatively affected. The same results were shown in the turnover numbers of the variants.

Analysis of the thermostability revealed differences in residues coordinating the zinc ion, showing stable to decreased thermostability for specific variants. The substitution of residues in the zinc cavity and at the entrance of the cavity showed a better thermostability in the presence of more hydrophilic residues.

Although variants of the zinc-binding site did not show any release of soluble products, activity on the polymeric substrate PBAT exhibited an increased amount of release of hydrolysis products, Ta and BTa, for all the other five variants. The increased release of hydrolysis products was especially obvious in variants that carried a substitution of the residues at the entrance of the cavity, while the variants of the zinc cavity showed a comparable release of PBAT building blocks.

The next part of this thesis describes the adaptation of *Clostridium botulinum* EstA (Cbotu_EstA) to be engineered to hydrolyze the common non-biodegradable polyester PET. As previously mentioned, Cbotu_EstA is another member of the I.5 lipase family which possesses a lid and a zinc-binding domain. The recombinantly expressed enzyme was reported to be able to hydrolyze the aliphatic/aromatic copolyester PBAT, but it seemed to lack hydrolytic activity on PET. Moreover, the structure of the enzyme shows the presence of an extra domain at the N-terminus of the protein covering the lid structure that inhibits interfacial activation. Analysis with molecular modeling techniques of the surface of Cbotu_EstA revealed a hydrophobic patch covered by the N-terminal domain.

Construction of the truncated variant of Cbotu_EstA (del71Cbotu_EstA) and its expression in *E. coli,* with further purification *via* IMAC, made it possible to biochemically characterize the enzyme on the soluble substrate *p*NPB and with

regard to its interaction with polyesters. The hydrolysis of *p*NPB showed a 10-fold increase of specific activity of the truncated variant as compared to the wild-type enzyme. A 4-fold increase in affinity and a 1.5-fold increase in turnover number against *p*NPB led to a 6-fold increase of the catalytic efficiency of del71Cbotu_EstA as compared to Cbotu_EstA.

Hydrolyzing enzymes have to recognize the substrate and to direct their activity, for instance, on the surface of polyesters. The truncation of the 71 amino acids of the N-terminal domain was successful in exposing hydrophobic patches which can be adsorbed on the hydrophobic surface of polyesters. The truncation of the N-terminal domain led to a 3.7-fold increase in adsorption onto the polyester PET film. Furthermore, the increased adsorption, in combination with the removal of the hindrance caused by the N-terminal domain, led to the release of Ta that reached 0.5 mol mol^{-1} of enzyme, which was not detectable for Cbotu_EstA. Although, Cbotu_EstA was able to release the oligomer MHET, a 7-fold higher release was detected after the incubation with del71Cbotu_EstA.

Members of the I.5 lipase family are enzymes which show the ability to hydrolyze the surface of polyesters and can be used both for recycling of polyester building blocks and for the hydrophilization of the surface for further functionalization in an environmentally friendly method. Additionally, the improved activity on polyesters was presented and achieved by the analysis of the 3D structure of the enzyme focused on specific domains. Further work would include the combination of the truncation of the N-terminal domain and the substitutions of amino acids present in the zinc-binding domain which could possibly increase the activity of the enzyme on PET.

Furthermore, cutinases have shown the ability to act on bulky polyesters, especially on PET materials, which contain hydrophobic surfaces; as the surface of cutinases possesses hydrophobic patches. The ability to hydrolyze hydrophobic polymer surfaces has been shown to lead to increased hydrolysis of the polymeric substrate.

Synthetic polyamides, as shown for polyesters, possess a hydrophobic surface. However, the presence of a stronger structure on the surface of synthetic polyamides, due to the presence of multiple H-bonds, does not easily allow their hydrolysis. On the other hand, amide bonds are efficiently hydrolyzed only by amidases and proteases, which contain a H-bond acceptor that stabilizes the transition state. Hence, the final part of the thesis focused on the conversion of “polyesterases” into “polyamidases”. The introduction of a H-bond acceptor in two

cutinases, namely *Humicola insolens* cutinase (HiC) and *Thermobifida cellulosilytica* cutinase 1 (TcC), in combination with their ability to adsorb on hydrophobic surfaces, improved the hydrolysis of the polyamide Nylon66. The variant HiC L64H/I167Q was able to reduce the hydrophobicity of the Nylon66 surface with the production of functional groups, e.g. carboxylic groups on the surface, and by releasing higher amounts of building blocks on Nylon66.

In conclusion, members of the carboxylesterase superfamily can be studied, and their structure can be analyzed, in order to improve their activity on specific substrates. Site-directed mutagenesis is an optimal approach to substitute and introduce specific residues, which can improve specific features of the enzymes.

8

Appendix

8.1 Scientific publications

Papers

1. **Antonino Biundo**, Altijana Hromic, Tea Pavkov-Keller, Karl Gruber, Felice Quartinello, Karolina Haernvall, Veronika Perz, Miriam S. Arrell, Manfred Zinn, Doris Ribitsch, Georg M. Guebitz - Characterization of a poly(butylene adipate-co-terephthalate)-hydrolyzing lipase from *Pelosinus fermentans*. *Appl. Microbiol. Biotechnol.*, **2015**, 100(4): 1753-64.
2. **Antonino Biundo**, Georg Steinkellner, Karl Gruber, Theresa Spreitzhofer, Doris Ribitsch, Georg Guebitz - Engineering of the zinc-binding domain of an esterase from *Clostridium botulinum* towards increased activity on polyesters. *Catal. Sci. Technol.*, **2017**, 7(6): 1440-7.
3. **Antonino Biundo**, Doris Ribitsch, Georg Steinkellner, Karl Gruber, Georg M. Guebitz - Polyester hydrolysis is enhanced by a truncated esterase: Less is more. *Biotechnol. J.*, **2016**, 11: 1-5.
4. **Antonino Biundo**, Raditya Subagia, Michael Maurer, Robert Vielnascher, Per-Olof Syrén, Doris Ribitsch, Georg Guebitz - Nylonidases by redesign of water networks. *Science.* Submitted.

Oral presentations as presenting author

1. **Antonino Biundo**, Altijana Hromic, Karl Gruber, Veronika Perz, Doris Ribitsch, Georg M. Guebitz - Enzyme optimization for polymer modification. *International Conference on Biochemistry and Molecular Biology (ICBMB)*, 17-19 April **2014**, Vienna, Austria

2. **Antonino Biundo**, Georg Steinkellner, Karl Gruber, Doris Ribitsch, Georg M. Guebitz - Novel polyesterases with potential in food waste treatment. *Cost action meeting*, 7-10 September **2015**, Tallinn, Estonia

3. **Antonino Biundo**, Georg Steinkellner, Karl Gruber, Doris Ribitsch, Georg M. Guebitz - Less is more: Hydrolysis of polyesters is enhanced by a truncation of an esterase. *FEMS*, 9-13 July **2017**, Valencia, Spain

Poster presentations (most relevant)

1. **Antonino Biundo**, Doris Ribitsch, Felice Quartinello, Veronika Perz, Georg M. Guebitz, Characterization of a poly(butylene adipate-co-terephthalate)- hydrolyzing lipase from *Pelosinus fermentans*, *SETAC* 2016, Nantes, France

2. **Antonino Biundo**, Doris Ribitsch, Per-Olof Syren, Georg M. Guebitz, Converting Polyesterases into Polyamidases, *Biotrans* 2015, Vienna, Austria

3. **Antonino Biundo**, Doris Ribitsch, Felice Quartinello, Veronika Perz, Caroline Gamerith, Georg M. Guebitz, Biochemical characterization of a novel PBAT-degrading enzyme from *Pelosinus*. *RPP8* 2015, Palma de Mallorca, Spain

4. **Antonino Biundo**, Doris Ribitsch, Veronika Perz, Georg M. Guebitz, Biochemical characterization of a PBAT-degrading enzyme from *Pelosinus fermentans*. *ÖGMBT* 2014, Vienna, Austria

5. **Antonino Biundo**, Doris Ribitsch, Veronika Perz, Enrique Herrero Acero, Georg M. Guebitz, Characterization of a new α/β hydrolase from *Pelosinus* sp. for polyesters hydrolysis, *Green Chemistry - GRC* 2014, Hong Kong

6. **Antonino Biundo**, Doris Ribitsch, Georg Steinkellner, Karl Gruber, Georg M. Guebitz, Polyester Hydrolysis is Enhanced by a Truncated Esterases: Less is More, *ESIB* 2016, Graz, Austria

8.2 Miscellaneous

Secondments

1. 9 - 13 December **2013**, Biotechnology and Sustainable Chemistry, Institute of Life Technology University of Applied Sciences of the Occidental Switzerland, Sion, Switzerland. Supervisors Dr. Stephanie Follonier and Prof. Manfred Zinn

2. 01 February - 30 April 2014, Biocatalysis Group, Royal Institute of Technology (KTH), Stockholm, Sweden. Supervisors Prof. Mats Martinelle and Prof. Karl Hult

Fellowships and awards

1. **2013-2015**, Marie Curie Fellowship, Seventh Framework Programme (FP7) for Research and Technological Development of the European Commission.

7.3 Acknowledgments

So many people have supported me and given me the strength to be able to write and to complete this thesis. They deserve to be appropriately thanked.

My supervisor **Prof. Georg Guebitz** for giving me the opportunity to move to Austria and to carry my PhD in his lab, for all the constructive advices, ideas and to give me the opportunity to attend conferences all around the world.

Doris Ribitsch for being a constant support and help during my project and to show me a second path when the route seemed to go through a single one.

Prof. Karl Gruber, **Georg Steinkellner** and all the **Structural Biology group** at UniGraz for their help in crystallography and for their great pictures of protein 3D structures.

Prof. Manfred Zinn and **Stephanie Follonier** for their support in biodegradable polyesters hydrolysis and for hosting me in their lab at HES-SO Valais.

All the **IFA-people** for the support in the last years. In particular a big thanks goes to **Elke** and **Petra** for solving all bureaucratic problems, **Marion** and **Marcus Pruckner** for the technical problems. A special thank goes to **Benjamin, Lydia, Lucy, Mariana, Günther** and **Cathrine** for sharing part of their lives outside of the lab ☺

My students **Johanna** and **Theresa** for performing great experiments in the lab and for their help. A special thank goes to **Luna**, **Felice** and **Radit** for their help inside the lab and for being good friends outside.

All the BET-group and especially **Barbara**, **Kati**, **Alex**, **Quique**, **Katrin G**, **Gregor**, **Caro and Orti**, **Karolina**, **Dani** for nice discussions not only about work.

Ale, **Sara, Marina, Zia Lucia, Valentina and Stefania** for bringing a bit of the Italian.

Giovanna to be b^3 together and **all my friends** close and far.

Martina and **Fra** for being the best sisters someone could ever have.

I miei genitori per avermi supportato in tutte le mie decisioni (buone o cattive) e per essere sempre speciali.

Theo να είναι μέρος της ζωής μου και να μου επιτρέψετε να εισέλθουν στη ζωή του.

7.4 Statutory declaration

I declare that I have authored this thesis independently, that I have not used other than the declared sources/resources, and that I have explicitly marked all material which has been quoted either literally or by content from the used source.

date	signature